Quantitatively Investigating the Genetic Response of the Euryhaline Sailfin Molly (*Poecilia latipinna*) to Manipulations of Environmental and Dietary Magnesium

Jacob Tyler Melissis

A thesis submitted to the Faculty of Graduate Studies in partial fulfillment of the requirements for the degree of Master of Science

Graduate Program in Biology

York University

Toronto, Ontario

Canada

July 2023

I: Abstract

Magnesium (Mg^{2+}) plays vital roles including aiding in DNA replication, cell signaling, hormone production, and musculoskeletal health. To date, research into the function and regulation of genes suspected to be involved in Mg^{2+} homeostasis has lacked a holistic approach. I therefore sought to quantitatively investigate the regulation of a multitude of genes including *solute carriers* (*slc*) *slc41a1*, *slc41a2*, *cyclin m3* (*cnnm3*), *transient receptor potential melastatin 7* (*trpm7*), as well as two *Na^+/K^+-ATPase* (*nka*) isoforms *nka-1α*, *nka-2α* in the gills, intestines, and kidneys of euryhaline sailfin mollies (*Poecilia latipinna*) during manipulations of environmental salinity and dietary Mg^{2+}. I further investigated how these manipulations would affect plasma Mg^{2+} levels using Ion Selective Microelectrodes (ISME) to better understand the function of these genes and the responses to salinity in this species. All Mg^{2+} transporters were ubiquitously expressed across all tissues examined, regardless of environmental salinity. Furthermore, saltwater acclimation alone did not affect plasma Mg^{2+} levels, but downregulation of *slc41a1*, *cnnm3*, and *trpm7* was observed in the gills and intestines, and downregulation of *cnnm3* and *trpm7* was observed in the kidneys. Increasing dietary Mg^{2+} led to acute elevation of plasma Mg^{2+} that was quickly normalized in both salinities. Freshwater-acclimated fish seemed to adapt to dietary manipulations by decreasing intestinal absorption, whereas saltwater-acclimated fish seemed to favour increased renal transport and decreased intestinal transport. This study was the first of its kind to quantitatively investigate the integrated roles of these genes in cellular Mg^{2+} homeostasis across multiple ionoregulatory epithelia in a euryhaline fish and highlight the need for more wholistic investigations in other species.

II: Acknowledgements

I would like to personally thank my friends, family, peers, colleagues and mentors for the support and guidance I have received throughout my time at York. I would like to thank Dr. Carol Bucking and my lab mates (both past and present) for the continued mentorship and encouragement throughout this process. I would like to thank Dr. Raymond Kwong and the members of his lab for the invaluable feedback they have given me, and for allowing me to use their equipment as needed. I would like to thank Dr. Andrew Donini for allowing us to use his equipment to conduct ISME for my experiments, as well as his help throughout the process of data acquisition and analysis. Dr. Carol Bucking's lab is funded by NSERC discovery grants and York University, making the experiments within this thesis possible.

Table of Contents

List of Tables and Figures

List of Abbreviations

AC- Accessory cell

ANOVA- analysis of variance

ATP- adenosine triphosphate

BLAST- Basic Local Alignment Search Tool

cDNA- complementary DNA

CFTR- Cystic Fibrosis Transient Receptor

Cldn- claudin

Cnnm3- Cyclin-m3

Cor- cobalt-resistant transporter

Ct- Cycle threshold

DCT- distal convoluted tubule

FCD- control diet for FW-acclimated fish

FTD- test diet for FW-acclimated fish

FW- freshwater

GIT- gastrointestinal tract

HEK- human embryonic kidney

ISME- Ion-Selective Microelectrode Technique

I-TASSER- Iterative Threading ASSEmbly Refinement

Mgt- Magnesium transporter

MIQE- Minimum Information for Publication of Quantitative Real-Time PCR Experiments

MRC- Mitochondria-rich cell

MS-222- tricaine methanesulfonate

MUSCLE- Multiple Sequence Comparison by Log- Expectation

NCBI- National Center for Biotechnology Information

Nka- Na^+/K^+-ATPase

Nkcc- $Na^+/K^+/2Cl^-$ cotransporter

NME- Na^{+}/Mg^{2+} exchanger

PCR- Polymerase Chain Reaction

PDB- Protein Data Bank

PNA^{+}- peanut lectin-sensitive

PNA^{-}- peanut lectin-insensitive

PPT- parts per thousand

PSI-BLAST- Position-Specific Iterative Basic Local Alignment Search Tool

PVC- Pavement cell

qPCR- quantitative real-time polymerase chain reaction

RMSD- Root Mean Square Deviation

RO- reverse osmosis

Rpl- Ribosomal Protein-Like

SCD- control diet for SW-acclimated fish

SIET- Scanning Ion-selective Electrode Technique

Slc- solute carrier

STD- test diet for SW-acclimated fish

SW-saltwater

TAE- Tris, Acetic acid, and EDTA (Ethylenediaminetetraacetic acid)

Trpm- Transient receptor potential melastatin

18s- Ribosomal protein 18s

Chapter 1: Introduction

1.1 The Importance of Studying Fish Physiology

Fish compose approximately one half of vertebrate biodiversity on earth with over 34,000 currently documented extant species (Froese and Pauly, 2022). Further, fish fill multiple ecological niches making them a vital part of the food chain and their ecosystems, as well as exposing them to a variety of environmental conditions. Therefore, understanding how fish respond to changes in their environment is essential for understanding how they survive. This is particularly true as contamination from various sources, such as industries, introduce foreign substances into aquatic ecosystems potentially impacting a diverse, ecologically important vertebrate. Hence, with this knowledge we may learn how to preserve fish populations and protect fragile ecosystems. Fisheries and aquaculture also play a large economic role in the world, generating 59.51 million jobs, and US $164 billion to the global economy in 2018 (FAO, 2020). As such, an understanding of their physiology has important economic and socio-economic impacts. Finally, fish share many physiological traits with higher vertebrates such as the need to regulate internal ionic/osmotic concentrations within narrow physiological ranges to survive (Hwang et al., 2011). This means that knowledge gained from piscine-focused studies not only illuminates their own physiology, but also potentially that of higher vertebrates. Supporting their role in research, fish are readily accessible, many being inexpensive and commercially available. Furthermore, many species will breed readily, making overall cost and supply convenient for scientists. When considering these factors, it becomes apparent that the use of fish as model organisms in physiological research is an important and worthwhile pursuit.

1.2 Introduction to Osmoregulation in Fish

Within their aquatic habitats, fish face the challenge of balancing their internal ion levels with the surrounding water (reviewed by Hwang and Lee, 2007). Due to the hypotonic nature of freshwater (FW) environments, FW fish must combat constant diffusive ion loss, as well as passive water gain (e.g. Griffiths, 1891; Fredericq, 1901; as reviewed by Potts, 1954; Perry et al., 2003; Evans, 2008; Griffith, 2017; Figure 1a). To overcome these challenges, these animals absorb ions from their environment through their gills (e.g. Krogh, 1937, 1938; reviewed by Potts, 1954; Evans et al., 2005; Evans, 2008; Hwang et al., 2011; Figure 1a), and through the food they eat (e.g. Taylor and Grosell, 2007, Bucking and Wood, 2007; Bucking et al., 2010; reviewed by Marshall and Grosell, 2005; Figure 1a). Additionally, tight junctions in the gills and integument prevent ion loss and water gain by acting as a physical barrier to the environment (Chasiotis et al., 2012; Kwong et al., 2013; Doyle et al., 2022; Figure 1a). Further, the kidneys also help maintain osmotic and ionic balance by creating copious amounts of dilute urine that maximize the amount of water being lost while minimizing the ion load lost from the plasma (Tang et al., 2010; Teranishi and Kaneko, 2010; reviewed by Hickman and Trump, 1969; Beyenbach, 1995; Takvam et al., 2021; Figure 1a).

In contrast, fish that live in marine habitats face the opposite osmotic and ionic challenges than those of their FW counterparts as they risk dehydration and passive ion gain from their hypertonic environments (Figure 1b). To survive, they must drink the surrounding sea water. Upon ingestion, water and ions are absorbed across the esophagus and intestines, where the ions are then transported via the plasma to the gills to be actively pumped back into the environment (reviewed by Evans et al., 2005; Hwang et al., 2011; Figure 1b). The kidneys additionally produce small volumes of highly concentrated urine, rich in Ca^{2+}, Mg^{2+}, Cl^- and

$SO4^-$ (e.g. Hickman, 1968; reviewed by Beyenbach, 2004; Takvam et al., 2021), thus minimizing water loss while also excreting the excess ions (Figure 1b).

Many fish species have adapted to living within a narrow salinity range and will not survive in environments that exceed these limits (reviewed by Gonzalez, 2012). These species are referred to as stenohaline and have adopted rigid osmoregulatory strategies to combat the environmental challenges of their specific environments, either FW or saltwater (SW) as discussed above. A much smaller percentage of fish species (~3-5%) have adapted to survive in a much wider range of salinities while still being able to balance their plasma osmolality within narrow physiological ranges (reviewed by Henry et al, 2012). These euryhaline species have physiological adaptations that allow them to switch their osmoregulatory strategies as the salinities of their environments change (reviewed by Evans, 1984). For example, the mummichog (*Fundulus heteroclitus),* a euryhaline teleost that commonly inhabits marshes and coastal estuaries in eastern Canada faces regular shifts in environmental salinity and can acclimate to salinities ranging from 0ppt FW to 120ppt SW, approximately 4x the salinity of SW (35ppt) (Griffith, 1974). When environmental salinity increases from evaporation or tidal changes, the direction of ion movement across the epithelia of the gills, kidneys and intestines shifts from net absorption in FW to net excretion in SW (Wood and Marshall, 1994) as the fish also increases its drinking rate along with decreasing urine production to combat dehydration (Potts and Evans, 1967). The reversal of ion and water transport in response to changes in environmental salinity makes euryhaline fish useful model organisms for learning about the differentiation and integration of transporter function (Foskett et al., 1983). Similar physiological adaptations have also been shown in the sailfin molly (*Poecilia latipinna)* (Gonzalez et al., 2005). Adaptations such as these are possible due to regulation of transport proteins and cellular

remodelling within the osmoregulatory organs, as well as hormonal changes that occur during the change in salinity (e.g. Foskett et al., 1983; Loretz et al., 2004; Kültz, 2012; Kültz, 2015).

1.3: Transcellular Ionoregulatory Pathways in Teleosts

Regardless of environmental conditions, the major osmoregulatory organs of fish are the gills, intestines, and kidneys (Seo et al., 2013), providing ion and water transport pathways to meet the unique homeostatic demands of fish.

1.3.a: Branchial Ionoregulation

The branchial epithelium of teleosts is composed of highly vascularized lamellar folds through which the blood must fully pass through before returning to the systemic circulation (reviewed by Evans et al., 2005). Due to its large surface area and direct exposure with the environment, branchial epithelium is a dominant site of ion transport in fish (Seo et al., 2013) and, along with the integument, forms a physical barrier between the external and internal fluids of the animal (Lai et al., 2015).

Within the gill lamellae, there are several cell types that express transporters responsible for maintaining ionic balance within the animal, namely Mitochondria-Rich Cells (MRCs) and Pavement Cells (PVCs.) The main contributor to ionic balance within the branchial epithelium is the MRC (also known as the ionocyte). These cells regulate ion balance through the expression of multiple channels, pumps and transporters on the apical and basolateral membranes (Kang et al., 2008). MRCs can be categorized into 4 distinct types based on the presence and distribution of various channels within them as identified by immunostaining in the embryos of Mozambique tilapia, (*Oreochromis mossambicus*; Hiroi et al., 2005). Furthermore, the 4 cell types are differentially regulated depending on the salinity of the environment (Hiroi et al., 2005). In type I

(immature) MRCs, only basolateral Na^+/K^+-ATPase (Nka) is present. Type II MRCs contain both basolateral Nka and apical $Na^+/K^+/2Cl^-$ (Nkcc) and are thought to be expressed for ion absorption in FW. Type III MRCs contain basolateral Nka and basolateral Nkcc. Type IV MRCs are specialized for ion secretion in a marine environment, and contain basolateral Nka, basolateral Nkcc and apical Cystic Fibrosis Transient Receptor (Cftr), but disappeared when fish were transitioned from SW to FW after 72h (Hiroi et al., 2005). Interestingly, it has been proposed that type III MRCs may be a dormant form of type IV MRC that begin to synthesize apical Cftr upon transition into a marine environment to aid in ion secretion in SW (Hiroi et al., 2005). Type I, II, and III MRCs are found in fish acclimated to FW while type I and IV MRCs are present in fish acclimated to SW (Hiroi et al., 2005).

Another cell type that is involved in branchial ionoregulation is the PVC which influences MRC function by covering or uncovering regulatory epithelia in response to changing rates of Na^+ and Cl^- efflux. When environmental salinity increases, type IV MRCs become uncovered to meet the increased demand for excretion, whereas a decrease in ambient salinity from SW to FW leads to the covering of and apoptosis of type IV MRCs, and the emergence of cuboidal type II MRCs (Laurent et al., 2006). Interestingly, in euryhaline fish it is thought that MRCs are smaller in size and separate from other ionoregulatory cells in FW but combine with accessory cells (AC) to form larger multicellular complexes upon transition to SW (Pisam and Rambourg, 1991; Shiraishi et al., 1997). Further, Type IV cells appeared and were upregulated upon transfer from FW to SW and disappeared shortly after transfer from SW to FW (Hiroi et al., 2005). Type II and III are not present in SW acclimated fish but are transcribed and upregulated upon acclimation to FW (Hiroi et al., 2005).

Functionally distinct branchial MRCs can also been divided into peanut lectin -sensitive (PNA^+) and peanut lectin-insensitive (PNA^-) subtypes (Galvez et al., 2002; Goss et al., 2001; Marshall and Grosell, 2005). Davis et al. (2002) demonstrated that PNA^+ MRCs exchange extracellular Cl^- for intracellular HCO_3^- at the basolateral membrane (Boisen et al., 2003). PNA^- cells, on the other hand, are involved in apical Na^+ uptake (Lin et al., 1994). In FW-acclimated fish, transport of ions via PNA cells is thought to either be driven via a negative electrochemical gradient into the cell established by H^+-ATPase (Wilson et al., 2000), or through coupled exchange of H^+ out of the cell and Na^+ into the cell (e.g. Choe et al., 2002; Clairborne et al., 1999; Edwards et al., 1999). Once inside of the intracellular space, Na^+ is secreted across the basolateral membrane via Nka. In SW-acclimated fish, the regulatory function of the branchial epithelium shifts from net absorption of ions to net secretion (Hwang and Lee, 2007). Changes in expression of PNA^+ and PNA^- cells as well as the activity of Nka and H^+-ATPase within each cell type therefore occur to meet shifting homeostatic demands. For example, when FW rainbow trout (*Oncorhynchus mykiss*) were transferred from FW to SW, the expression of PNA^- cells greatly decreased while the expression of PNA^+ cells greatly increased. H^+-ATPase activity also decreased in both cell types upon SW acclimation, whereas Nka activity increased significantly in PNA^- cells and decreased significantly in PNA^+ cells (Hawkings et al., 2004). Additionally, plasma Cl^- is transported across the basolateral membrane and into the cell by Nkcc to establish a favourable electrochemical gradient by which Na^+ can enter the cell via Nka before ultimately being excreted into the environment. $HCO3^-$ is then exchanged for Cl^- at the apical membrane via Cftr, (Laverty and Skadhauge, 2012). Three major contributors to monovalent ion balance within MRCs are Nka, Cftr, and $Na^+/K^+/ 2Cl^-$ cotransporter 1 (Nkcc1) and are some of the most

targeted proteins in studies involving salinity acclimation (Ding et al., 2020, Hwang and Lee, 2007).

Most branchial models have focused on monovalent ion transport as described above. There is also evidence that divalent cations such as Mg^{2+} have transport pathways within the gill (e.g. Bijvelds et al. 1996; Marshall 2002). Although specific pathways for divalent ion transport have not been identified thus far, the presence of RNA believed to code for Na^{+}/Mg^{2+} exchangers (NMEs) such as *slc41a1* (Islam et al., 2013; Kodzhahinchev et al, 2017; Arjona et al., 2019) and *cnnm3* (Islam et al., 2014) has been shown in the gills of various fish species using quantitative Polymerase Chain Reactions (qPCR) (*Takifugu rubripes,* Islam et al., 2013;2014; *Carassius auratus*, Kodzhahinchev et al., 2017; *Danio rerio*, Arjona et al., 2019). It has also been demonstrated that, when consuming a Mg^{2+}-poor diet in FW, the total body Mg^{2+} content exceeds the amount that could reasonably be gained from dietary intake (Bijvelds et al., 1996a). Further, it has been suggested that the negative transepithelial potential maintained across the branchial membrane is too small to support passive Mg^{2+} uptake across the gills, and therefore branchial Mg^{2+} absorption is likely an active process (Bijvelds et al., 1998). Despite this limited evidence of gill transport, the kidneys and gastrointestinal tract (GIT) are likely comparatively more important in the transport of divalent cations (Larsen et al., 2014; Bucking et al, 2009; Bucking and Wood, 2007; Hansen et al., 2021).

1.3.b: Ionoregulatory Function of the GIT

Physiological studies of the piscine GIT have demonstrated that the intestine functions as an osmoregulatory organ that contributes to the regulation of both monovalent and divalent cations taken in from the surrounding water and the diet in an environmentally dependent manner (e.g. Marshall and Grosell, 2005, Taylor and Grosell, 2007, Bucking and Wood, 2007).

In SW, marine fish ingest the surrounding water to combat passive water loss, and it is first desalinized in the anterior portion of the alimentary canal, predominantly across the esophagus (Grosell, 2006). Indeed, the esophagus is a unique portion of the GIT with a low permeability to water and which nearly exclusively transports Na^+ and Cl^- both passively and through transporters such as Nka (Hirano and Mayer-Gostan, 1976, Parmelee and Renfro, 1983). The Na^+ and Cl^- that are absorbed across the esophagus are quickly transported to the branchial epithelium for excretion (Ando et al., 2003). As the imbibed SW travels from the esophagus to the anterior intestine, the salinity has decreased by more than 50% and active transport of Na^+ and Cl^- becomes increasingly important, as water starts to get absorbed (Marshall and Grosell, 2006; Whittamore, 2011). In fact, water absorption in the anterior intestine is solute linked (Larsen et al., 2009) and occurs in tandem with NaCl cotransport that creates as more favourable osmotic gradient in the local intercellular space, allowing water to move across the intestinal mucosa passively (Thiagarajah and Verkman 2006; Larsen et al., 2009; Whittamore, 2011). Divalent ions such as Ca^{2+}, Mg^{2+}, and SO_4^{2-}, on the other hand, are poorly absorbed across the intestine of SW fish (Whittamore, 2011). To prevent the excess accumulation of free divalent cations within the intestinal lumen, SW-acclimated fish secrete bicarbonate into the intestine, increasing the pH and forming $CaCO_3$ and $MgCO_3$ precipitates. The precipitation of these divalent cations further lowers the osmotic pressure and allows for more water to become absorbed into the blood via osmosis (Whittamore, 2011). The resultant intestinal fluid is highly concentrated with bicarbonate salts and divalent ions and is excreted through the rectum into the environment (Walsh et al., 1991 Wilson et al., 2002).

In FW- acclimated fish, drinking the surrounding water is thought to be minimal to reduce water gain from their hypotonic environment (Bucking and Wood, 2006a). Furthermore,

it is thought that the branchial epithelium has a lower permeability to divalent cations such as Ca^{2+} and Mg^{2+} than it does for monovalent ions (Flik et al., 1993). It is therefore expected that the majority of divalent ion uptake in FW-acclimated fish is via the diet (e.g. Bijvelds et al., 1998; Bucking and Wood, 2006a, b; Bucking and Wood, 2007; Wood and Bucking, 2010). For example, when guppies (*Poecilia reticulata*) were fed a low Mg^{2+} diet, it was found that they were unable to sufficiently uptake Mg^{2+} from the environment and suffered a reduced growth rate and increased mortality (Shim and Ng, 1988). Similar findings were also documented when a variety of other FW fish were fed a Mg^{2+}-poor diet including common carp (*Cyprinnus carpio*), rainbow trout (*Oncorhynchus* mykiss), channel catfish (*Ictalurus punctatus*) (Ogino and Chiou, 1976; Ogino et al., 1978; Gaitlin et al., 1982, respectively). Absorption of dietary ions by enterocytes can occur passively down an electrochemical gradient, or actively through coupled uptake via specific transporters that either use the gradients created by the movement of other ions (often Na^{+}) to drive uptake, or through the hydrolysis of ATP (Kuz'mina, 2021). In particular, Na^{+} absorption in the intestine is initiated by the basolateral Nka of the enterocyte (Loretz, 1995), which establishes a negative internal electrochemical gradient through which apical transporters such as Nkcc (Musch, 1982) transport ions into the enterocyte whereafter ion specific pumps finally transfer the ions into the serosal layer to enter the blood (Bucking and Wood, 2006b).

It has been shown that, although digesting a meal rich in Na^{+} will increase plasma osmolality by a significant margin (15-20%, Bucking and Wood, 2006a), the overall transport rate of Na^{+} is still much less than that of branchial MRCs (150 μmol Na^{+} kg^{-1} fish weight, vs. 200 μmol $kg^{-1}hr^{-1}$ in FW, respectively, Marshall and Grosell, 2005; Grosell et al., 2000) suggesting that the diet may not play as significant a role in monovalent ion homeostasis as the

branchial epithelium. 70-90% of required Mg^{2+}, on the other hand, is thought to be taken in via dietary intake (e.g. Bijvelds et al., 1998; Dabrowska et al., 1991; Shearer, 1989). The branchial epithelium is thought to have a low permeability to Mg^{2+}, and indeed in various studies of fish fed a Mg^{2+}-poor diet it was shown that environmental uptake was unable to adequately compensate for the loss of dietary Mg^{2+}, ultimately leading to health complications and increased mortality (e.g. Dabrowska et al., 1991; Bijvelds et al., 1998; Shim and Ng, 1988; Ogino and Chiou, 1976; Ogino et al., 1978; Gaitlin et al., 1982). Despite the importance, Mg^{2+} absorption across the intestinal epithelium is not well understood (e.g. Wood and Bucking; 2010), however it has been shown using inert markers in the rainbow trout that a large portion of dietary Mg^{2+} is absorbed across the stomach and the anterior portion of the intestine (Bucking and Wood, 2007).

1.3.c: Renal Ionoregulation in Teleosts:

Although MRCs (and PVCs) in the branchial epithelium, as well as enterocytes of the GIT provide critical pathways to address osmoregulatory challenges faced by fishes, excess ions or fluid in the plasma are also filtered out as urine via the renal epithelium. In FW the kidneys use high rates of glomerular filtration to produce large quantities of urine while the distal tubules actively reabsorb ions to produce copious amount of dilute waste and preserve ion balance. This effectively further combats water gain either passively from ambient water, or ingested alongside food (Bucking and Wood, 2006a), while simultaneously combatting ion loss. Reabsorption of monovalent ions in the proximal tubule is driven by basolateral Na^+/K^+-ATPase and apical Nkcc as in the gill (Dantzler, 2003; Marshall and Grosell, 2005). Divalent ions such as Mg^{2+} are likely also absorbed in the proximal tubule (Bucking et al., 2009) although the exact transport mechanism is still under study.

As euryhaline fish transition to SW, the physiology of the kidney shifts towards reabsorption of imbibed water and excretion of ions, especially Mg^{2+}, Ca^{2+}, and $SO4^{-}$ (Marshall, 2013; Marshall and Grosell, 2006). As a result, glomerular filtration and urine flow rates decrease and the small volume of urine produced becomes ion-rich. Furthermore, proteins involved in the excretion of ions become upregulated (e. g. Nka-1β, Nkcc1), leading to a shift in the direction of monovalent ion movement from absorption into the blood to secretion into the lumen of the proximal tubule to form preurine (Madsen et al., 2020). Following this shift in electrochemical gradient, divalent cations such as Mg^{2+} are then excreted into the urine via coupled transcellular transport in the proximal tubule (Marshall and Grosell, 2005; Beyenbach, 2000). In SW, the kidney plays a larger role in the excretion of excess divalent ions such as Mg^{2+} and SO_4^{-} than it does in the transport of monovalent ions (Larsen et al., 2014).

1.4: The Physiological Importance of Mg^{2+}

Magnesium (Mg^{2+}) is the fourth most abundant extracellular cation in the body and is the second most abundant intracellular cation in animals next to K^{+} (Romani and Scarpa, 1992; Houillier, 2014). Mg^{2+} serves a wide variety of roles in the body and is a key contributor to cell and molecular signalling interactions, nucleic acid stability, maintenance of electrolyte balance, cellular growth, neuromuscular signalling, bone and muscle development, enzymatic reactions, regulation of intracellular proteins by causing changes in conformation, and as a cofactor to the transport of Ca^{2+} and K^{+} (Arjona et al., 2013; Houillier, 2014). The majority of Mg^{2+} in the cell is bound to various proteins and complexes, and thus only a small percentage (<5%) is found as free ions (Houillier, 2014). Mg^{2+} is present in higher concentrations in the tissues that are more metabolically active such as the liver, heart, kidneys, and brain (Wabbaken et al., 2003). Large quantities of Mg^{2+} are stored as hydroxyapatite in bone and are also stored in the muscle for use

in contractile reactions (Komiya and Runnels, 2015). Due to the role of Mg^{2+} in many physiological processes, strict regulation of intracellular Mg^{2+} is imperative to maintaining proper physiological functions and therefore survival of the organism. The most abundant source of Mg^{2+} uptake in FW fish is via dietary intake, with a small portion of Mg^{2+} absorption coming from the environment via branchial transport (Arjona et al., 2013). The adverse effects of improper Mg^{2+} balancing in animals have been well documented in the literature and include retarded growth, skeletal malformation, and improper cellular signalling leading to various disease states (e.g. De Baaj et al., 2015; Hurd et al., 2013; Swaminathan, 2003; Heron, 2018; Komiya and Runnels, 2015).

1.5: The Study of Mg^{2+} Transport in Fish

Despite the well-documented significance of Mg^{2+} in the literature, the study of the molecular mechanisms involved in its regulation has been poorly explored (e.g. Islam et al., 2013; Kodzhahinchev et al., 2017; Arjona et al, 2019; Hansen et al., 2021). However, the transporters involved in Mg^{2+} homeostasis have gained more attention in recent years (e. g. Islam et al., 2013, 2014; Arjona et al., 2019; Hansen et al., 2021). Indeed, the discovery of a novel bacterial Mg^{2+} channel called MgtE (Magnesium transporter E) in *Bacillus firmus* was a significant step in the discovery of eukaryotic Mg^{2+} transporter homologs (Fleig et al., 2014). Our understanding of Mg^{2+} transport now includes Na^{2+}/Mg^{2+} exchangers (NMEs) such as Solute carriers (Slc) 41a1-3 and Cyclin-m3 (Cnnm3), and channels such as Transient receptor potential melastatin (Trpm) 6/7 (Islam et al., 2013, 2014; Kodzhahinchev et al., 2017; Arjona et al., 2019; Hansen et al., 2021). Most of the evidence that this variety of channels and transporters are involved in the movement of Mg^{2+} at the cellular level is from mammalian models (e.g. Giménez-Mascarell et al., 2018, Hansen et al., 2021), however there is a recent

growing body of research in teleosts (Islam et al., 2013, 2014; Kodzhahinchev et al., 2017; Arjona et al., 2019) that also supports their role. From all of these studies, it is generally agreed upon that there is an apical pathway that brings Mg^{2+} into the cell (possibly involving Trpm6/7, Hansen et al., 2021), and a basolateral extrusion mechanism that is likely an active process that utilizes exchangers such as proteins from the Slc41 and Cnnm families (Hansen et al., 2021). However, there are several contradictory studies, for example placing Slc41 members on the apical membrane of cells (e.g. Islam et al., 2013; 2014), creating a body of literature that is inconsistent and making the generation of cellular and physiological models difficult.

1.7: Objective

The aim of this thesis was to expand the current state of knowledge of Mg^{2+} homeostasis in fish by utilizing a novel model organism (the sailfin molly, *P. latipinna*), with a strong focus on better understanding the role Mg^{2+} transporters play in Mg^{2+} homeostasis when exposed to environmental and dietary challenges. The sailfin molly (*P. latipinna)* is a tropical euryhaline teleost that inhabits a wide range of environments, including ponds, creeks, lakes, marshes, swamps, and estuaries (CABI, 2019). In their natural habitat, these fish primarily reside in either fresh or brackish waters but have been shown in studies to be tolerant of hypersaline conditions up to 80ppt (Nordlie et al., 1992) making them an ideal candidate for physiological studies involving environmental manipulations. Furthermore, these fish eat a primarily herbivorous diet which is rich in micronutrients such as Mg^{2+} and may present interesting physiological differences when exposed to variation in diet composition than their carnivore or omnivore counterparts. qPCR was used to study changes in the expression of genes suspected to play roles in the balance of Na and Mg^{2+} in vertebrates (*slc41a1, slc41a2, trpm7, cnnm3, nka-1α, nka-1β*) following dietary and environmental manipulations.

My first major objective was to identify the presence of RNA coding for *slc41a1*, *slc41a2*, *trpm7*, and *cnnm3* across a variety of tissues in sailfin mollies acclimated to 0ppt FW or 35ppt SW using qPCR. Salinity exposure experiments (0ppt FW, or 35ppt SW) were then used to determine the impact of salinity on the regulation of my target genes in a time-dependent manner regulation in the gills, kidneys, and intestines using qPCR and determine the impact of acclimation on plasma concentration of Mg^{2+} using the Ion-Selective Microelectrode technique (ISME; Chapter 2). Finally, I determined the impact of dietary Mg^{2+} when acclimated to either 0ppt FW or 35ppt SW on the regulation of transporters in the gills, kidneys, and intestines using qPCR as well as plasma Mg^{2+} concentrations over time using the Ion-Selective Microelectrode technique (ISME; Chapter 3).

1.8: Research Impact

Although there has recently been more of a focus on the physiological mechanisms behind Mg^{2+} homeostasis in teleosts (e.g. Islam et al., 2013, 2014; Kodzhahinchev et al., 2017; Arjona et al., 2019; Hansen et al., 2021) there are many important details that have yet to be investigated. For example, none of the studies mentioned above have investigated the integrated roles of the environment and diet in a euryhaline species. Furthermore, the integrated roles of multiple transporters thought to be responsible for the absorption and excretion of Mg^{2+} in fish have been largely overlooked, with only two species being investigated (Arjona et al., 2019 (*Danio rerio*); Hansen et al., 2021 (*Opsanus beta*)), only one of which being euryhaline, and in both cases the role of the diet and intestinal epithelia were overlooked, instead primarily focusing on the renal handling of Mg^{2+}. This is despite evidence that dietary intake may play a larger role in Mg^{2+} homeostasis than the gills or kidneys (e.g. Bijvelds et al., 1998; Dabrowska et al., 1991; Shearer, 1989; Bucking and Wood 2007; Wood and Bucking, 2010). This thesis is the first to

investigate the integrative roles of Slc41a1, Slc41a2, Cnnm3, and Trpm7 on Mg^{2+} homeostasis in response to both environmental and dietary manipulations in three major ionoregulatory organs in a euryhaline fish. Through my observations I hope to build on the foundation of knowledge of how Mg^{2+} is being handled in fish, and consequently apply this knowledge to higher vertebrates to better understand and treat conditions that may be caused by a lack of Mg^{2+} in the diet, or through underlying genetic conditions that may negatively affect the functionality of the investigated genes.

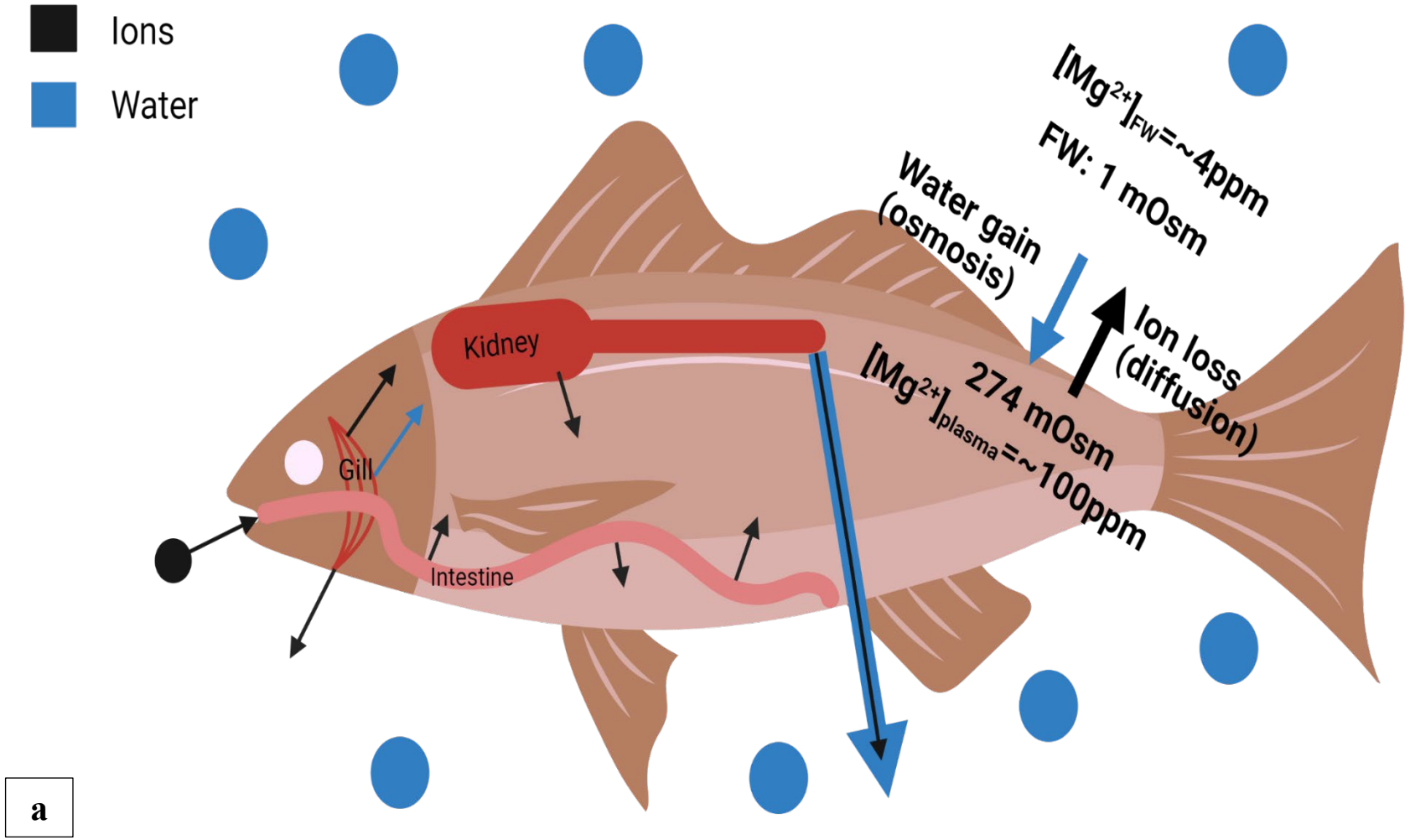
Ions
Water
$[Mg^{2+}]_{FW}$=~4ppm
FW: 1 mOsm
Water gain
(osmosis)
Ion loss
(diffusion)
Kidney
274 mOsm
$[Mg^{2+}]_{plasma}$=~100ppm
Gill
Intestine

a

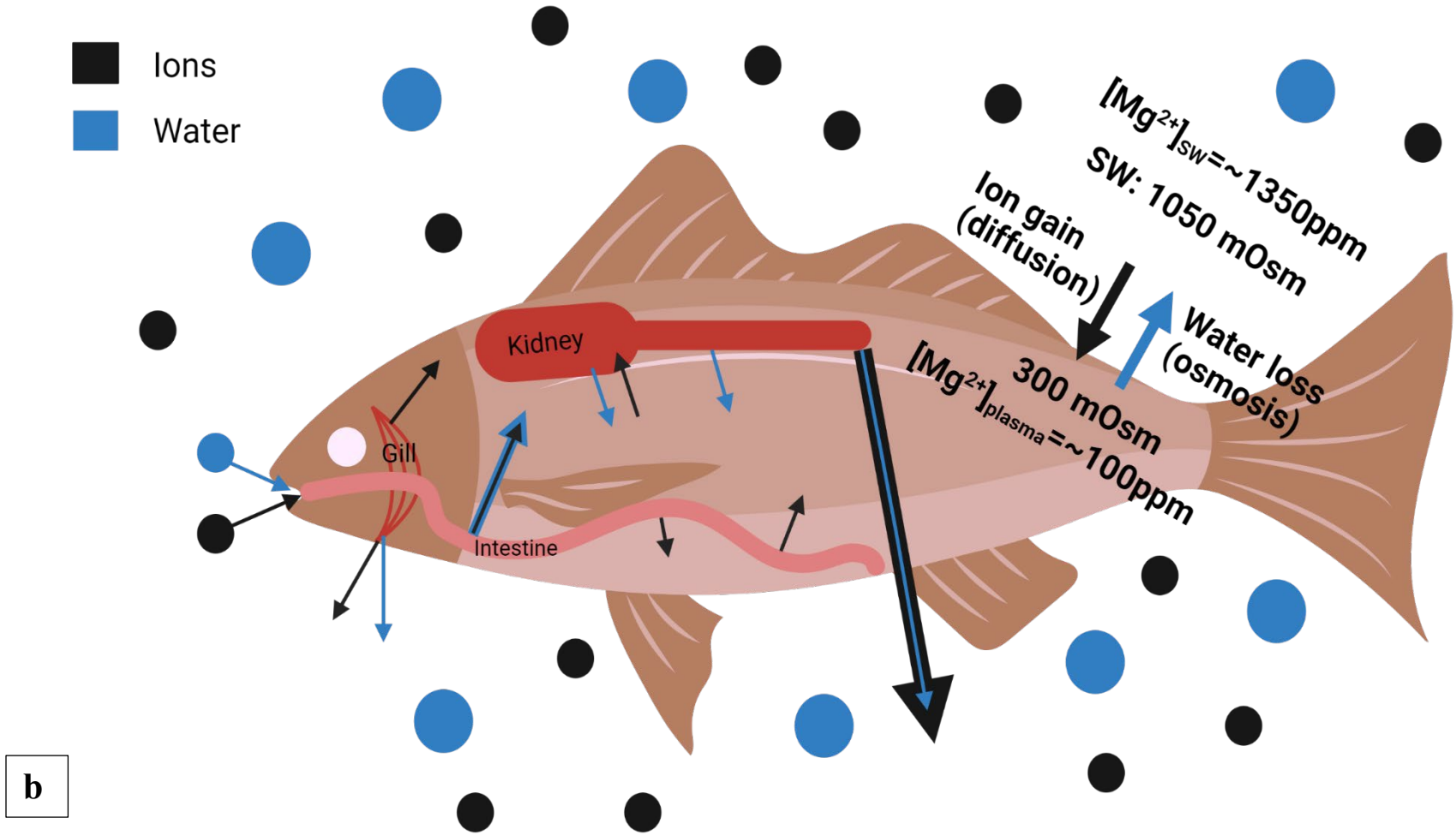

Figure 1: Osmoregulatory strategies of fish in FW (a) and SW (b). Under hypoosmotic stress, FW fish face challenges of passive ion loss and passive water gain across their gills and skin. They must actively absorb ions from the surrounding water across their gills, absorb ions from their diets, and utilize their kidneys to reabsorb ions and excrete large volumes of dilute urine (a). Fish in marine environments face the challenges of passive water loss and ion gain across their gills and skin. They must actively excrete ions across their gills, drink the surrounding water and desalinize it across their intestines and excrete small volumes of concentrated urine. Figure constructed using Biorender.

Chapter 2: Determining the Role of Ambient Salinity on the Expression of Several Ion Transporters

2.1 Introduction:

Despite its vital biological roles, studies on the regulation of Mg^{2+} at the cellular level are scarce. This scarcity could be due to the difficulty in studying magnesium transport using classical techniques. For example, there is a relative lack of stable radioisotopes for the study of Mg^{2+} transport across cellular membranes (Bijvelds et al., 1998). Furthermore, many of the ionophores and fluorescent tags that are currently used in the study of Mg^{2+} transport are also highly sensitive to Ca^{2+}, causing difficulties in gathering reliable data (McGuigan et al., 1993). Regardless, it is expected that for Mg^{2+} to be successfully absorbed transcellularly, it likely enters the cell through a channel and must be excreted via another transporter, possibly through an active transporter or one linked to a Na^{+}-gradient (Yamazaki et al., 2013) as has been observed in *Caenorhabditis elegans* (Taramoto et al., 2005, 2010) and briefly discussed in Chapter 1.

It has been shown in mammalian models that members of the *trpm* family, (Trpm6 and Trpm7) on the apical cellular membrane are involved in passive uptake of Mg^{2+} into the cell down its electrochemical gradient (Voets et al., 2004; Ryazanova et al., 2010). Regarding basolateral extrusion, it has been proposed that Na^{+}/Mg^{2+} exchangers (NMEs) utilize the Na^{+} gradient generated by the basolateral Na^{+} /K^{+} ATPase (Nka) to remove excess Mg^{2+} from the cell (Hansen et al., 2021). Indeed, urinary concentrations of Mg^{2+} and Na^{+} in teleosts acclimated to SW show a negative correlation (Natochin and Gusev 1970), suggesting that Na^{+} may play a role in Mg^{2+} transport. These NMEs are hypothesized to include members of the Slc41 (Slc41a1,

Slc41a2, Slc41a3) and Cnnm (Cnnm2, Cnnm3)) families (Stuiver et al., 2011; Kolisek et al., 2012; Yamazaki et al., 2013; Islam et al., 2014). Despite evidence of potential physiological significance these proteins remain understudied, especially in fish.

2.1.1 : Trpm6 and Trpm7 Facilitate Cellular Mg^{2+} Absorption

Trpm proteins have been shown experimentally to facilitate Mg^{2+} absorption in both the kidneys and intestines of mammals (Schlingmann et al., 2002; Giménez-Mascarell et al., 2018), forming an apical channel that transports primarily Mg^{2+}, but potentially small amounts of other divalent cations such as Ca^{2+} (Voets et al., 2004; Ryazanova et al., 2010; Hansen et al., 2021). Knockdown of *trpm6* in mice has led to renal wasting of Mg^{2+} into the urine, suggesting a significant role in epithelial Mg^{2+} reabsorption from the glomerular filtrate (Schlingmann et al., 2002; Voets et al., 2004; Giménez-Mascarell et al., 2018). Additionally Trpm7 has been shown in mammalian cells to mediate cellular absorption of divalent ions including Mg^{2+} by forming transmembrane channels (Ryazanova et al., 2010; Yu et al., 2014; Loewen et al., 2016). Further, a knockdown of *trpm7* in the embryos of zebrafish (*Danio rerio*) was found to impair Mg^{2+} and Ca^{2+} homeostasis, leading to kidney stone formation (Elizondo et al., 2010), although no similar studies exist for *trpm6* in fish. Although structurally similar, being the only two members of the *trpm* family to contain an intrinsic kinase domain (Runnels et al., 2001; as reviewed by Schlingmann et al., 2007), Trpm6 and Trpm7 are functionally distinct from one another, and are differentially regulated (Li et al., 2006). Although there is evidence of apical localization of both isoforms in the kidneys of mammals (Schlingmann et al., 2002; Giménez-Mascarell et al., 2018), there is only one study to date that investigated these proteins in relation to Mg^{2+} transport in fish which determined that both proteins were significantly upregulated in proximal tubular cells in the gulf toadfish (*Opsanus beta*), upon acclimation to hyperosmotic conditions (60ppt),

suggesting their function may be conserved among vertebrates (Hansen et al., 2021). Although tissue localization of *trpm7* RNA has been shown in the pronephros of developing zebrafish (*Danio rerio*; Wingert et al., 2007), no cellular localization of this protein in adult fish has been achieved to date, and no localization of *trpm6* has been achieved in any fish. Based on their transmembrane divalent ion permeability, however, it was suggested that Trpm6/7 may be localized to the basolateral membrane in the kidneys of fish (Hansen et al., 2021). These predictions are, however, at odds with what has been previously observed in mammalian models, and therefore further experimental evidence is required to support the basolateral localization of Trpm6/7. Due to the existing body of evidence suggesting a role in apical absorption of Mg^{2+} in mammalian models, along with the scarcity of information about these proteins in teleosts, I sought to investigate the role Trpm6/7 may have in Mg^{2+} transport in euryhaline sailfin mollies when exposed to altered environmental ion loads.

2.1.2 : Transcellular Mg^{2+} Transport via Na^{+}/Mg^{2+} Exchangers (NMEs)

Two families of proteins (Cnnm and Slc41) have been identified in fish and are suspected of being NMEs (Stuiver et al., 2011; Kolisek et al., 2012; Yamazaki et al., 2013; Islam et al., 2014). Firstly, Cnnm2 and Cnnm4 have been localized to the basolateral membranes of mammalian DCT cells (Stuiver et al., 2011; Yamazaki et al., 2013). In fish, *cnnm3* mRNA was localized to the lateral membrane of the proximal tubule in the kidney of euryhaline mefugu (*Takifugu obscurus*) acclimated to SW and demonstrated upregulation when compared to mefugu acclimated to FW (Islam et al., 2014). It was also found that *cnnm3 m*RNA was higher in the kidneys of euryhaline gulf toadfish (*Opsanus beta*) after acclimation to hypersaline conditions (60ppt SW) (Hansen et al., 2021). Furthermore, when *cnnm3* mRNA was expressed in *Xenopus laevis* oocytes, the cellular concentration of Mg^{2+} significantly decreased, suggesting

that Cnnm3 may be involved in excretion of Mg^{2+} from cells (Islam et al., 2014). Secondly, Slc41a1 was discovered in human embryonic kidney (HEK-293) cells (Wabakken et al., 2003). The involvement of this protein in Mg^{2+} homeostasis was suggested due to structural similarities with the bacterial MgtE transporter (Smith et al., 1995). This was further supported when the introduction of *slc41a1* mRNA into a bacterial cell was able to rescue Mg^{2+}-dependent cell growth, despite absence of functional Mg^{2+} (*cobalt-resistant*) *corA*, *mgtA*, and *mgtB* (Wabbaken et al., 2003). The molecular mechanism of Na^+/Mg^{2+} exchange via Slc41a1 is proposed to be an active process involving the influx of 2 Na^+ for every 1 Mg^{2+} excreted from the cell. (Kolisek et al., 2012). Studies in the SW killifish (*Fundulus heteroclitus*) using the ^{26}Mg isotope led to the proposition that Mg^{2+} secretion may involve accumulation of Mg^{2+} in cytosolic vesicles of unknown origin in proximal tubule cells before fusing with the apical membrane to be eliminated from the cell (Chandra et al., 1997). This proposition was further supported when *slc41a1* mRNA was localized to vesicles in the apical cytoplasm of the proximal tubules in the kidneys of SW-acclimated mefugu (Islam et al., 2013). This accumulation of vesicular Mg^{2+} may be achieved by Slc41 proteins on the vesicular membrane that exchange intravesicular Na^+ for cytosolic Mg^{2+} (Islam et al., 2013; Hansen et al., 2021).

There is evidence that Slc41a1 may be present in many eukaryotic organisms (Islam et al., 2013; Kodzhahinchev et al., 2017; Arjona et al., 2019). Despite evidence that this protein may serve an evolutionarily conserved role, studies of Slc41a1 in fish are rare. In an investigation of *slc41a1* expression and localization in various tissues of SW pufferfish: torafugu (*Takifugu rubripes*) and its closely related euryhaline relative mefugu (*Takifugu obscurus*), it was found that *slc41a1* mRNA was localized to the vacuoles of the apical cytoplasm of the renal tubular cells, and that renal expression of *slc41a1* was markedly elevated upon transfer from FW

to SW, suggesting that it may be involved in secreting excess Mg^{2+} out of the kidneys and into the urine for excretion (Islam et al., 2013). Furthermore, in stenohaline FW goldfish (*Carassius auratus*), Mg^{2+}-poor water led to a marked decrease in *slc41a1* expression (Kodzhahinchev et al., 2017). A knockdown experiment in larval FW zebrafish (*Danio rerio*) was performed by Arjona et al. (2019) which led to Mg^{2+} deficiency and upregulation of other genes (*trpm6*, *cnnm2a*, *cnnm2b*, *slc41a2*) suspected to play a role in Mg^{2+} transport (Arjona et al., 2019). It was also found that when *slc41a1* was knocked down, the closely related *slc41a3* was upregulated (Arjona et al., 2019), which, combined with the ubiquitous expression of *slc41a3* mRNA in pufferfish tissues (torafugu (*Takifugu rubripes*), and mefugu (*Takifugu obscurus*)), Islam et al. (2013) suggests that their associated proteins may serve similar physiological roles in fish. Recently, Hansen et al. (2021) demonstrated that when gulf toadfish (*Opsanus beta*) were exposed to hypersaline conditions, expression of *slc41a1* and *slc41a3* mRNA were both elevated in the proximal tubules of the kidney, suggesting they may serve a role in the excretion of excess Mg^{2+} from the blood and into the urine of fish living in a hypersaline marine environment. (Hansen et al., 2021). The functional role of Slc41a2 has not been explored nearly to the same extent as Slc41a1, or even Slc41a3. It has however been identified in various vertebrate species including humans (*Homo sapiens*; e.g. Sahni et al., 2006), mice (*Mus musculus*; e.g. Goytain and Quamme, 2005) and Atlantic salmon (*Salmo salar*; e.g. Esbaugh et al., 2014) and its structure was characterized to be a plasma-membrane protein with an N-terminus-outside/C-terminus-inside 11-TM (transmembrane)-span topology, consistent with its functioning as a trans-plasma-membrane transporter (Sahni et al., 2007). Regarding the physiological role of Slc41a2, it has been shown in DT40 cells deficient in *trpm7* that Slc41a2 was able to facilitate $^{36}Mg^{2+}$ uptake in a dose-dependent manner, allowing cell growth in the absence of supplemental Mg^{2+} suggesting

a role in direct transmembrane Mg^{2+} uptake in vertebrate cells (Sahni et al., 2007). In Atlantic salmon smolts (*Salmo salar*), *slc41a2* was upregulated along with *trpm7* in response to SW acclimation in both the gills and intestines (Esbaugh et al., 2014) demonstrating a potential role in Mg^{2+} homeostasis in fish. No such evidence for Slc41a2 function in the kidneys of fish currently exists, however, in a study of the mouse (*Mus musculus*) kidney, patch-clamp analysis was unable to detect a Mg^{2+} current specific to Slc41a2 suggesting that Slc41a2 may serve a more significant role in non-renal tissues, such as the skin, gills, and intestines (Goytaine and Quamme, 2005). Overall, the physiological role of Slc41a2 is currently poorly understood, especially in fish, and I wanted to better understand the role it plays in Mg^{2+} homeostasis in the gills, intestines, and kidneys of sailfin mollies.

It is worth noting that despite evidence of ubiquitous transporter expression across various tissues in fish (e.g. Islam et al., 2013; Kodzhahinchev et al., 2017; Arjona et al., 2019), the study of Mg^{2+} transport in fish has primarily focused on the kidney (e.g. Islam et al., 2013, 2014; Hansen et al., 2021). Other osmoregulatory organs of fish such as the gills and GIT are much rarer. This is despite the fact that these organs play significant roles in ionoregulation as discussed in Chapter 1 (e.g. Evans et al., 2005 (gill); Marshall and Grosell, 2005; Bucking and Wood, 2006a ,2006b, 2007 (intestine)). It is thus probable that the regulation of these transporters, follows different patterns when exposed to varying levels of environmental Mg^{2+} in these tissues. Kodzhahinchev et al. (2017) demonstrated in stenohaline FW goldfish (*Carassius auratus*) that exposure to reduced environmental Mg^{2+} led to a significant decrease in *slc41a1* expression in the intestine, with no significant changes observed in the gills or kidneys, proposing that this may have been a mechanism to preserve dietary Mg^{2+} assimilation when environmental sources were depleted (Kodzhahinchev et al., 2017). The lack of significant

change in *slc41a1* expression in the gills and kidneys also led to a proposition that the observed changes in the intestine may have provided satisfactory compensation to Mg^{2+} homeostasis, although they cautioned that analysis of total Mg^{2+} intake may be necessary to validate this claim (Kodzhahinchev et al., 2017). Arjona et al. (2019) demonstrated the dependence of branchial *slc41a1* expression on environmental Mg^{2+} concentration in stenohaline FW zebrafish (*Danio rerio*) when decreasing ambient Mg^{2+} led to a significant increase in *slc41a1* expression in the gills suggesting a potential role in absorption of environmental Mg^{2+} across the gills of zebrafish (Arjona et al., 2019). This contrasted with the findings of Kodzahinchev et al. (2017) in goldfish (*Carassius auratus*) where no changes in branchial *slc41a1* expression were observed during restriction in environmental Mg^{2+} (Kodzhahinchev et al., 2017). Interestingly, neither study observed changes in renal *slc41a1* expression in response to environmental Mg^{2+} restriction (Kodzhahinchev et al., 2017; Arjona et al., 2019). Arjona et al. (2019) did not investigate the role of the intestine in Mg^{2+} homeostasis but based on their findings in the gills and kidneys, it is possible that Slc41a1 in both the gills and intestines plays a role in Mg^{2+} homeostasis. The study of Slc41a1 in the gills and intestines of fish has not been quantitatively investigated in the context of salinity acclimation over time in euryhaline fish, and no studies so far have investigated the regulation of other transporters involved in Mg^{2+} homeostasis in the gills and intestines of euryhaline fish during salinity acclimation.

Due to the scarcity of data on the role of Slc41a1 in Mg^{2+} homeostasis in the gills, kidneys, and intestines of fish, the purpose of my study was to expand the current state of knowledge on how Slc41a1 and related transporters (Slc41a2, Cnnm3, Trpm7, NKA) are regulated in response to increased salinity in the environment in the previously unstudied sailfin molly (*P. latipinna*). I also wanted to understand the correlation of transporter expression and

physiological factors such as Mg^{2+} concentrations of plasma. To do this I compared FW-acclimated individuals and SW-acclimated individuals at 1, 7, 14, and 30 days of acclimation to 35ppt SW.

Specifically, I first wanted to determine the genetic expression profile of *slc41a1*, *slc41a2*, *cnnm3*, and *trpm7* in a variety of tissues within the sailfin molly when fully acclimated (>30days of exposure) to 0ppt FW or 35ppt SW. Based on the findings of previous studies (Islam et al., 2013; Kodzhahinchev et al, 2017; Arjona et al., 2019), I hypothesized that *slc41a1*, *slc41a2*, *cnnm3*, and *trpm7* would be ubiquitously expressed across all observed tissues although I predicted that the presence of mRNA for each transporter would vary between tissues, presumably being highest in more metabolically active tissues such as the brain, liver, kidneys and heart, as was demonstrated for *slc41a1* in zebrafish (*Danio rerio*, Arjona et al., 2019), as well as *slc41a1, slc41a2, slc41a3* and *cnnm3* in mefugu and torafugu (*Takifugu obscurus*, *Takifugu rubripes*, Islam et al., 2013, 2014). I also hypothesized that there would be a difference in transporter expression in the tissues of fish acclimated to FW when compared to fish that had been acclimated to SW, and that this expression would be tissue dependent. Specifically, I predicted that genes that code for proteins thought to be involved in Mg^{2+} excretion (*slc41a1*, *slc41a2*, *cnnm3*) would be upregulated in the osmoregulatory tissues of SW- acclimated fish, whereas genes that code for proteins thought to be involved in Mg^{2+} absorption (*trpm7*) would be downregulated in SW-acclimated fish.

I then wanted to determine how the time course of acclimation to environmental salinity would affect genetic expression by comparing the expression of *slc41a1, slc41a2*, *cnnm3*, *trpm7*) and *nka* paralogs between fish acclimated to 0ppt FW or 35ppt SW over the course of 30 days using qPCR. I also wanted to measure changes in plasma Mg^{2+} concentration using the Ion-

Selective Microelectrode technique (ISME) during the acclimation process to get a better understanding of the connection between transporter expression and the amount of Mg^{2+} in the plasma.

Based on my current understanding of my genes of interest, and the function of the gills, intestines, and kidneys in ionoregulation in fish, I established predictive cellular models to represent each tissue (Figures 2, 3, 4).

In the gills of FW-acclimated fish, the levels of Mg^{2+} within the plasma are much higher than those of the surrounding water, meaning that Trpm7 must be localized to the basolateral membrane, as an apical position would drive passive ion loss and be physiologically disadvantageous. I also predicted that Nka isoforms would be basolateral, as this has been demonstrated in a wide variety of fish (reviewed by Evans et al., 2005). Mg^{2+} that enters branchial cells passively through Trpm7 is exchanged by Cnnm3 at the lateral membrane (as observed in the renal cells of mefugu (Islam et al., 2014)) for $2Na^{+}$ in the lateral membrane space due to the activity of basolateral Nka isoforms, where it would reenter the plasma. This would function to conserve and/or prevent magnesium loss. Finally, Slc41a1 is thought to serve an absorptive role within the gills (Arjona et al., 2019), but it has not been localized in the gills of an adult fish, making positioning it within this model difficult. Finally, I suspected Slc41a2 to be localized similarly to Slc41a1 and to also serve an absorptive role in the gills due to their genetic similarity (Figure 2). Therefore, as the ionic gradient changes during SW acclimation, and the gills shift from net absorption to net excretion, I expect to see a decrease in the expression of *trpm7*, *cnnm3*, *slc41a1*, and *slc41a2*.

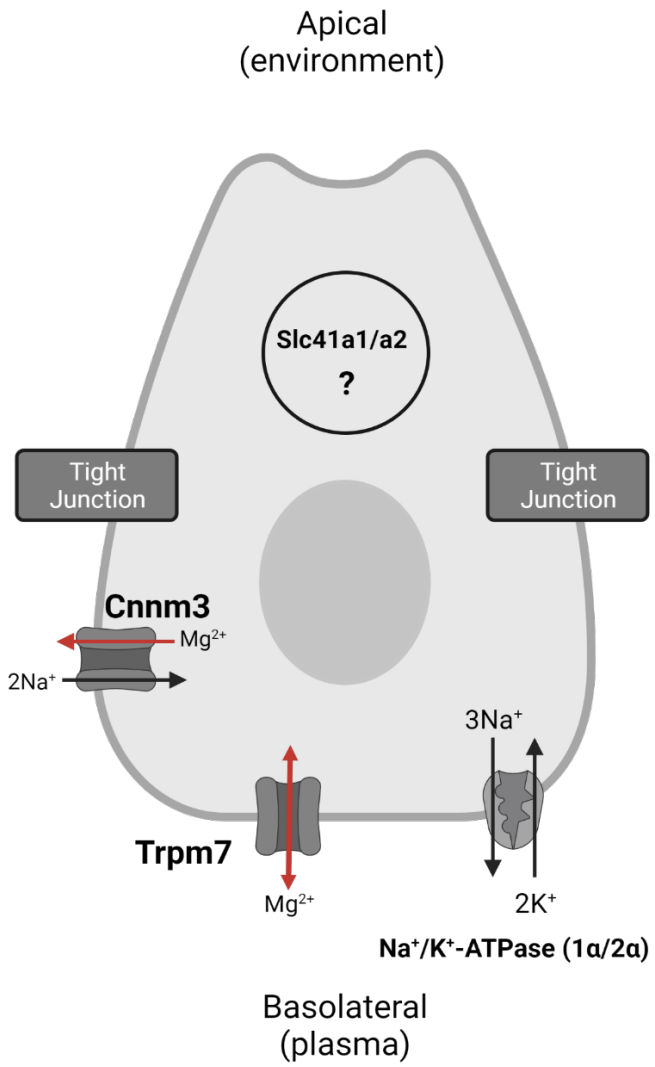

Figure 2: Proposed cellular model of branchial Mg^{2+} transport in *P. latipinna*. Mg^{2+} enters the cell passively through a channel formed by Trpm7 at the basolateral membrane. Nka isoforms at the basolateral membrane actively exchange $2K^{+}$ into the cell for $3Na^{+}$ out of the cell. The transmembrane Na^{+} gradient established by NKA isoforms is then used by Cnnm3 on the lateral membrane to remove Mg^{2+} from the cell in exchange for $2Na^{+}$. Slc41a1/a2 both serve a role in Mg^{2+} absorption, although its exact position within the cell is unknown. Created with BioRender.com

The intestines are thought to be the dominant site of Mg^{2+} absorption in FW acclimated fish (e.g. Bucking and Wood, 2007; reviewed by Wood and Bucking, 2011), leading me to hypothesize that there would be genetic changes within the intestines during SW acclimation. Sadly, the intestine has been largely overlooked as an ionoregulatory organ in fish, providing scant evidence to base my predictions on. For the most part, I expected to see genetic regulation like those in the gills, however, *slc41a1* has been shown to decrease during environmental Mg^{2+} restriction in goldfish, suggesting that it may serve an excretory role in this tissue (Kodzhahinchev et al., 2017). Based on the available evidence, I proposed a model where basolateral Nka creates extracellular Na^{+} gradients used by laterally localized Cnnm3 in exchange for intracellular Mg^{2+}. Once in the intermembrane space, Mg^{2+} would travel down its gradient and into the plasma. Apically localized Trpm7 facilitates the passive diffusion of luminal Mg^{2+} into enterocytes. Finally, Slc41a1/a2 on the membranes of apically associated vacuoles remove cytosolic Mg^{2+} in exchange for vacuolar Na^{+} before fusing with the apical membrane to excrete Mg^{2+} back into the lumen (Figure 3). Based on my model, I predicted that SW acclimation would lead to downregulation of *trpm7* and *cnnm3*. Since less Mg^{2+} would be entering the cell, the need for excretion should also decrease, and therefore I also expected to see downregulation of *slc41a1/a2*.

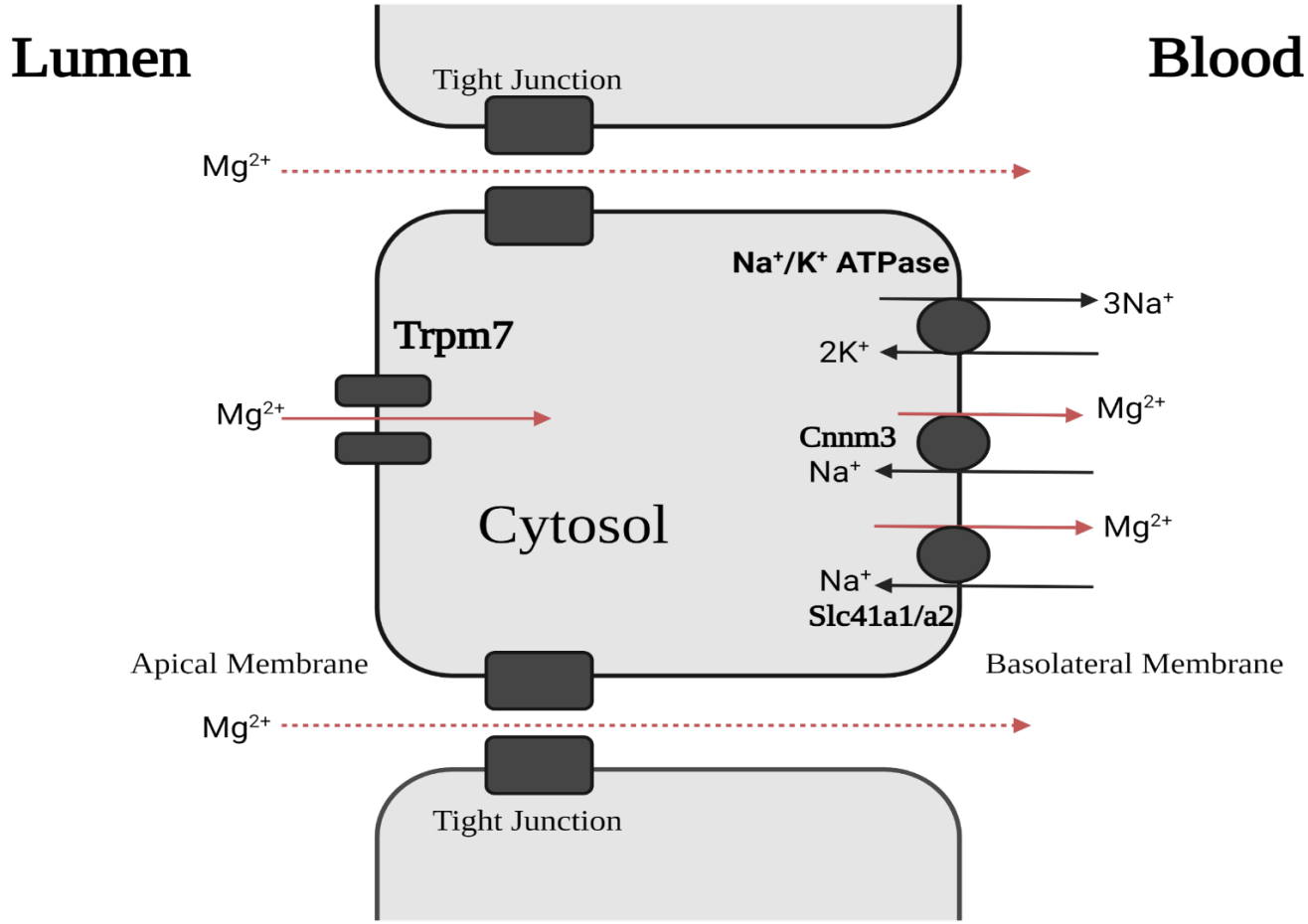

Figure 3: Proposed cellular model of intestinal Mg^{2+} transport in *P. latipinna.* Mg^{2+} in the lumen enters the cell through apically localized Trpm7 channels. Nka isoforms at the basolateral membrane actively exchange 2 extracellular K^+ for 3 intracellular Na^+. The transmembrane Na^+ gradient established by Nka isoforms is then used by Cnnm3 on the lateral membrane to remove Mg^{2+} from the cell in exchange for $2Na^+$ where it is absorbed into the plasma. Slc41a1/a2 facilitate Mg^{2+} entry into apically associated vesicles in exchange for Na^+, eventually fusing with the apical membrane to remove Mg^{2+} from the cell. Created with BioRender.com

The kidneys of FW acclimated fish are responsible for the removal of excess water and the reabsorption of ions from the preurine. During SW acclimation, however, I expected to see a shift from net ionic reabsorption to net secretion. I hypothesized that this would occur through changes at the genetic level. I proposed a cellular model in which Cnnm3 on the lateral membrane (as shown by Islam et al., 2014) exchanges the extracellular Na^+ produced by Nka activity at the basolateral membrane for intracellular Mg^{2+}, facilitating entry into the blood. Slc41a1 has been localized to apically associated vacuoles in the kidneys of mummichog (Chandra et al., 1997) and mefugu (Islam et al., 2013) and has been observed to upregulate in the presence of excess dietary Mg^{2+} (Kodzhahinchev et al., 2017) and during SW acclimation (Islam et al., 2013; Hansen et al., 2021) suggesting an excretory role, however it should be noted that elevating dietary Mg^{2+} led to downregulation of *slc41a1* in the kidneys of zebrafish (Arjona et al., 2019). Finally, due to its position in mammalian models (e.g. Schlingmann et al., 2002; Giménez-Mascarell et al., 2018), I positioned Trpm7 at the apical membrane to facilitate Mg^{2+} reabsorption from the preurine (Figure 4). Based on my current understanding of these transporters, I predicted that *slc41a1* (and by association, *slc41a2*) would increase to aid in Mg^{2+} excretion. I further predicted to see decreased *trpm7* and *cnnm3* expression as a mechanism to decrease the movement of Mg^{2+} from the preurine back into the blood. Finally, I hypothesized that plasma Mg^{2+} would change during SW acclimation, predicting that levels would increase initially before being normalized.

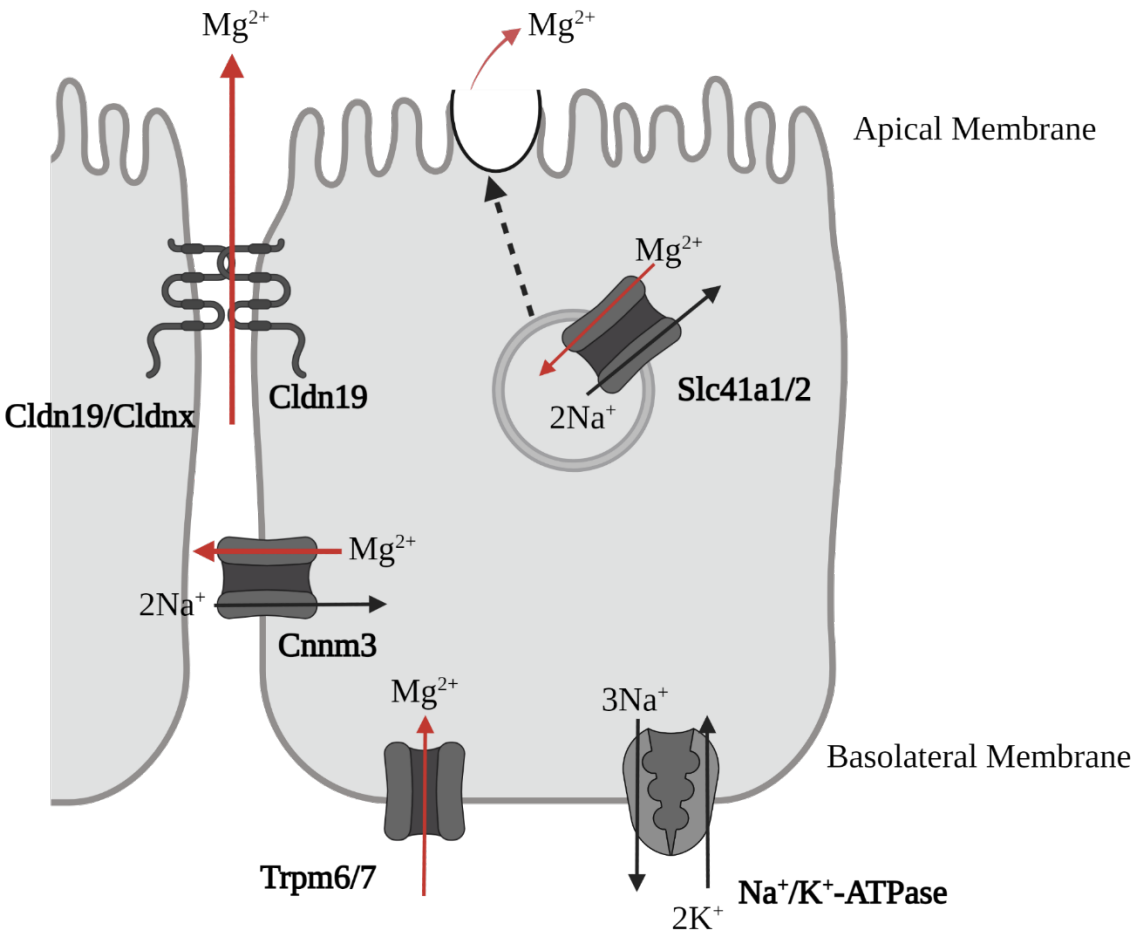

Figure 4: Proposed cellular model of renal Mg^{2+} transport in *P. latipinna*. Basolateral Nka isoforms actively pump intracellular Na^{+} into the plasma where it is exchanged for intracellular Mg^{2+} by Cnnm3 on the lateral membrane. Extracellular Mg^{2+} then moves down its concentration gradient, ultimately ending up in the plasma. At the apical brush border, Trpm7 forms a channel to facilitate Mg^{2+} reabsorption from the preurine. Finally, Slc41a1/a2 localized to the plasma membrane of apically associated vacuoles exchange intracellular Mg^{2+} for Na^{+} before eventually fusing with the apical membrane and excreting the accumulated Mg^{2+} into the preurine. Created with BioRender.com

2.2 : Materials and Methods

2.2.1 : Animal Husbandry

Sailfin mollies were housed in static 37.85L glass aquaria (approximately 20 fish per tank) containing dechlorinated Toronto city tap water and supplied with biological filters. Sea salt mixture (Instant Ocean; PetSmart) was then gradually added to half of the tanks, raising the salinity by ~12ppt/day as monitored by a refractometer until the desired salinity of 35ppt was achieved. Increases in environmental salinity were incremental to minimize any potential stress on the animals. The water temperature was maintained at ~23ºC using standard tank heaters and monitored daily with a thermometer for accuracy. Water quality was monitored daily with an API FW/ SW master test kit (Big Al's) following the manufacturer's instructions, and 30% water changes occurred weekly to eliminate any accumulated waste within the tanks. The average Mg^{2+} concentration of Toronto city tap water is $3.50x10^{-1}$ mmol/L and the pH of Toronto city tap water is 7.5 (City of Toronto, 2021). All experiments were conducted according to approved York Animal Use protocols (2017-R3).

2.2.2 : Tissue Sampling

2.2.2.1 : Tissue Expression Analysis

The purpose of this experiment was to confirm the presence of RNA for *slc41a1*, *slc41a2*, *cnnm3*, and *trpm7* in *P. latipinna*. Sailfin mollies acclimated to 0ppt FW (n=3) or 35ppt SW (n=3) were sacrificed using a lethal dose (250mg/L) of tricaine methanesulfonate (MS-222). A spinal transection was then performed before extracting the gills, heart, liver, intestines (divided into anterior and posterior segments), brain, kidneys, skin, and white muscle. Extracted tissues were encased in aluminum foil and immediately snap-frozen on dry ice and stored at -

80°C for later use. To prevent cross contamination, dissecting equipment was kept clean throughout the dissecting process and sterilized in 70% ethanol to remove any trace amounts of tissue or debris.

2.2.2.2 : Impact of Salinity on Transporter Expression

To determine the impact of the environment on transporter expression, fish were acclimated to FW (0 ppt), and full-strength SW (35 ppt). 5 fish were randomly sampled, and tissues (kidneys, gills, anterior and posterior intestines) were extracted after 1 day, 7 days, and 30 days of acclimation to 35 ppt SW, using the expression of FW-acclimated fish as a control. Tissues were snap frozen on dry ice and stored at -80°C for later use.

2.2.3 : RNA Extraction

The protocol for RNA extraction and isolation using TRIzol was adapted from the manufacturer's instructions. Tissues (50-100mg) were homogenized using glass homogenizers in 0.5 mL of TRIzol reagent and the resulting solutions were aliquoted into 1.5mL sterile microcentrifuge tubes. Tubes were incubated on ice for 5-10 minutes to ensure proper dissociation of proteins had occurred. 100µL of chloroform was then added to each tube, briefly vortexed to ensure complete incorporation into the sample, and incubated on ice for 2-3 minutes. samples were centrifuged at 4°C and 12000xg for 15 minutes. The top, aqueous phase containing the RNA was then transferred from the original centrifuge tube and into another sterile 1.5mL sterile microcentrifuge tube. The remaining DNA and protein contents were then discarded. RNA was isolated by adding 250µL of isopropanol to each sample. Samples were then incubated on ice for 10 minutes, briefly vortexed to ensure proper mixing, and then centrifuged for 10 minutes at 4°C and 12000xg. Precipitated RNA formed a small, white, gel-like pellet at the

bottom of the tube. Supernatant was discarded, leaving only the RNA pellet, which was subsequently washed with 0.5mL of 75% ethanol, vortexed briefly, and 5 minutes at 4°C and 7500xg. Supernatant was discarded and the pellets were air dried before resuspension in 20-50µL of sterile, molecular grade water.

RNA quality was then checked both on a non-denaturing 2% gel stained with ethidium bromide and using a microplate reader (BioTek Syngergy HT machine (BioTek Instruments Inc, Winooski, Vermont, USA)) to assess the 260/280 absorption ratio. A sample was of acceptable quality if two distinct bands were present on the gel, and the 260/280 ratio registered a value between 1.8 and 2.2. Samples that did not meet these quality standards were not reverse transcribed into cDNA for use in qPCR, instead being discarded and replaced with new samples that met my standards.

2.2.4 : cDNA Synthesis

400ng of RNA was then reverse transcribed into 10 µL of cDNA using a GoScipt™ reverse transcription kit by PROMEGA following manufacturer's instructions whereby RNA was combined with 0.5µg of Primer ($Oligo(dT)_{15}$), and nuclease-free water to a volume of 5µL in a sterile 200µL PCR tube, mixed briefly and heated to 70ºC in a heating block for 5 minutes before being chilled in an ice bath for 5 minutes. In another sterile PCR tube, a reverse transcription reaction mix (15µL total volume) containing 4.0µL of GoScript™ 5x reaction buffer, 3.2µL of 25mM $MgCl_2$, 1µL of PCR nucleotide mix (containing 0.5mM each dNTP), 1 µL of GoScript™ reverse transcriptase, and 5.2 µL of nuclease free water. The contents of the two tubes were then combined, gently mixed with a pipette, and placed in a heating block. cDNA was annealed at 25ºC for 5 minutes, extended at 42ºC for 60 minutes, and the reaction was inactivated by incubating at 70ºC for 15 minutes. cDNA samples were subsequently diluted 1:3

with molecular grade water to a final working concentration of 10ng/µL. Samples were stored at -21°C for later use.

2.2.5 : Primer Design and Optimization

Primers were designed for 6 test genes: *slc41a1*, *slc41a2*, *cnnm3*, *trpm7,* and 2 *nka* paralogs *nka-1α* and *nka-2α* as well as 3 control genes: *18s*, *rpl-7*, and *rpl-17* in sailfin mollies (Table 1). Control genes were selected based on literature involving the transfer of fish from FW to SW (e.g. *18s*, Kodzhahinchev et al., 2017; *rpl-7*, Ellis et al., 2019; *rpl-17*, Robledo et al., 2014). Coding sequences were retrieved using the Ensembl™ genetic database. In the event of multiple isoforms for one specific gene, all isoforms were aligned using the CLUSTALW algorithm, and primers were specifically designed for novel regions within the coding sequences of the target gene. Primer pairs for genes were generated to amplify a target sequence in the 100-200BP range using Primer 3. Primer sequences were then BLASTed against other genes from *P. latipinna* in the NCBI database to test for any unwanted secondary structures or nonspecific products.

Primer validity was tested by PCR reaction using pooled cDNA generated from various tissues of sailfin mollies (see ubiquitous expression of Mg^{2+} transporters in sailfin mollies for a full list of tissues) acclimated to 0ppt FW and 35ppt SW using the following cycling protocol for Taq polymerase adapted from the manufacturer's instructions:

1) Initial denaturation: 95°C for 3m
2) Denaturation: 95°C for 30s
3) Annealing: (primer-specific temperature) for 30s
4) Extension: 72°C for 1m

Repeat step 2-4 for 40 cycles

5) Final Extension: 72°C for 10m

PCR reactions were then run on a 2% TAE agarose gel stained with redsafe gel dye, at 70V and 40.0A for 40 minutes before being imaged under UV light. PCR products that generated a single clean band in the expected size range were then purified using a GeneJET PCR Purification kit (Thermofisher Scientific) following the manufacturer's protocol whereby a 1:1 volume of binding buffer was added to the completed PCR mixture. If the resultant solution was yellow, it was at an optimal pH and the reaction was continued. A 1:2 volume of 100% isopropanol was then added to the mixture from step 1 and mixed thoroughly (optional step for DNA fragments ≤500bp). Up to 800µL of the solution from step 2 were then added to purification columns (included in the kit) and centrifuged at room temperature for 1 minute at 12000xg, the flow-through was discarded. 700µL of wash buffer (diluted with ethanol as per manufacturer's instructions) were then added to the column and centrifuged at room temperature for 1 minute at 12000xg. The flow-through was again discarded. To prevent inhibition of downstream reactions, all residual ethanol was removed from the column by centrifuging the empty column again (see step 4). Flow-through was again discarded. The purification tubes were then transferred to clean RNAse- and DNAse-free microcentrifuge tubes and 20µL of elution buffer (minimum recommended amount to account for low DNA quantities in the samples) was added to the center of each purification membrane before being centrifuged at room temperature for 1 minute at 12000xg. Purified samples were stored at -20ºC until they were sent for sequencing. The concentrations of the purified DNA samples were measured spectrophotometrically with a BioTek Syngergy HT machine (BioTek Instruments Inc, Winooski, Vermont, USA), and samples were prepared according to the specifications set by Sick Kids Sanger sequencing lab:

7µL of purified cDNA (10ng total DNA) added to PCR tubes and mixed with 50ng of custom primer template (Table 1). Returned sequences were then BLASTed in the NCBI database (https://blast.ncbi.nlm.nih.gov/) to confirm that the designed primers amplified the intended genes. Primers that met these criteria were then used in qPCR.

Table 1: Primer Sequences and Annealing Temperatures for Test and Control Genes

Target Gene	Primer Sequence (5'-3')	Annealing Temperature (°C)
1. slc41a1	F: GACCCCAACCTTCCTCAATTCT R: CACCACAATCTCCGACCTCT	60
2. slc41a2	F: AGCTGTAGCAGCCGTCATAC R: TTCGACCCCACAATTACCCC	60
3. cnnm3	F: TGAAGAAGCGTGGGAGCAT R: ACAGCAGGCTCAAGTTTACGG	60
4. trpm7	F: GCTCACCTTTACACTCTACT R: AAAATGGCTGCATCAGTTGC	62
5. nka-1a	F: GCCCCGAAACCCCAAAACAG R: TGTAAAGAACCCAGCTGAGG	60
6. nka-2a	F: AGAGGAACACTGGCGATGAT R: GGAGGGTCGTCTCATCTTTGA	62
7. 18s	F: GGCCGTTCTTAGTTGGTGGA R: TCAATCTCGGGTGGCTGAAC	60
8. rpl-7	F: GTCTCGTATGGCTCGCAAAG R: TCAGCTTGACAAACACACCG	60
9. rpl-17	F: CGCAAAGCCAACAAGTACCT R: AACTCTGCGCTTTTCTTGGG	60

2.2.6 : qPCR Analysis of Gene Expression

All qPCR assays were conducted according to the MIQE guidelines (Bustin et al., 2010). 10µL reactions containing 5 µL Powertrack SYBR green qPCR master mix (Thermofisher Scientific), 500nM of forward and reverse primers (see table 1 for sequences), 10 ng of cDNA, and molecular grade water were pipetted into 96-well plates in technical duplicates. Sealed plates were then centrifuged for 1 minute and loaded into a Roche light cycler 96. The program for qPCR was as follows: enzyme activation at 95°C for 2 minutes followed by 40 cycles of amplification using a denaturation temperature of 95°C for 5 seconds and an annealing/extension step at a primer-specific temperature (Table 1) for 30 seconds. Amplification was followed by a dissociation step as specified by the manufacturer. Dissociated products were analyzed using Roche LC96 software to confirm the amplification of one specific product in the reaction, and to confirm that the cDNA was of acceptable quality. cDNA was of acceptable quality when technical replicates could consistently amplify within half of a cycle, and when dissociation curves did not contain any bumps that would suggest degradation. Samples of cDNA that did not meet these requirements were discarded and new cDNA was created to replace it (see section 3.4). A 10-fold dilution series was used to generate a standard curve to determine the efficiency of each primer. A negative control containing molecular grade water in place of cDNA was utilized to confirm the absence of primer-dimers and a non-reverse transcription control containing 10 ng of randomly pooled RNA from a variety of tissues and treatments was used on non-intron spanning targets to confirm the absence of genomic DNA amplification. Ct values of each sample were averaged, and relative expression of each test gene was normalized to the geometric average of the corresponding Ct values for *18s*, *Rpl-7*, and *Rpl-17* using the Pfaffl method:

$$rrrrrrrrr = \frac{(EE_{ttttttttttt})^{\Delta CCtt(ccccccttttcccc-ssttsssscctt)_{ttttttttttt}}}{(EE_{ttttrrttttttccccttt})^{\Delta CCtt(ccccccttttcccc-ssttsssscctt)_{ttttrrttttttccccttt}}}$$

where E represents the efficiency of the reaction, expressed as 1+ efficiency as a decimal (i.e. a 100% efficient reaction would give an E value of 2), ΔCt represents the difference in cycles it takes for the sample to reach a threshold fluorescence reading between the control and test treatments, expressed as the mean of technical duplicates, and the ratio represents the change in expression of the target gene compared to the control treatment (Pfaffl, 2001).

2.2.7 : Determining Plasma Magnesium Concentration

An ion-selective microelectrode filled with a selectophore specific for magnesium (magnesium ionophore II; Sigma-Aldrich Co), was used to estimate the magnesium concentration in plasma pooled from 3 fish. Serial dilutions were created for plasma samples using distilled water, (1 g ml^{-1}, 0.1 ml^{-1} and 0.01g ml^{-1}) to generate a standard response curve. All samples were then placed under mineral oil and the magnesium concentration was quantified using ion selective micro-electrodes (ISME) (as described in Donini and O'Donnell 2005). The electrodes were calibrated using 0.5, 5, 10 and 100mM $MgCl_2$ solutions and the concentration was calculated using the following equation:

$a^h = a^c \times 10^{(\Delta V/S)}$,

where a^h is the ion concentration in the sample, a^c is the ion concentration in the calibration solution, ΔV is the voltage difference between the two and S is the slope measured in response to a 10-fold change in ion concentration (using the two calibration solutions most closely bracketing the sample being measured).

2.2.8 : Phylogenetic Analysis of Target Genes

Coding sequences for *slc41a1*, *slc41a2*, *cnnm3*, and *trpm7* were obtained for all fish species from Ensembl genome browser. Sequences were aligned using the MUSCLE algorithm in MEGA 11 software (Tamura et al., 2021) and phylogenetic trees were generated using the maximum likelihood method using 500 bootstrap replicates. The maximum likelihood method was chosen over maximum parsimony as it provided a model derived from statistical probability instead of the fewest number of changes. I chose to run 500 bootstraps based on the phylogenetic analysis performed by Kodzhahinchev et al. (2017) in *C. auratus*.

2.2.9 : Statistics

Statistical analyses were carried out using Sigmaplot 14.5 (Systat). All qPCR data was tested for normality using a Shapiro Wilk's test. Samples that did not pass normality were logarithmically transformed to become normal. Once normalized, data was tested for outliers using a Grubb's test. If an outlier was identified using this test, it was removed from the subsequent analysis. Data was also tested for homogeneity of variance using a Brown-Forsythe test. If data passed both normality and homogeneity of variance, ANOVA tests were carried out as follows: Effect of acclimation to 35ppt SW on transporter expression within the target tissues, as well as the concentration of Mg^{2+} in the plasma were subjected to a one-way ANOVA test, and tissue expression profile experiments were subjected to a one-way repeated measures ANOVA test. Tukey's posthoc test for multiple pairwise comparisons was used on data that was statistically significant. Data that did not pass either normality or homogeneity of variance was tested for statistical significance using ANOVA on ranks ($p<0.05$ was considered significant for all tests)

2.3 : Results

2.3.1 : Expression Profiles of Mg^{2+} Transporters in 0ppt FW and 35ppt SW

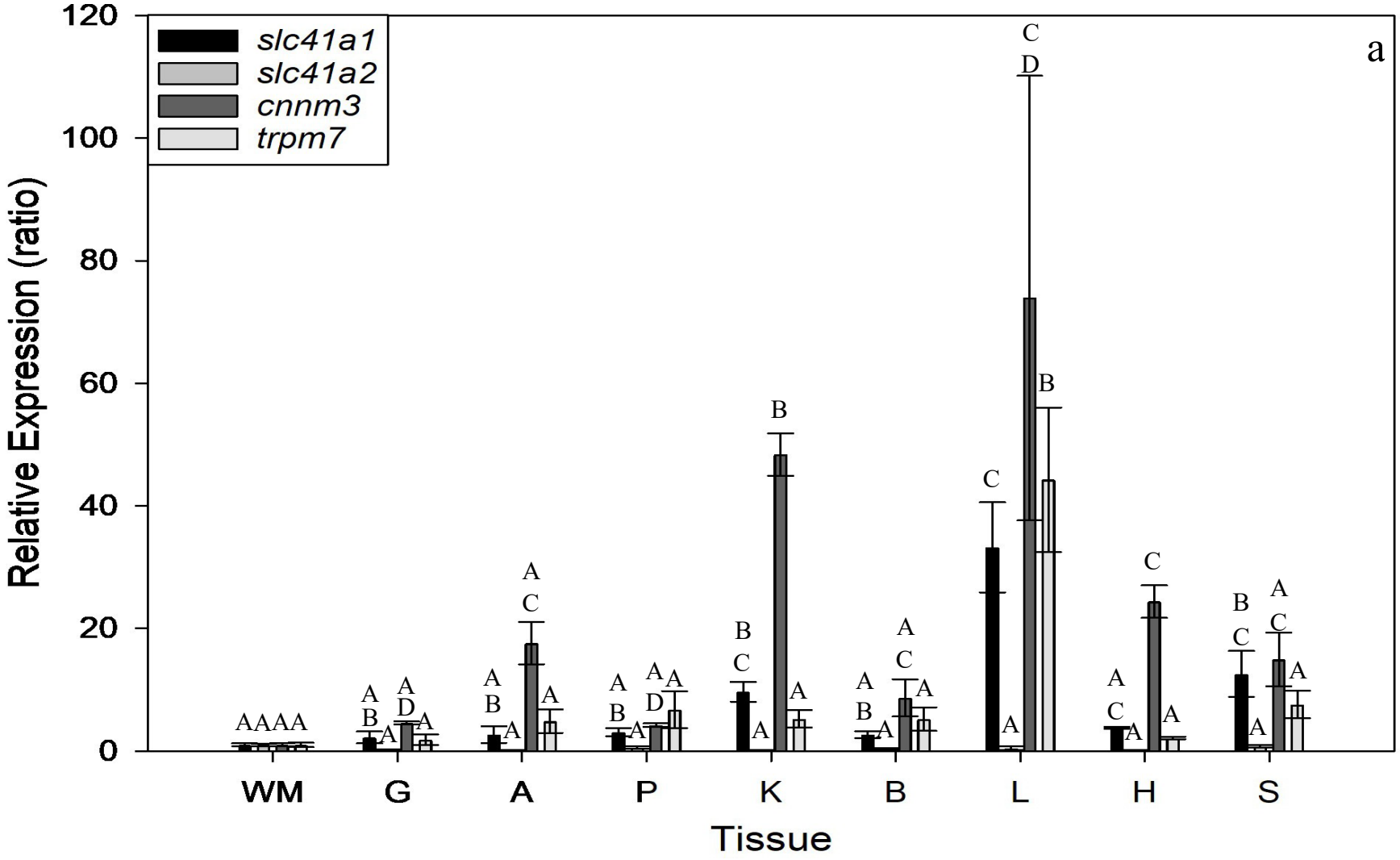

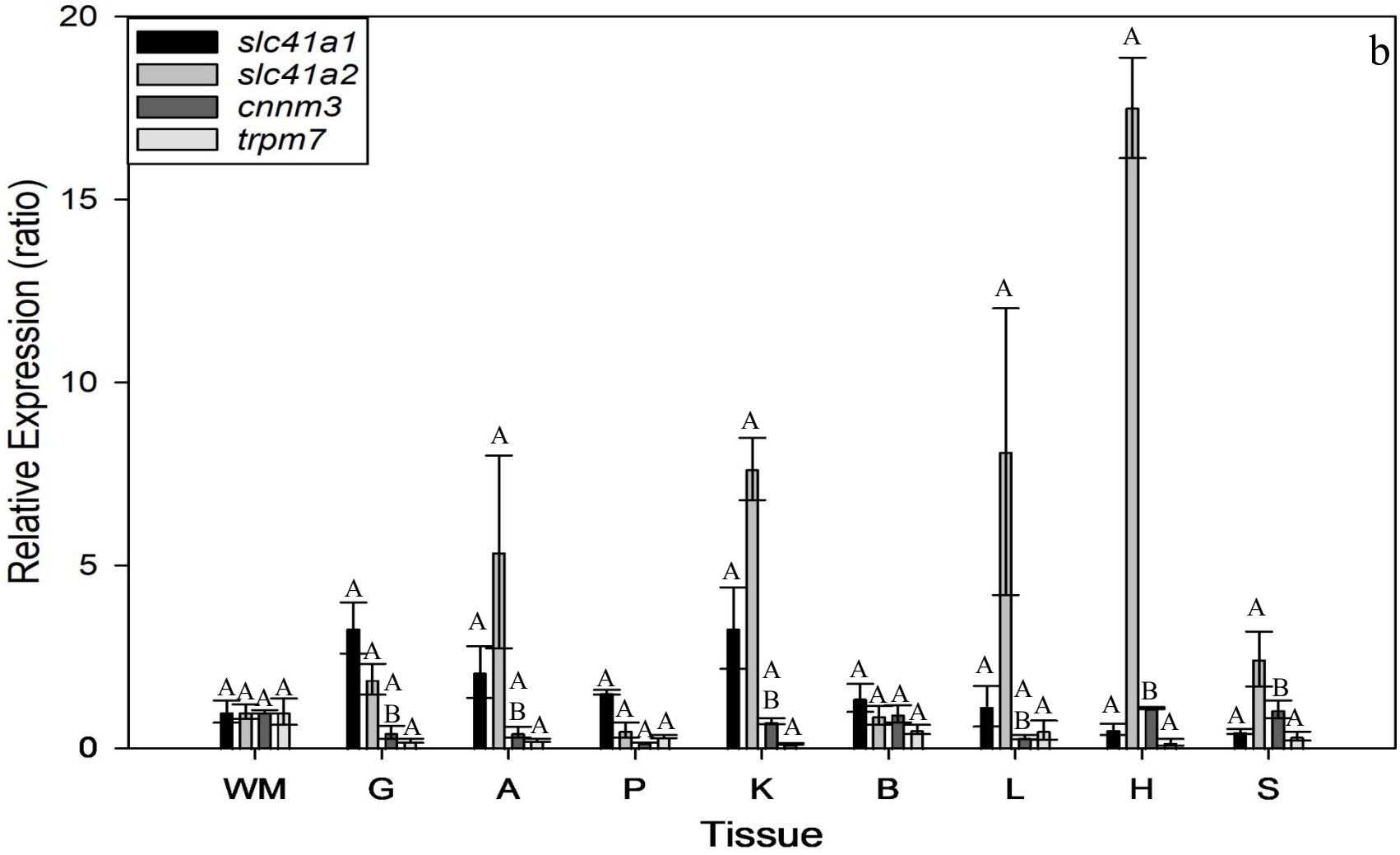

Figure 5: Expression profile of Mg^{2+} transporters in white muscle (WM), gill (G), anterior intestine (A), posterior intestine (P), kidney (K), brain (B), liver (L), heart (H), and skin (S) of *P. latipinna* acclimated to 0ppt FW (a), and 35ppt SW (b) for 30 days (n=3). Bars represent the mean ±SEM of the expression ratio using white muscle as a neutral control (i.e. set to 1). Statistical significance was tested within each gene using a one-way repeated measures ANOVA followed by Tukey's post hoc test for multiple pairwise comparisons. Within each gene bars that do not share the same letter are significantly different from one another ($p<0.05$). Comparisons between genes were not made.

Expression of *slc41a1*, *slc41a2*, *trpm7*, and *cnnm3* was observed in all tested tissues of *P. latipinna* exposed to 0ppt FW and 35ppt SW for 30 days (Figures 5a and 5b, respectively). In FW-acclimated fish, *slc41a1* expression was highest in the liver, kidneys, and skin ($p=0.001$). Although ANOVA testing of SW-acclimated individuals confirmed statistical significance between the different tissues ($p=0.024$), post-hoc analysis was unable to determine where the differences were within the dataset. Similarly, *slc41a2* expression was significantly different between the sampled tissues under both salinity conditions ($p= 0.043$ and $p= 0.027$ for FW and SW, respectively), however post hoc analysis was again unable to determine where these differences were in either treatment. Expression of *trpm7* in individuals acclimated to FW was highest in the liver, with no significant differences in expression throughout the other tested tissues ($p=0.002$; Figure 5a). Interestingly, I did not observe significant tissue dependent *trpm7* expression in SW acclimated fish ($p=0.306$) (Figure 5b). *cnnm3* expression in FW acclimated fish was highest in the kidneys, heart, and liver ($p<0.001$; Figure 5a). In individuals acclimated to 35ppt SW, expression was more consistent across tissues, with differences only being observed between the posterior intestine and the heart and skin ($p=0.008$; Figure 5b).

2.3.2 : Influence of Environmental Salinity on Plasma Mg^{2+} Concentrations

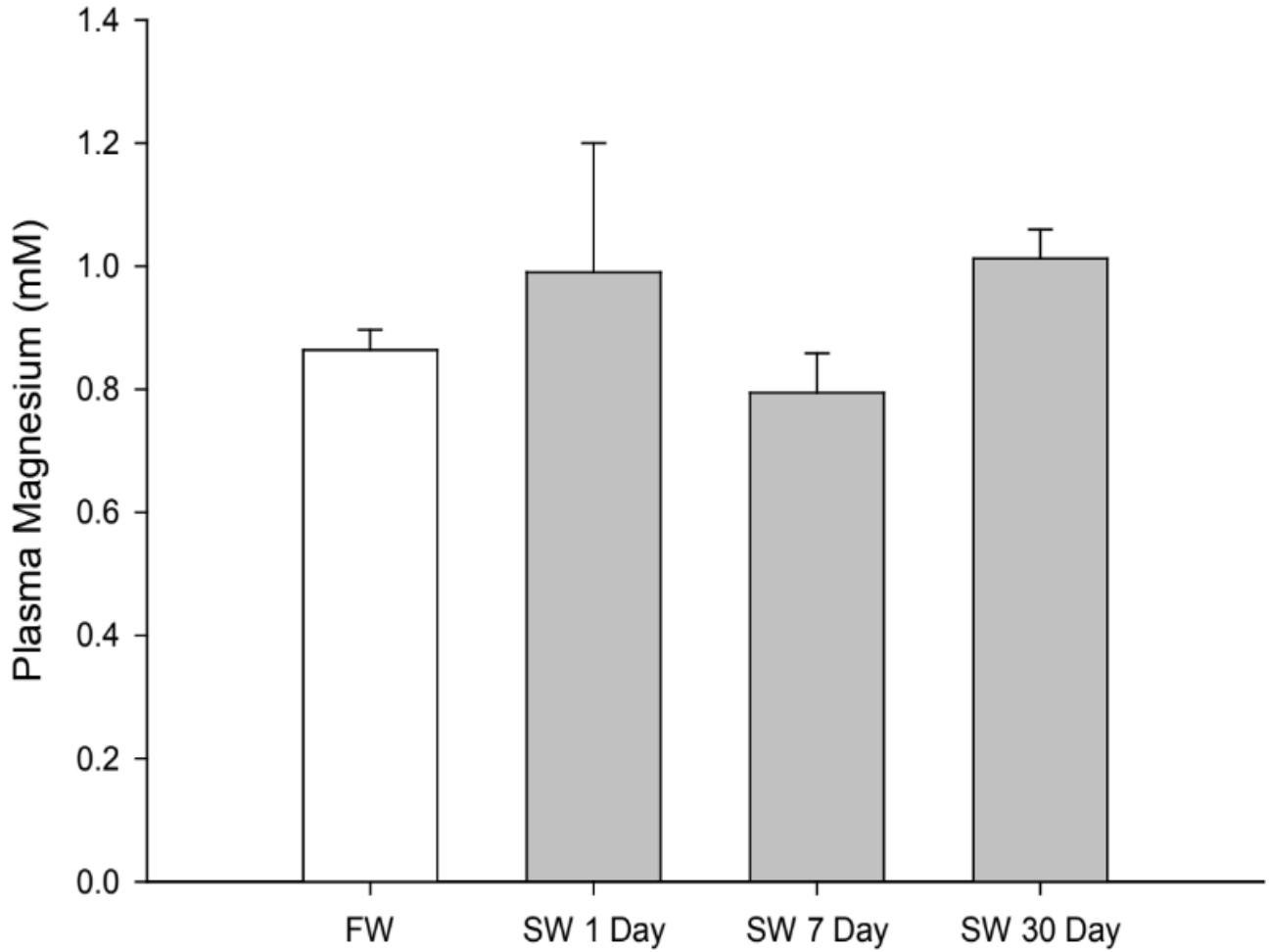

Figure 6: Plasma Mg^{2+} concentrations of *P. latipinna* acclimated to 35ppt SW for 1, 7, and 30 days on pooled samples of plasma (n=4) measured using the Ion-Selective Microelectrode Technique (ISME). Bars represent the mean + SEM. Raw data did not pass equal variance testing, therefore ANOVA on ranks was performed ($p>0.05$).

NOTE: Calcium concentrations were also tested and revealed no differences in plasma concentrations. This was done to confirm any changes were not being driven by calcium detection by the magnesium ionophore.

The median concentrations of Mg^{2+} in the plasma of *P. latipinna* throughout the treatment groups exposed to 35ppt SW did not change significantly ($p=0.14$) when compared to 0ppt FW controls at any time point. The average plasma value was 0.9 mM±0.12 across all timepoints and treatments (Figure 6).

2.3.3 : Influence of Environmental Salinity on Transporter Expression

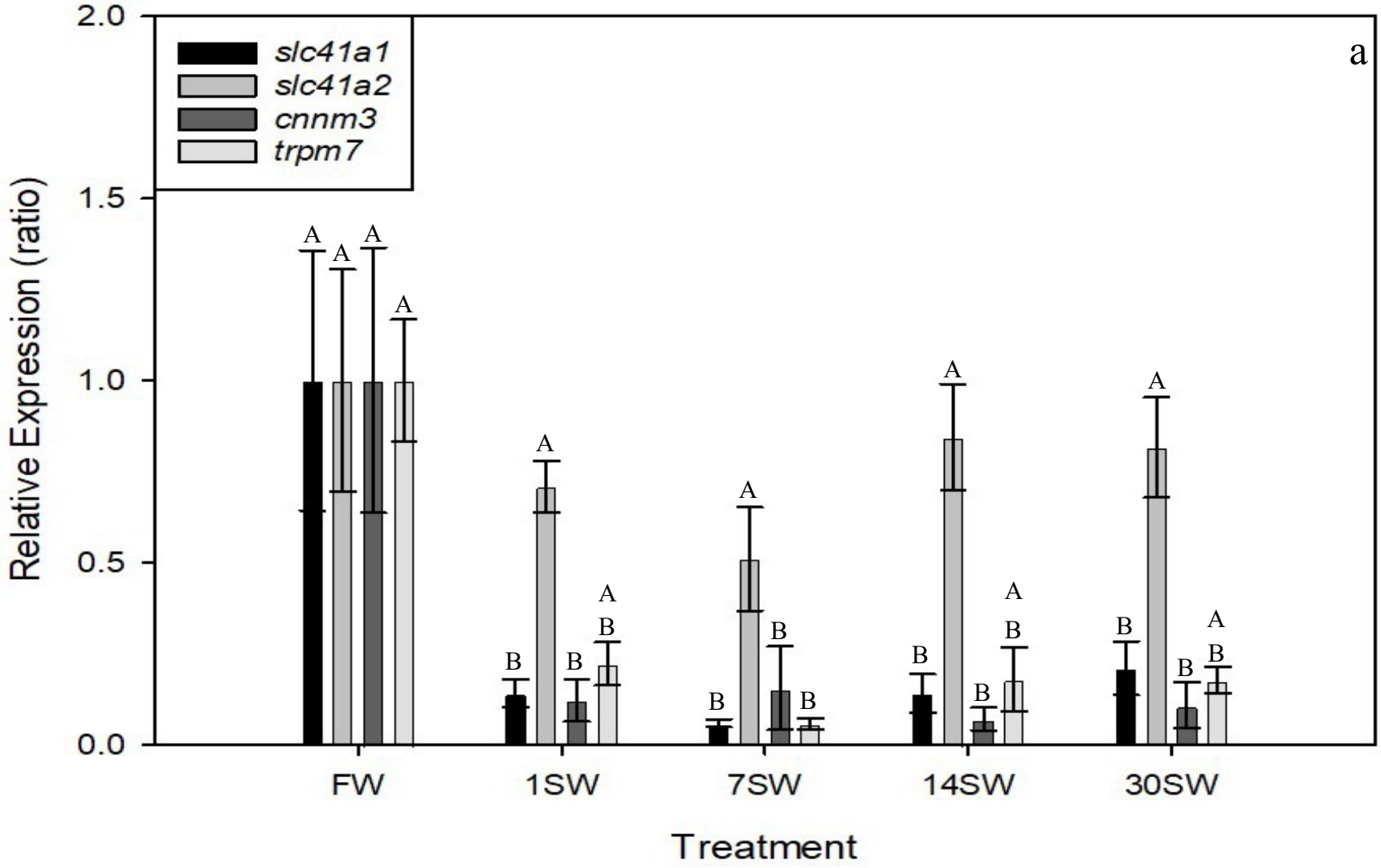

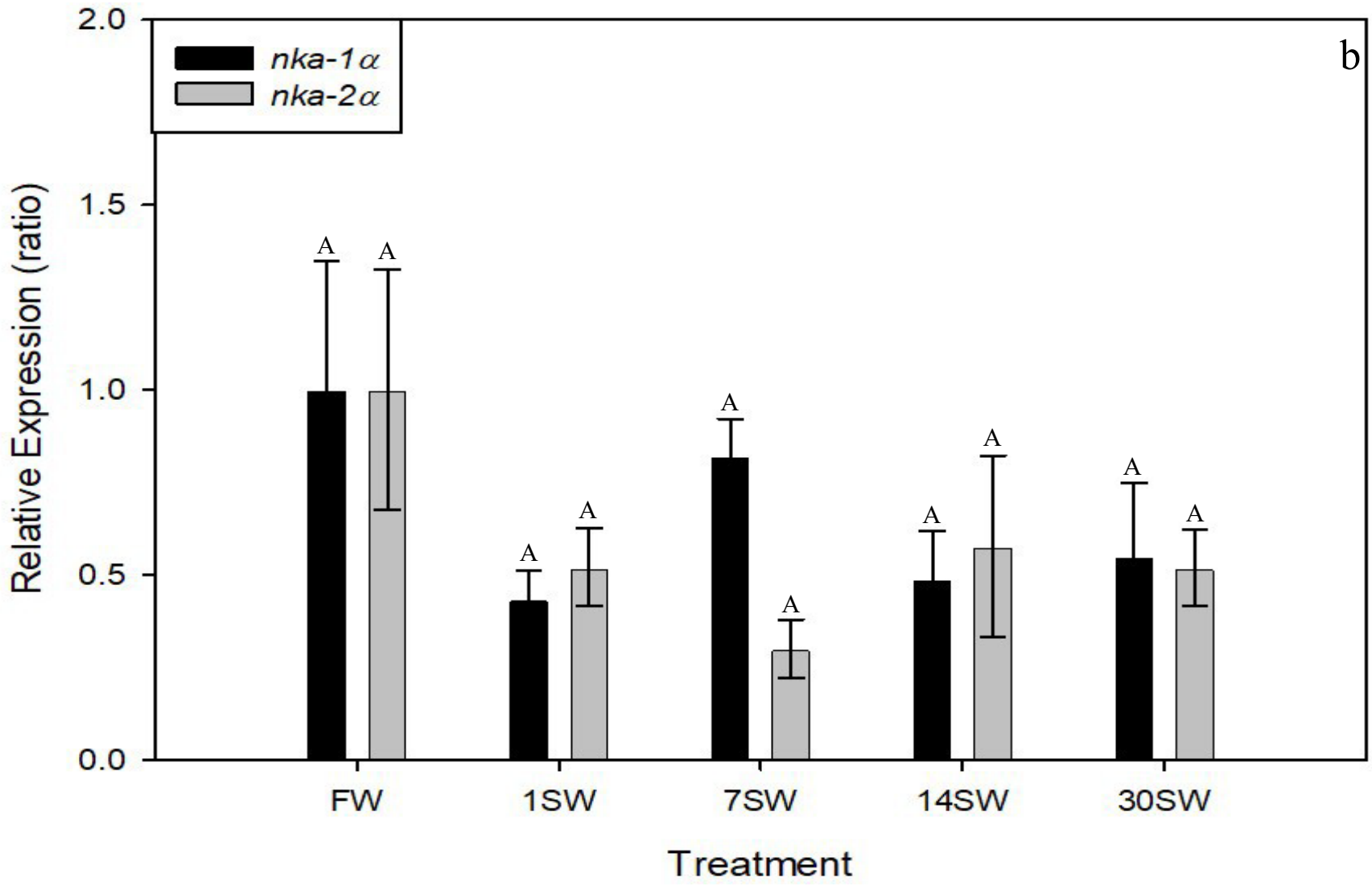

Figure 7: Relative mRNA expression of Mg^{2+} transporters (a) and *nka* isoforms (b) in the gills of *P. latipinna* exposed to 35ppt SW at 1, 7, 14, or 30 days (n=4-5). Bars represent the mean ± SEM of the expression ratio compared to controls exposed to 0ppt FW (control ratio =1). Statistical significance was determined with one-way ANOVA ($p>0.05$) followed by Tukey's post hoc test for multiple pairwise comparisons. Within each gene, bars that do not share a letter are significantly different from one another. Comparisons between genes were not made.

Acclimation of *P. latipinna* to 35ppt SW led to significant decreases in branchial expression of *slc41a1* (P=0.01), *cnnm3* (P=0.002), and *trpm7* (P=0.002). Changes in expression of *slc41a1* and *cnnm3* were observed after 1 day of acclimation, whereas *trpm7* expression was not significantly different from controls until 7 days had passed. No significant changes in the expression of *slc41a2*, *nka-1α*, or *nka-2α* were observed in the gills (Figure 7).

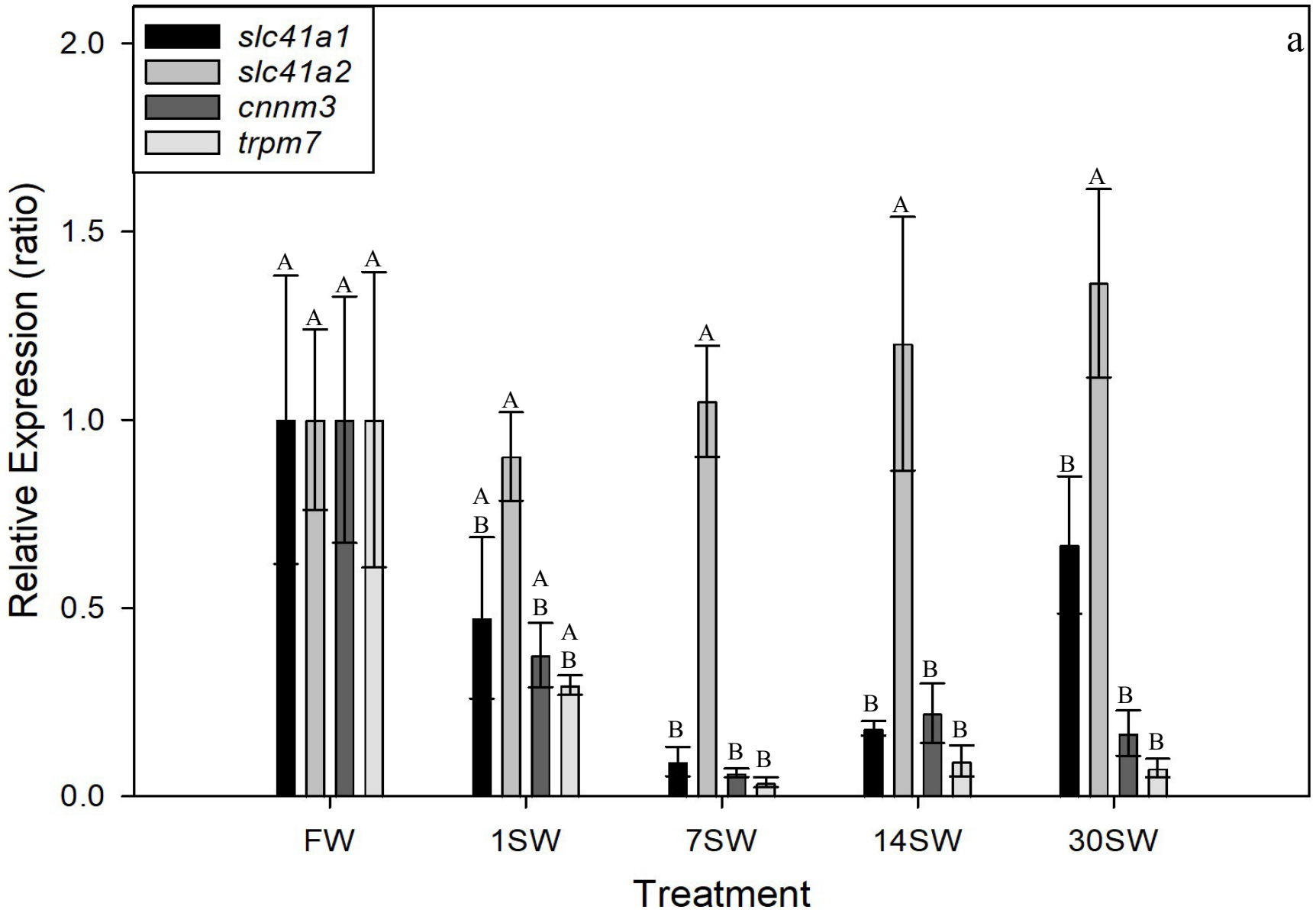
slc41a1
slc41a2
cnnm3
trpm7
a
Relative Expression (ratio)
2.0
1.5
1.0
0.5
0.0
FW
1SW
7SW
14SW
30SW
Treatment

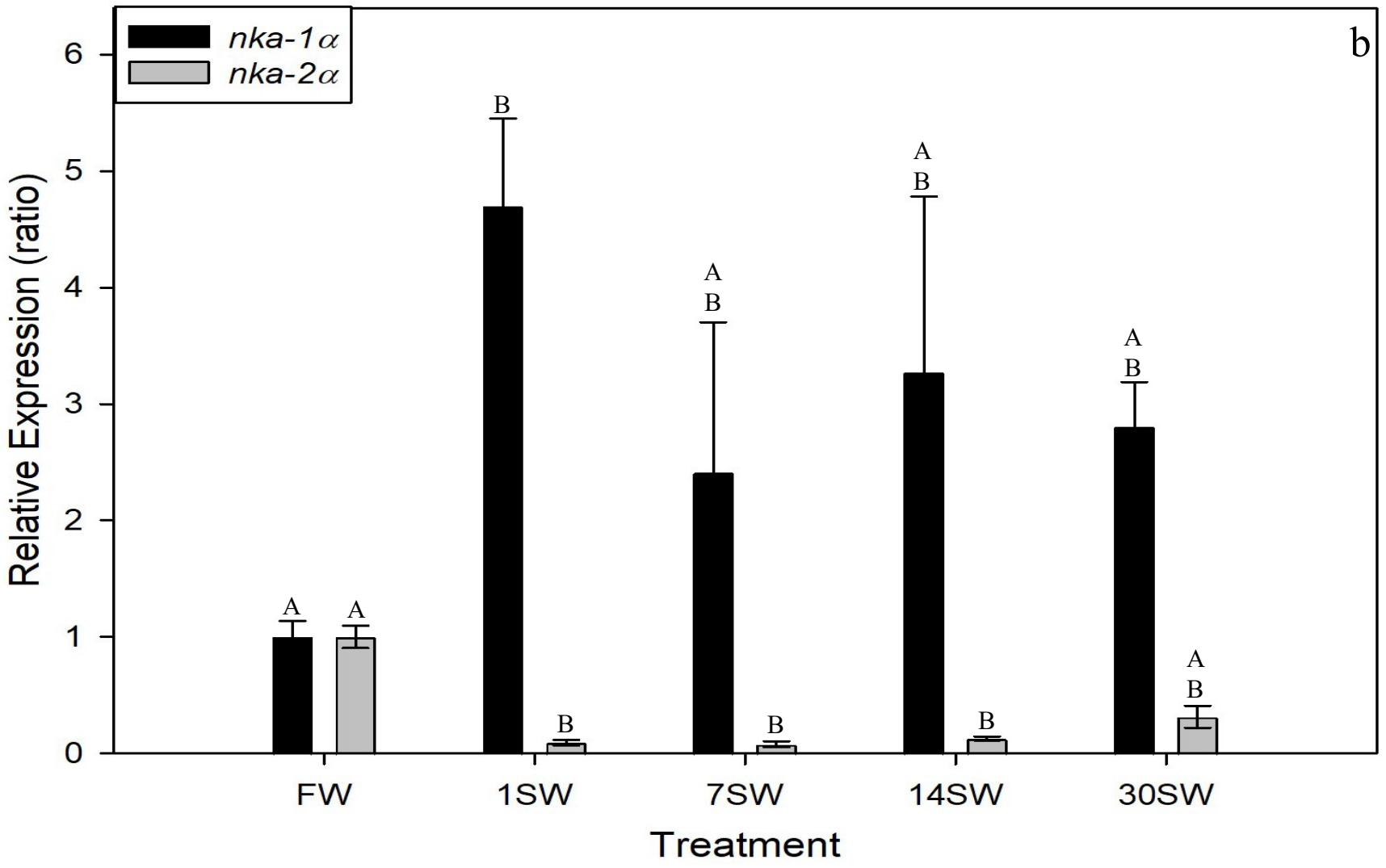

Figure 8: Relative mRNA expression of Mg^{2+} transporters (a) and *nka* isoforms (b) in the anterior intestine of *P. latipinna* exposed to 35ppt SW at 1, 7, 14, or 30 days (n=4-5). Bars represent the mean ± SEM of the expression ratio compared to controls exposed to 0ppt FW (control ratio =1). Statistical significance was determined with one-way ANOVA followed by Tukey's post hoc test for multiple pairwise comparisons. Within each gene, bars that do not share a letter are significantly different from one another ($p<0.05$). Comparisons between genes were not made.

In the anterior intestine, acclimation to 35ppt SW led to significant decreases in the expression of *slc41a1* (P=0.03), *cnnm3* (P=0.028), *trpm7* (P=0.04), and *nka-2α* (P=0.018). Acclimation to 35ppt SW led to increased expression of *nka-1α* (P=0.005). Interestingly, changes in expression of *nka* isoforms occurred after 1 day of exposure whereas the expression of Mg^{2+} transporters were not significantly different until 7 days had passed. No significant changes in *slc41a2* expression were observed within the anterior intestine (Figure 8).

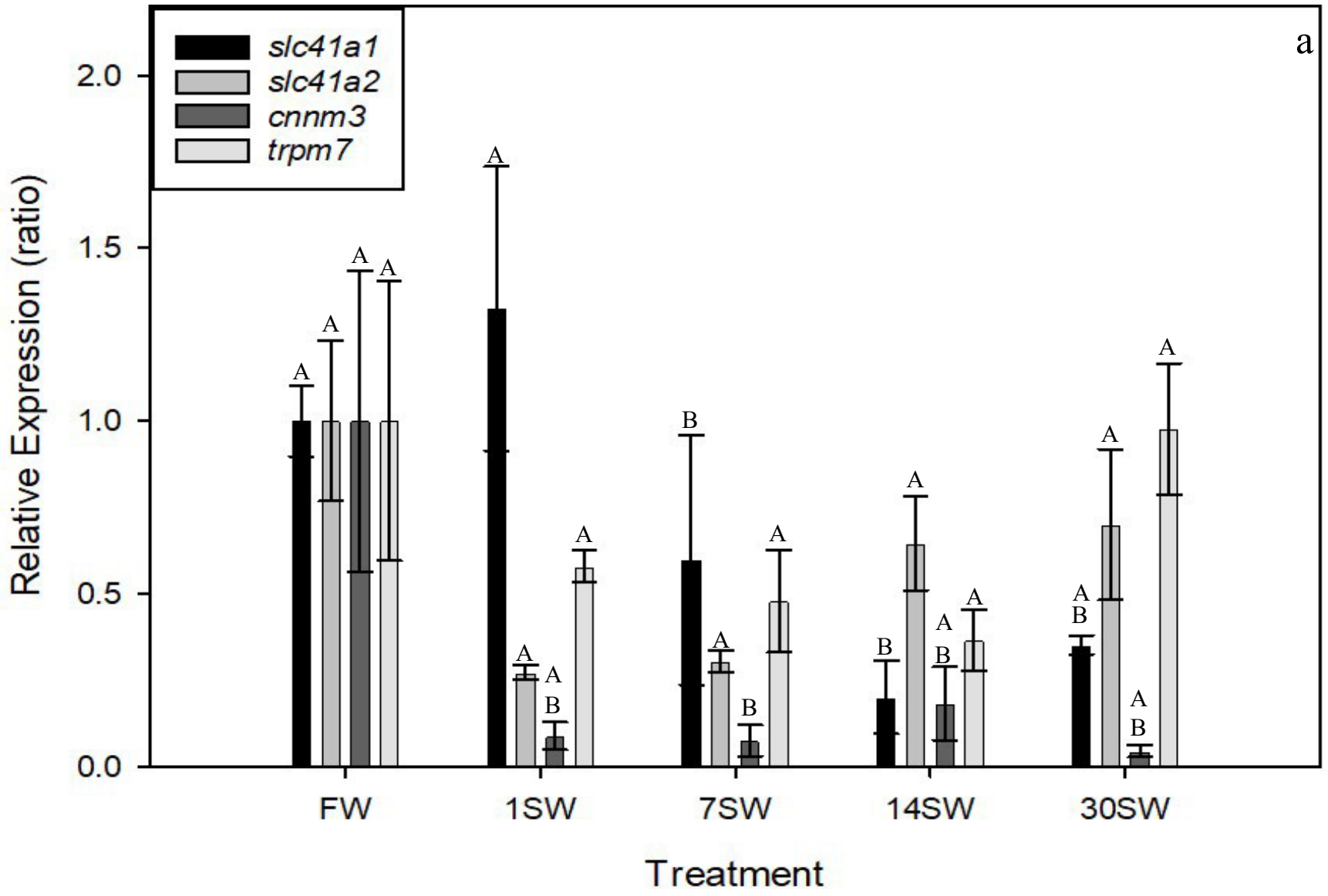
a
slc41a1
slc41a2
cnnm3
trpm7
Relative Expression (ratio)
2.0
1.5
1.0
0.5
0.0
FW
1SW
7SW
14SW
30SW
Treatment

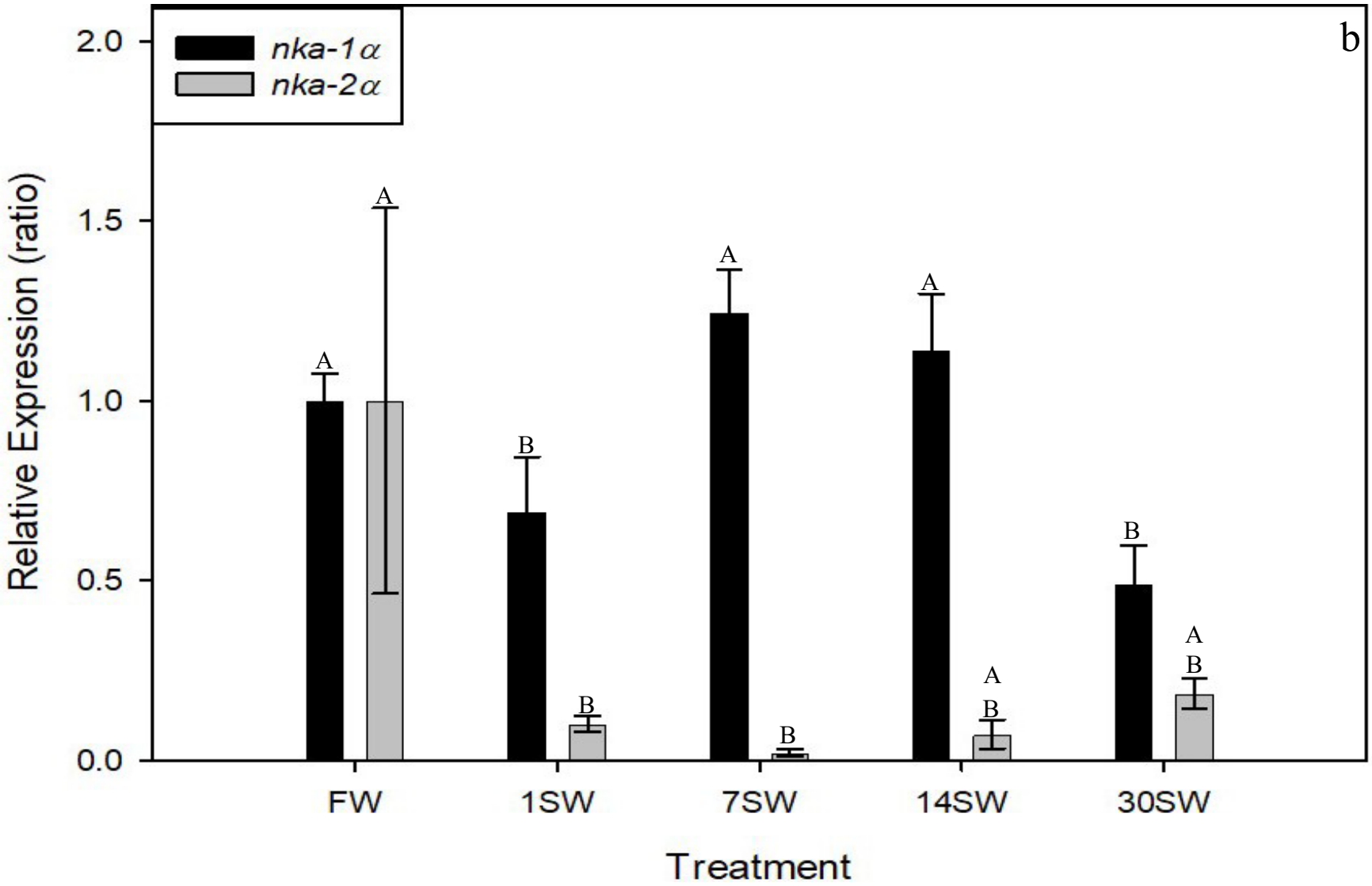

Figure 9: Relative mRNA expression of Mg^{2+} transporters (a) and *nka* isoforms (b) in the posterior intestine of *P. latipinna* exposed to 35ppt SW at 1, 7, 14, or 30 days (n=4-5). Bars represent the mean ± SEM of the expression ratio compared to controls exposed to 0ppt FW (control ratio =1). Statistical significance was determined with one-way ANOVA followed by Tukey's post hoc test for multiple pairwise comparisons. Within each gene, bars that do not share a letter are significantly different from one another ($p<0.05$). Comparisons between genes were not made.

In the posterior intestine, SW acclimation led to significant decreases in the expression of *slc41a1* (P=0.009), *cnnm3* (P=0.018), *nka-1α* (P=0.001), and *nka-2α* (P=0.013), with no significant changes in the expression of *slc41a2* or *trpm7* being observed. As was observed in the anterior intestine, the expression of *nka* isoforms changed significantly after 1 day of exposure, whereas significant changes in the expression of *slc41a1* and *cnnm3* were only observable after 7 days (Figure 9).

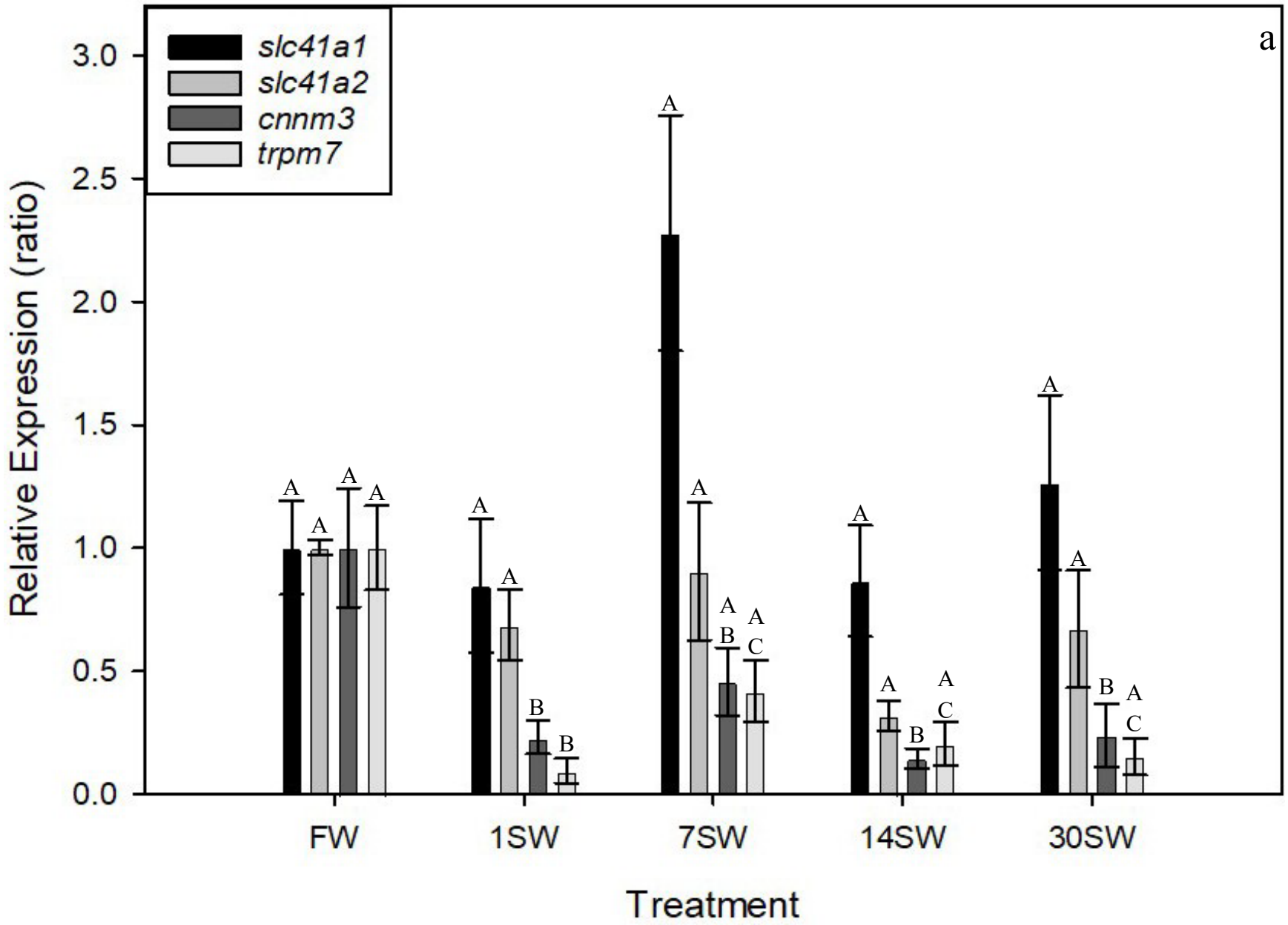
a
slc41a1
slc41a2
cnnm3
trpm7
Relative Expression (ratio)
3.0
2.5
2.0
1.5
1.0
0.5
0.0
A A A A
A A B B
A A B A A C
A A B A C
A A B A C
FW
1SW
7SW
14SW
30SW
Treatment

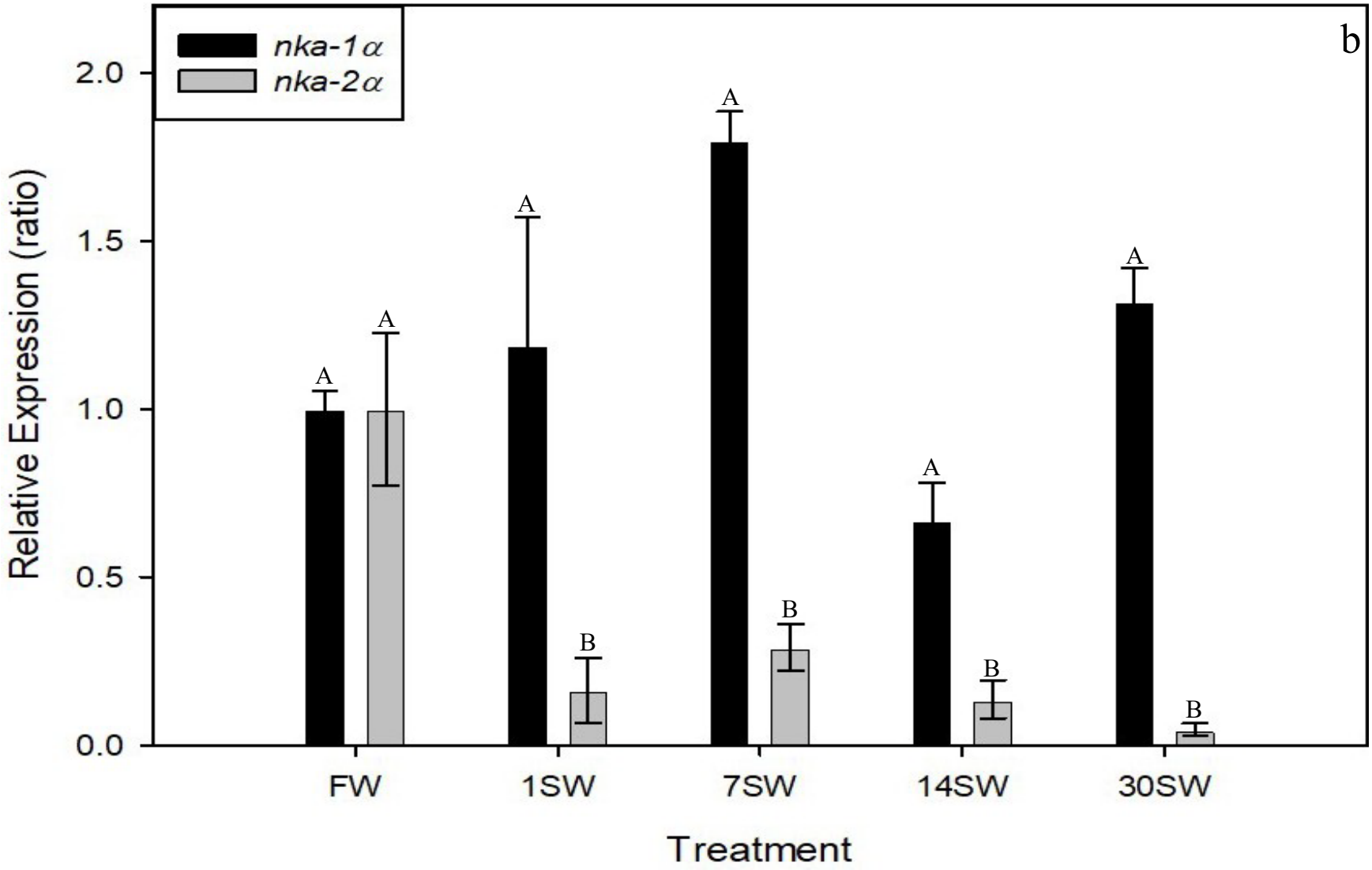

Figure 10: Relative mRNA expression of Mg^{2+} transporters (a) and *nka* isoforms (b) in the kidneys of *P. latipinna* exposed to 35ppt SW at 1, 7, 14, or 30 days (n=4-5). Bars represent the mean ± SEM of the expression ratio compared to controls exposed to 0ppt FW (control ratio =1). Statistical significance was determined with one-way ANOVA followed by Tukey's post hoc test for multiple pairwise comparisons. Within each gene, bars that do not share a letter are significantly different from one another ($p<0.05$). Comparisons between genes were not made.

Renal expression of *cnnm3* (P=0.036), *trpm7* (P<0.001), and *nka-2α* (P=0.001) significantly decreased after acclimation to 35ppt SW. Significant changes in expression occurred within 1 day of exposure if they had occurred at all. Interestingly, measured quantities of *trpm7* mRNA were lowest after 1 day of exposure to the treatment but began to increase by 7 days to levels not significantly different from FW controls. These levels would remain consistent for the remainder of the experiment. No significant changes in the expression of *slc41a1*, *slc41a2*, or *nka-1α* were observed (Figure 10).

In summary, acclimation of *P. latipinna* to 35ppt SW led to significant changes in the expression of all studied transporters except for *slc41a2*. Increasing environmental salinity (and therefore, [Mg^{2+}]) caused large decreases in the expression of *slc41a1* mRNA in the gills and anterior portion of the intestine, whereas a less pronounced, yet still significant decrease in *slc41a1* mRNA could be observed in the posterior intestine, but changes began to rectify towards control levels after 30 days of exposure. In contrast, no significant changes in the relative quantity of *slc41a1* mRNA were observed in the kidneys after 30 days of SW acclimation. The expression of *cnnm3* mRNA in the studied tissues followed a similar pattern to what was observed in *slc41a1* in the gills, anterior and posterior intestines, however, unlike what was observed in *slc41a1*, quantities of *cnnm3* mRNA within the kidneys of SW-acclimated fish also significantly decreased during SW acclimation. Like what was observed for *slc41a1* and *cnnm3* mRNA during SW acclimation, expression of *trpm7* mRNA significantly decreased in the gills and anterior intestines. Unlike *slc41a1* and *cnnm3*, however, no significant changes were observed within the posterior intestines. Like *cnnm3*, but unlike *slc41a1*, expression of *trpm7* mRNA significantly decreased in the kidneys. No significant changes in the relative expression of either studied *nka* isoform (*nka-1α* and *nka-2α*) were observed in the gills of *P. latipinna* after

30 days of SW acclimation. In the anterior intestine, SW acclimation resulted in a significant increase in the expression of *nka-1α*, but a significant decrease in *nka-2α*. Expression of both *nka* isoforms significantly decreased in the posterior intestine, however the differences in *nka-2α* was more pronounced than what was observed for *nka-1α*, where expression was only significantly lower than controls at 7- and 30-days of acclimation. Finally, expression of *nka-2α* within the kidneys significantly decreased during SW-acclimation, whereas levels of *nka-1α* remained unchanged.

2.3.4 : Phylogenetic Analysis of Mg^{2+} Transporters

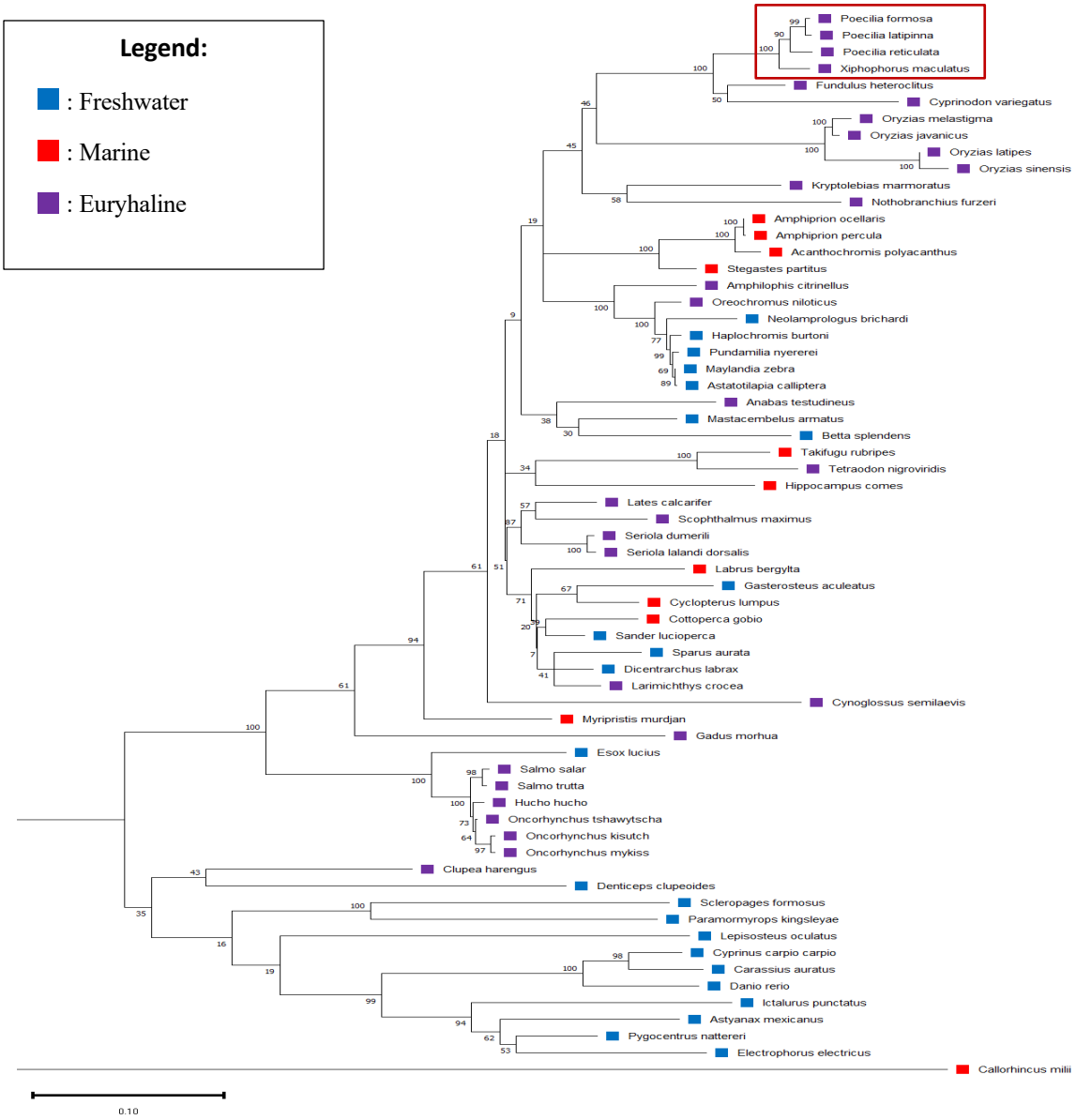

Figure 11: Phylogenetic analysis of *slc41a1* coding sequences from many fish species using Ensembl. The evolutionary history was inferred by using the Maximum Likelihood method and General Time Reversible model (Nei and Kumar, 2000). The tree with the highest log likelihood (-13823.56) is shown. The percentage of trees in which the associated taxa clustered together is shown next to the branches. Initial tree(s) for the heuristic search were obtained automatically by applying Neighbor-Join and BioNJ algorithms to a matrix of pairwise distances estimated using the Maximum Composite Likelihood (MCL) approach, and then selecting the topology with superior log likelihood value. A discrete Gamma distribution was used to model evolutionary rate differences among sites (5 categories (+G, parameter = 0.7526)). The rate variation model allowed for some sites to be evolutionarily invariable ([+I], 36.51% sites). The tree is drawn to scale, with branch lengths measured in the number of substitutions per site. This analysis involved 64 nucleotide sequences. Codon positions included were 1st+2nd+3rd+Noncoding. All positions containing gaps and missing data were eliminated (complete deletion option). There was a total of 846 positions in the final dataset. Evolutionary analyses were conducted in MEGA11 (Tamura et al., 2021). FW species are labelled with a blue square, SW species are labelled with red squares, and euryhaline species are labelled with purple squares. A red box surrounds *P. latipinna* and other members of the Poecilid family.

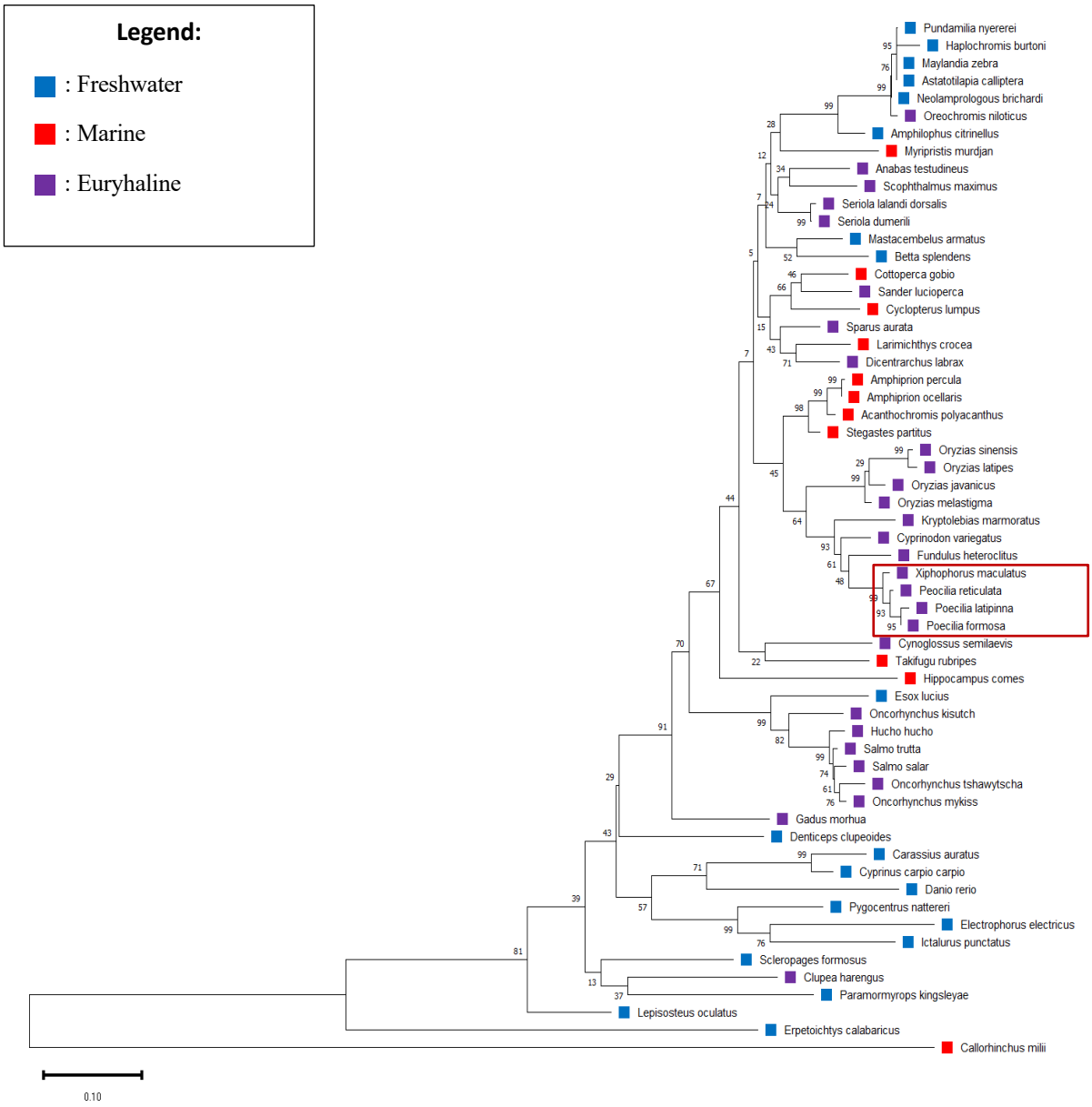

Figure 12: Phylogenetic analysis of *cnnm3* coding sequences from many fish retrieved from Ensembl. The evolutionary history was inferred by using the Maximum Likelihood method and Tamura-Nei model (Tamura and Nei, 1993). The tree with the highest log likelihood (-10031.27) is shown. The percentage of trees in which the associated taxa clustered together is shown next to the branches. Initial tree(s) for the heuristic search were obtained automatically by applying Neighbor-Join and BioNJ algorithms to a matrix of pairwise distances estimated using the Tamura-Nei model, and then selecting the topology with superior log likelihood value. A discrete Gamma distribution was used to model evolutionary rate differences among sites (5 categories (+G, parameter = 0.3224)). The tree is drawn to scale, with branch lengths measured in the number of substitutions per site. This analysis involved 59 nucleotide sequences. Codon positions included were 1st+2nd+3rd+Noncoding. All positions containing gaps and missing data were eliminated (complete deletion option). There were a total of 676 positions in the final dataset. Evolutionary analyses were conducted in MEGA11 (Tamura et al., 2021). FW species are labelled with a blue square, SW species are labelled with red squares, and euryhaline species are labelled with purple squares. A red box surrounds *P. latipinna* and other members of the Poecilid family.

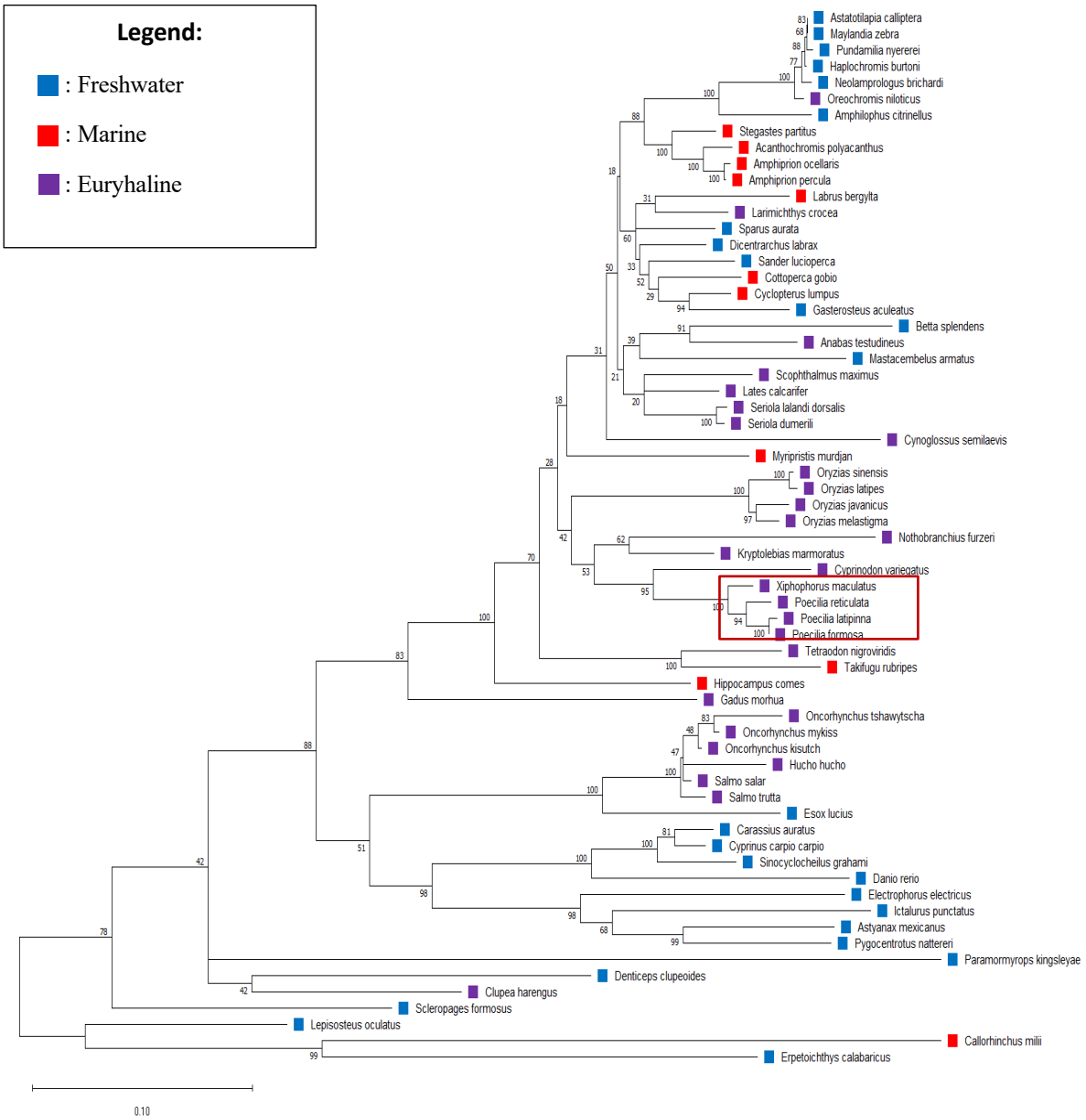

Figure 13: Phylogenetic analysis of *trpm7* coding sequences from many fish retrieved from Ensembl. The evolutionary history was inferred by using the Maximum Likelihood method and Kimura 2-parameter model (Kimura, 1980). The tree with the highest log likelihood (-19227.51) is shown. The percentage of trees in which the associated taxa clustered together is shown next to the branches. Initial tree(s) for the heuristic search were obtained by applying the Neighbor-Joining method to a matrix of pairwise distances estimated using the Maximum Composite Likelihood (MCL) approach. A discrete Gamma distribution was used to model evolutionary rate differences among sites (5 categories (+G, parameter = 0.5715)). The rate variation model allowed for some sites to be evolutionarily invariable ([+I], 19.92% sites). The tree is drawn to scale, with branch lengths measured in the number of substitutions per site. This analysis involved 65 nucleotide sequences. Codon positions included were 1st+2nd+3rd+Noncoding. All positions containing gaps and missing data were eliminated (complete deletion option). There were a total of 1187 positions in the final dataset. Evolutionary analyses were conducted in MEGA11 (Tamura et al., 2021). FW species are labelled with a blue square, SW species are labelled with red squares, and euryhaline species are labelled with purple squares. A red box surrounds *P. latipinna* and other members of the Poecilid family.

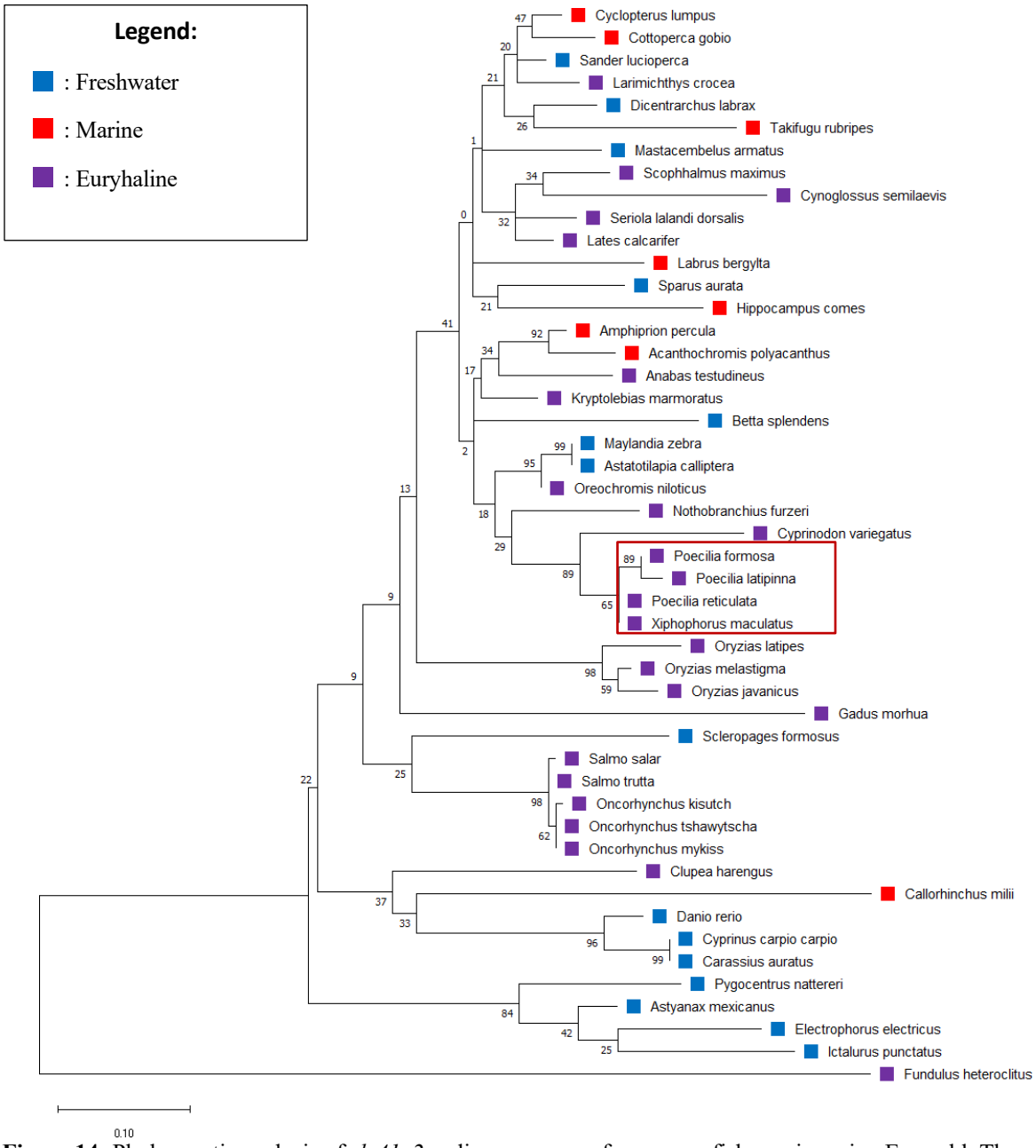

Figure 14: Phylogenetic analysis of *slc41a2* coding sequences from many fish species using Ensembl. The evolutionary history was inferred by using the Maximum Likelihood method and Kimura 2-parameter model (Kimura, 1980). The tree with the highest log likelihood (-2935.79) is shown. The percentage of trees in which the associated taxa clustered together is shown next to the branches. Initial tree(s) for the heuristic search were obtained by applying the Neighbor-Joining method to a matrix of pairwise distances estimated using the Maximum Composite Likelihood (MCL) approach. A discrete Gamma distribution was used to model evolutionary rate differences among sites (5 categories (+G, parameter = 1.0599)). The tree is drawn to scale, with branch lengths measured in the number of substitutions per site. This analysis involved 48 nucleotide sequences. Codon positions included were 1st+2nd+3rd+Noncoding. All positions containing gaps and missing data were eliminated (complete deletion option). There were a total of 176 positions in the final dataset. Evolutionary analyses were conducted in MEGA11 (Tamura et al., 2021). FW species are labelled with a blue square, SW species are labelled with red squares, and euryhaline species are labelled with purple squares. A red box surrounds *P. latipinna* and other members of the Poecilid family

All phylogenetic trees demonstrated a familial grouping of genetic relationships, with *P. latipinna* sharing the most genetic similarity the amazon molly (*Poecilia Formosa*), closely followed by other members of the poecilid family such as guppies (*Poecilia reticulata*) and the southern platyfish (*Xiphophorus maculatus*). The same pattern can be observed across other genera such as medaka (*Oryzias spp*) and salmonids. Past the immediate genus and species groupings, however, variations in between the trees start to appear. In the *slc41a1* tree (Figure 11), for example, *P. latipinna* and other Poecilid species were located farthest from the outgroup, whereas Poecilids are in a more central position for *cnnm3*, *trpm7*, and *slc41a2* (Figures 12-14, respectively). For *slc41a1* and *cnnm3* (Figure 11, 12, respectively), the species with the highest similarity to the Poeciliidae family was the mummichog (*Fundulus heteroclitus*), followed by the sheepshead minnow (*Cyprinodon variegatus*). In contrast, phylogenetic analysis of *slc41a2* produced a tree (Figure 14) in which the mummichog was positioned as an outgroup, suggesting low genetic similarity to sailfin mollies for this gene. It was not possible to determine where the mummichog would be in the *trpm7* tree (Figure 13), as its sequence was removed from the dataset by the software due to an incomplete sequence. Branch lengths within the *slc41a1* tree were the shortest indicating comparatively lower rates of genetic change, followed by *trpm7*, *cnnm3*, and *slc41a2* (Figures 11, 13, 12, and 14, respectively). It is also worth noting that, within the tree generated for *trpm7* (Figure 13), reedfish (*Erpetoichthys calabaricus*) were positioned alongside the elephant shark (*Callorhinchus millii*) suggesting *trpm7* in this species is more like chondrichthyans than bony fish. Finally, the only tree that suggested an environmental influence on its phylogenetic relationships was *trpm7* (Figure 13), with stenohaline species being more prevalent towards the top and bottom of the tree (Indicating the largest and smallest distances

from the outgroup respectively), and euryhaline species being primarily located in a median position.

2.4 : Discussion

2.4.1 : Influence of Salinity on Plasma Mg^{2+}

Acclimation of *P. latipinna* to 35ppt SW for 30 days did not lead to significant changes in plasma Mg^{2+} (Figure 6). This observation was somewhat expected as the rapidly changing environments of many euryhaline species drive physiological changes that allow them to rapidly switch from net ion absorption to excretion to survive. This was exemplified when euryhaline mefugu were able to maintain consistent levels of Mg^{2+} in their plasma during salinity acclimation (Islam et al., 2013). Furthermore, the rapid physiological response to manipulations of environmental Mg^{2+} was also demonstrated when zebrafish were able to maintain plasma Mg^{2+} concentration when exposed to both elevated and decreased levels of environmental Mg^{2+} (Arjona et al., 2013), suggesting that the rapid regulation of internal Mg^{2+} levels is not exclusive to euryhaline species. Plasma Mg^{2+} concentrations may have been maintained by a decrease in Mg^{2+} absorption, or an increase in Mg^{2+} excretion driven by changes at the genetic or protein level. Indeed, increased renal expression of *slc41a1* and *cnnm3* were both observed in the kidneys of euryhaline mefugu during salinity acclimation alongside increased urinary output of Mg^{2+} (Islam et al., 2013, 2014). While I did not test for regulation at the protein level, I did observe changes in the relative quantities of *cnnm3* and *trpm7* in the kidneys in response to increased environmental salinity whereas renal expression of *slc41a1* mRNA remained stable throughout the exposure (Figure 10), suggesting *slc41a1* may not be regulated at the genetic level in the kidneys of this species.

2.4.2 : Tissue Expression of Mg^{2+} Transporters in P. latipinna

Due to the physiological roles Mg^{2+} is known to play in animals, it was hypothesized that the expression of my genes of interest would be ubiquitously expressed in *P. latipinna*, regardless of salinity. Furthermore, I hypothesized that there would be significant tissue-dependent expression of all studied genes. Indeed, all studied genes were found to be ubiquitously expressed under both environmental conditions and significant tissue-dependent distribution of mRNA was observed in most cases (Figure 7), however, tissue-dependent expression of *trpm7* was not observed in SW-acclimated fish (Figure 7b). Ubiquitous expression of *slc41a1*, *slc41a2*, and *cnnm3* has been experimentally demonstrated in a variety of fish species (e.g. *T. rubripes, T. obscurus* (*slc41a1*, *slc41a2*, *cnnm3*), Islam et al., 2013, 2014; *C. auratus* (*slc41a1*), Kodzhahinchev et al., 2017; *D. rerio* (*slc41a1*), Arjona et al., 2019). Although my study is the first to observe ubiquitous *trpm7* expression in a fish (Figure 5), similar results have been observed in mice (Groenestege et al., 2006; reviewed by Schlingmann et al., 2007; Quamme, 2008). Significant tissue-dependent expression of *slc41a1* has been quantitatively demonstrated in goldfish (Kodzhahinchev et al., 2017), supporting the findings of my study, however no quantitative evidence exists for ubiquitous *slc41a1* expression in SW-acclimated fish, or for *slc41a2*, *cnnm3*, or *trpm7* in any fish (Figures 5a and 5b, respectively), making my study the first study to date to achieve this in a euryhaline fish.

In FW-acclimated *P. latipinna*, *slc41a1* expression was highest in the liver, kidneys, and skin (Figure 5a). Elevated levels of *slc41a1* in the kidneys and liver has also been reported in other species acclimated to FW including mefugu acclimated to FW (Islam et al., 2013), goldfish (Kodzhahinchev et al., 2017), and zebrafish (Arjona et al., 2019). A tissue-dependent distribution for *slc41a1* mRNA was also observed in SW-acclimated *P. latipinna*, however post-hoc analysis

was unable to identify where the exact differences were, although levels in the gills and kidneys appeared to be elevated compared to other tissues (Figure 5b). Similar findings have been reported in SW-acclimated mefugu (*T. obscurus*), and its close marine relative, torafugu (*T. rubripes*), where the kidneys were shown to be the dominant site of *slc41a1* expression using semi-quantitative methods (Islam et al., 2013).

Like *slc41a1*, *slc41a2* expression was also ubiquitous, and significant tissue-dependent expression was observed regardless of environmental salinity. Post hoc analysis was not, however, able to identify which tissues contained higher levels of this gene in either salinity (Figures 5a, 5b). Although studies of *slc41a2* expression in fish are rare, semi-quantitative experiments by Islam et al., (2013) demonstrated elevated expression of *slc41a2a* and *slc41a2b* in the kidneys of *T. obscurus* acclimated to FW, and in the kidneys and intestines of *T. obscurus* and *T. rubripes* acclimated to SW (Islam et al., 2013) likely confirming that this transporter is present in multiple tissues and responsive to environmental salinity if not environmental magnesium.

Like *slc41a1*, *cnnm3* expression was also found to be tissue-dependent in FW-acclimated fish, with the highest levels being seen in the kidneys, heart, and liver (Figure 5a). In SW, *cnnm3* expression was most pronounced in the heart and skin (Figure 5b). My study is the first to quantitatively determine a pattern of *cnnm3* expression in a euryhaline fish acclimated to both FW and SW. The most similar available study used semi-quantitative PCR to achieve a similar objective in two species of pufferfish (mefugu, *T. rubripes*; torafugu, *T. obscurus*) however they found the ubiquitous expression of *cnnm3* to be more uniform across studied tissues, although a quantitative analysis would be necessary to confirm this (Islam et al., 2014).

Like *slc41a1* and *cnnm3*, *trpm7* expression in FW-acclimated fish was highest in the liver, however levels within the kidneys, heart, and skin were not elevated, contrasting what I saw in other genes of interest (Figure 5a), however, unlike the patterns of *slc41a1* and *cnnm3* expression I observed, a tissue-specific distribution of *trpm7* mRNA was not detected in SW-acclimated fish (Figure 5b). To my knowledge, this study is the first to quantitatively demonstrate tissue-specific distribution of *trpm7* in a fish, although its ubiquitous expression has been observed in mammalian models, including mice (*Mus musculus*, e.g., Kunert-Keil et al, 2006), rats (*Rattus norvegicus*, e.g., Runnels et al., 2001), and in human embryonic cells (e.g. Nadler et al., 2001; Fonfria et al., 2008) suggesting that ubiquitous *trpm7* expression may be evolutionarily conserved.

2.4.3 : Influence of SW Acclimation on Transporter Expression

2.4.3.1 : Influence of SW Acclimation on Branchial Transporter Expression

SW acclimation led to significant decreases in the genetic expression of *slc41a1*, *cnnm3*, and *trpm7* within the branchial epithelium (Figure 7a). No changes were observed in the expression of *slc41a2* (Figure 7a), *nka-1α* or *nka-2α* (Figure 7b). Although the study of Mg^{2+} homeostasis at the genetic level has gained attention in the last decade (e.g. Islam et al., 2013, 2014; Kodzhahinchev et al., 2017; Arjona et al., 2019; Hansen et al., 2021), the effect of SW acclimation on the genetic regulation of Mg^{2+} transporters within the branchial epithelium of a euryhaline fish has not previously been quantitatively investigated, making my study the first to achieve this.

The only two previous studies that have quantitatively investigated the relationship between environmental Mg^{2+} on the genetic expression of branchial transporters have focused

exclusively on *slc41a1* in stenohaline FW fish (Kodzhahinchev et al., 2017; Arjona et al., 2019). Here, decreasing environmental Mg^{2+} led to increased *slc41a1* mRNA in the gills of zebrafish (Arjona et al., 2019), but did not cause a change at the genetic level in goldfish (Kodzhahinchev et al., 2017). The lack of changes observed in the gills of goldfish could mean that *slc41a1* is regulated at the protein level instead of at the genetic level, or that the regulation of *slc41a1* in other tissues such as the intestines may be sufficient to maintain homeostasis in goldfish (Kodzhahinchev et al., 2017). In zebrafish, however, there was upregulation of *slc41a1* mRNA in the branchial epithelium in response to the decrease in environmental Mg^{2+} (Arjona et al., 2019). Despite evidence in other tissues that Slc41a1 is involved in the secretion of cellular Mg^{2+} (Islam et al., 2013; Kodzhahinchev et al., 2017; Hansen et al., 2019), the only study to date to observe a significant change within the gills of zebrafish exposed to Mg^{2+}-poor water observed upregulation, leading them to believe Slc41a1 is absorptive within the gills (Arjona et al., 2019). I therefore predicted that *slc41a1* would be downregulated in the gills of sailfin mollies during SW acclimation, and my findings support this prediction (Figure 7a). Interestingly, Arjona et al. (2019) argued based on their data that Slc41a1 was not an NME, but rather a Mg^{2+} channel (Arjona et al., 2019). While this supports their results and mine, there is a large enough body of evidence supporting Slc41a1 as an NME that I am hesitant to fully agree with that conclusion. Therefore, although it seems that Slc41a1 is absorptive in the gills of sailfin mollies, its exact position in branchial cells remains unconfirmed.

Based on its similarity to *slc41a1*, I expected to see similar changes to *slc41a2* levels during this experiment. Although I did not observe a significant change here, the data did not outright disagree with my predictions either. Indeed, the lack of changes to *slc41a2* (Figure 7a), *nka-1α*, and *nka-2α* (Figure 7b) within the gills may have been due to post transcriptional

regulation that was undetectable with qPCR. I predicted Slc41a2 to serve a similar role to Slc41a1, and the lack of significant change observed here is insufficient to reject this prediction. When environmental salinity increases, euryhaline fish must shift from net ion absorption to net ion secretion (Chapter 1). Within branchial cells, this active secretion should occur at the apical membrane, however, an increase in plasma Mg^{2+} levels would be necessary to drive passive movement into the cell at the basolateral membrane (Figure 2). As one was not observed (Figure 6), perhaps this pathway was not activated due to regulation at other tissues.

Unlike *slc41a1*, no previous evidence regarding the genetic regulation of *cnnm3* or *trpm7* in the gills of fish currently exists. Significant decreases in *trpm7* and *cnnm3* mRNA with increasing environmental magnesium concentrations were observed in this experiment (Figure 7a). I propose that this decrease in expression was caused by a physiological need to reduce environmental magnesium absorption (which would be required in freshwater but not in saltwater; Chapter 1), suggesting potential absorptive roles for both genes as predicted in Figure 2. Indeed, *cnnm3* mRNA has been localized to the lateral membrane of renal tubules in euryhaline mefugu (Islam et al., 2014), influencing my own predictions (Figure 2). I thought that Cnnm3 was likely involved in the movement of intracellular Mg^{2+} into the lateral membrane space, and that it would be downregulated during SW acclimation. My results do not contradict this prediction.

From the results of this experiment, I return to my predictive branchial model (Figure 2). Here I proposed that Trpm7 forms a channel at the basolateral membrane allowing Mg^{2+} to enter the cell by diffusion while Nka isoforms at the basolateral membrane actively pump $2K^+$ into the cell in exchange for $3Na^+$ out of the cell. The electrochemical gradient established by Nka is utilized by Cnnm3 on the lateral membrane to move $2Na^+$ into the cell in exchange for $1Mg^{2+}$

into the intermembrane space, where it reenters the blood. Slc41a1/a2 are localized on the membranes of apically associated vacuoles before fusing with the apical membrane and excreting Mg^{2+} into the environment (Figure 2). Vacuolar localization has been demonstrated in the kidneys of other euryhaline fish (mummichog; Chandra et al., 1997; mefugu; Islam et al., 2013). I placed Trpm7 at the basolateral membrane since passive transport would be physiologically disadvantageous on the apical membrane. Overall, my results do not contradict my model as discussed above and previously.

2.4.3.2 : Influence of SW Acclimation on Intestinal Transporter Expression

SW acclimation led to decreased expression of *slc41a1*, *cnnm3*, and *trpm7* mRNA in both the anterior (Figure 8a) and posterior (Figure 9a) intestines of sailfin mollies. Like my observations in the gills (Figure 7), the intestinal expression of *slc41a2* mRNA remained relatively unchanged during SW acclimation (Figure 8a (anterior), Figure 9a (posterior). In contrast however, *nka-1α* levels increased in the anterior intestine (Figure 8b) but decreased in the posterior intestine (Figure 9b), while the expression of *nka-2α* decreased in both sections (Figure 8b (anterior), Figure 9b (posterior)). Due to the lack of attention piscine intestines have received as ionoregulatory organs (as discussed in Chapter 1) (e.g. Marshall and Grosell, 2005; Bucking and Wood, 2006a ,2006b, 2007), to my knowledge, this study is the first to investigate the relationship between environmental salinity and the genetic regulation of intestinal Mg^{2+} transport in a euryhaline fish. In goldfish, acclimation to a Mg^{2+}-poor environment led to decreased intestinal *slc41a1*, pointing to a likely role in Mg^{2+} excretion (Kodzhahinchev et al., 2017). While initially it may seem that my findings disagree with Kodzhahinchev et al. (2017), euryhaline fish such as the sailfin molly possess physiological adaptations that allow them to survive rapid changes in environmental salinity (Chapter 1). One such adaptation is an overall

decrease in intestinal transcellular permeability in SW (Sundell et al., 2003). This is especially true for divalent cations such as Ca^{2+} and Mg^{2+}, as their absorption across the intestinal lumen would hinder the osmotic gradient required for essential water uptake during drinking (e.g. Kurita et al., 2008; Wilson et al., 2002; Walsh et al., 1991), a theory that is supported by the presence of $CaCO_3$ and $MgCO_3$ in the intestinal lumen of SW-acclimated fish (Shehadeh and Gordon, 1969; Walsh et al., 1991). It is therefore possible that the decrease I observed in SLC41a1 expression when moving from freshwater (where absorption of Mg^{2+} is required) to saltwater (where Mg^{2+} is in excess and requires secretion) is not indicative of an absorptive role, but rather indicative of the lack of need for intestinal excretion, as large amounts of Mg^{2+} aren't likely being absorbed in the first place. This is also reflected in the lack of change to plasma Mg^{2+} (Figure 6) I saw earlier.

Unfortunately, the effect of SW acclimation on intestinal genetic expression of *slc41a2*, *cnnm3*, and *trpm7* has not been quantitatively demonstrated in fish to date, making mine the first to achieve this. I suspect that the lack of change in *slc41a2* expression (Figure 8a, 9a) is suggestive of post-translational regulation, which I was unable to detect with qPCR. Due to its genetic similarity to *slc41a1*, however, I suspect that it would function in a similar manner, although this has yet to be validated experimentally. The observed decreases in *cnnm3* and *trpm7* (Figure 8a, 9a) are also supported by a decrease in intestinal permeability. Decreased Trpm7 would reduce absorption from the lumen and into the cell, and decreased Cnnm3 would reduce the Mg^{2+} absorption across the basolateral membrane and into the plasma.

Finally, my observed differences in the genetic regulation of *nka-1α* between the anterior (Figure 8b) and posterior (Figure 9b) intestines are supported by previous literature, as the region-specific activity of Nka proteins has been demonstrated in the intestines of salmon smolts

(Sundell et al., 2008), and the different regions of the piscine intestine have been shown to differ in their ion transport characteristics (e.g. Bucking and Wood 2006a, 2006b, 2007). Conversely, *nka-2α* expression changed in a more consistent way regardless of intestinal region, perhaps suggesting a more uniform role throughout this tissue in sailfin mollies (Figures 8b and 9b).

My initial proposed model of intestinal Mg^{2+} transport (inspired by Quamme 2008; Figure 3) placed Trpm7 at the apical membrane of enterocytes, allowing for the flow of Mg^{2+} down its electrochemical gradient and into the cell, where it is exchanged at the serosal membrane by NMEs (Slc41a1, Slc41a2, and Cnnm3) for $2Na^{+}$, utilizing gradients established by basolateral NKA transporters. I believe that the results support my predictions, as well as my proposed intestinal model (Figure 3).

2.4.3.3 : Influence of SW Acclimation on Renal Transporter Expression

SW acclimation led to decreased quantities of *cnnm3*, *trpm7* (Figure 10a), and *nka-2α* (Figure 10b). No significant changes in *slc41a1*, *slc41a2* (Figure 10a), or *nka-1α* (Figure 10b) were observed in this tissue. Most quantitative studies of cellular Mg^{2+} homeostasis in fish have focused primarily on the kidneys. Further, of the genes I have investigated, *slc41a1* has been the primary focus in fish. In goldfish (*C. auratus*) and zebrafish (*D. rerio*), decreasing environmental Mg^{2+} did not result in significant changes in renal *slc41a1* expression (Kodzhahinchev et al., 2017; Arjona et al., 2019, respectively), suggesting that other tissues such as the gills (Arjona et al., 2019) or the intestines (Kodzhahinchev et al., 2017) may offer sufficient compensation to physiological Mg^{2+} levels during environmental challenge.

Alternatively, it is possible that renal *slc41a1* is regulated at the protein level, perhaps through endosomal recycling, as has been proposed previously (Mandt et al., 2008). Based on the

changes I observed in branchial (Figure 7a) and intestinal (Figures 8a and 9a) *slc41a1* expression, along with the lack of observed changes within the plasma (Figure 6), it is possible that the genetic regulation of *slc41a1* within the gills and intestines is sufficient to maintain plasma Mg^{2+} concentrations, reducing the need for renal excretion. In mefugu and gulf toadfish, transfer from FW to SW led to increased renal *slc41a1* (Islam et al., 2013; Hansen et al., 2021 respectively) and *cnnm3* (Islam et al., 2014; Hansen et al., 2021, respectively) supporting an excretory role for both proteins.

These findings, when taken alongside the localization of *cnnm3* mRNA to the lateral membrane of renal cells in mefugu (Islam et al., 2014), suggest that Cnnm3 is moving Mg^{2+} out of the cell and into the lateral membrane space. From there, Hansen et al. (2021) proposed that Mg^{2+} would follow its concentration gradient, ending up in the preurine for excretion, traveling through tight junction complexes established by Claudin 19 and another unidentified Claudin (Hansen et al., 2021). Trpm7 has not yet been localized in the kidneys of adult fish, however, based on its perceived role in renal reabsorption in mammalian models, it is thought to be localized to the apical membrane (e.g. Voets et al., 2004; Giménez-Mascarell et al., 2018). My findings (Figure 10a) are in line with a role in reabsorption, as SW-acclimated fish produce low volumes of concentrated urine to reduce ion loading (Chapter 1). From my observations, as well as the other studies of renal Mg^{2+} transport in fish, I built upon my previous model (Figure 4, Chapter 2; adapted from Hansen et al., 2021): Basolaterally localized Nka isoforms exchange intracellular Na^{+} for extracellular K^{+}, establishing an extracellular Na^{+} gradient that is used by Cnnm3 at the lateral membrane to drive cellular Mg^{2+} excretion. Mg^{2+} in the intercellular space then moves passively, either through tight junctions and into the preurine when plasma levels are elevated, or back into the plasma. At the apical brush border, Trpm7 forms a channel to facilitate

Mg^{2+} reabsorption from the filtrate. Slc41a1/a2 on the membranes of apically associated vacuoles exchange intracellular Mg^{2+} for vacuolar Na^{+}, ultimately fusing with the apical membrane to excrete Mg^{2+} into the preurine (Figure 4). When environmental salinity increases, plasma Mg^{2+} levels are kept stable (Figure 6), likely through regulation at the branchial (Figure 7) and intestinal (Figures 8-9) levels, reducing the need for renal Mg^{2+} transport in sailfin mollies. As a result, *trpm7* and *cnnm3* are downregulated at the genetic level (Figure 10a) and the vacuoles containing Slc41a1/a2 are recycled intracellularly, explaining the lack of genetic change I observed (Figure 10a).

2.4.4 : Phylogenetic Analysis

Phylogenetic analyses of *slc41a1*, *cnnm3*, *trpm7*, and *slc41a2* (Figures 11-14, respectively) were carried out to draw comparisons between my findings and those of previous studies on Mg^{2+} transporters in fish (i.e., Islam et al., 2013, 2014; Kodzhahinchev et al., 2017; Arjona et al., 2019; Hansen et al., 2021), predicting that the phylogenetic relationships between the model organisms used in other studies may shed some light on why previous studies may have produced contradictory results. My phylogenetic analyses of *slc41a1* (Figure 11), *slc41a2* (Figure 14), and *cnnm3* (Figure 12) all produced trees that did not appear to be dictated by environmental salinity, leading us to believe that coding sequences for these genes may have changed many times throughout evolutionary history. This may be why environmental Mg^{2+} restriction led to increased branchial *slc41a1* levels in the zebrafish (Arjona et al., 2019), but did not lead to a change in *slc41a1* levels within the gills of goldfish (Kodzhahinchev et al., 2017). It is also possible that different species of fish regulate these transporters differently in species-specific ways, potentially resulting in conflicting data at the gene level, when perhaps data on protein activity and regulation may lead to similar conclusions on a more wholistic level.

Furthermore, environmental Mg^{2+} manipulations did not influence the quantity of *slc41a1* mRNA in the kidneys of zebrafish (Arjona et al., 2019), goldfish (Kodzhahinchev et al., 2017), or sailfin mollies, but did lead to significantly higher levels of *slc41a1* in the kidneys of euryhaline mefugu (Islam et al., 2013) and gulf toadfish (Hansen et al., 2021).

My analysis of *trpm7* coding sequences (Figure 13) revealed a possible exception to what I observed with *slc41a1*, *slc41a2*, and *cnnm3* (Figures 13, 16, 14, respectively), with a more salinity-dependent distribution of species suggesting that this gene may have evolved to support the physiological needs of fish living in different environmental conditions. Still, the genetic regulation I observed at the level of the kidneys is the opposite of what was observed in the gulf toadfish, but this may be attributed to their aglomerular kidneys, as they would likely filter ions differently than glomerular species (Hansen et al., 2021).

2.4.5 : Conclusions and Future Perspectives

The purpose of this experiment was to better understand the integrated roles of various genes thought to be involved in Mg^{2+} homeostasis in sailfin mollies. More specifically, I sought to better understand how these genes were regulated in response to increasing environmental salinity. I first wanted to confirm that the target genes involved in Mg^{2+} homeostasis were expressed in all tissues of *P. latipinna* regardless of environmental salinity, which my data demonstrated. I further predicted that tissue-specific expression would differ depending on environmental salinity, and this was found to be the case. My next objective was to analyze the effects of SW-acclimation on Mg^{2+} concentrations within the plasma, which revealed exceptional regulation of Mg^{2+} transport as homeostatic balance was maintained throughout. Finally, I hypothesized that the levels of mRNA would change upon acclimation to SW, and that these changes would be time dependent. In the gills, I predicted that SW acclimation would lead to

decreases in *slc41a1*, *slc41a2*, *cnnm3*, and *trpm7* due to their proposed roles in branchial absorption which I observed apart from *slc41a2*, where no significant change occurred (Figure 7a), supporting my proposed cellular model (Figure 2). In the intestines, I predicted that a decrease in permeability to divalent cations would lead to decreases in all studied Mg^{2+} transporters, and again, the results support this prediction (Figures 8a and 9a), and my proposed cellular model (Figure 3). Finally, I predicted renal *slc41a1*/*a2* expression would increase, while *cnnm3* and *trpm7* would decrease. While I did observe decreases in *cnnm3* and *trpm7*, no significant changes occurred for *slc41a1* or *slc41a2*, although the lack of a decrease is not sufficient to refute my predictions either. My renal model is largely supported by my results (Figure 4).

In conclusion, it seems that all studied genes are indeed working in tandem to maintain physiological concentrations of Mg^{2+} in sailfin mollies, as is exemplified by the lack of change in plasma concentrations (Figure 5). Further, a decrease in Mg^{2+} uptake across the intestine and gills might be a primary physiological adaptation to increased salinity, leading to a decreased demand for Mg^{2+} excretion, explaining the consistent decreases I observed across tissues for all genes. The upregulation of *nka-1α* in the anterior intestine (Figure 8b) was likely to drive osmotic water uptake, as was demonstrated in trout (Bucking and Wood, 2006a). The lack of change in *slc41a2* in any studied tissue across this experiment may be indicative of regulation at a level undetectable using qPCR, or sufficient compensation by my other genes of interest, although it would be difficult to draw a concrete conclusion regarding the physiological role of Slc41a2 based on the current data from this experiment alone. Future comparisons of the regulation of my genes of interest at various levels, along with analysis of urine and whole body

Mg^{2+} contents may be useful in providing a more wholistic picture of how this species regulates Mg^{2+} during SW acclimation.

Chapter 3: Investigating the Integrated Affects of Dietary Magnesium and Environmental Salinity on Transporter Expression

3.1 : Introduction:

As previously discussed, fish live in environments that provide consistent challenges to osmo- and ionoregulation (Chapter 1). For a long time, it was assumed that the kidneys and gills were primarily responsible for compensating with ionoregulatory challenges in FW fish, and that the intestines played a small role, if any, in ionoregulation. However, in SW fish, the intestine works to combat passive water loss to the hyperionic environment by absorbing water and excreting ions as salts and therefore is a significant ionoregulatory organ (e.g. Wood and Bucking, 2010). Importantly, both paradigms were based around fasted fish. Recently, researchers have recognized that fasting is not reflective of how these animals exist in nature, as they would feed either opportunistically or on a diurnal cycle (Wood and Bucking, 2010). As diets may contain large quantities of ions (e.g. Taylor and Grosell, 2006a; Wood et al., 2007b; Klinck et al., 2007; Bucking and Wood, 2006a, b, 2007; D'Cruz and Wood, 1998; Kjoss et al., 2005; Baldisserotto et al., 2006; Wood et al., 2010; reviewed by Wood and Bucking, 2010), the role of dietary ions in ion regulation has undergone increasing amounts of investigation.

Once a meal is ingested and enters the alimentary canal, digestion begins. During the process of digestion gastric secretions containing acids, bile, water, and digestive enzymes enter the lumen of the gut to help break down the ingested food, and free up ions to be absorbed across the intestinal mucosa and into the blood, briefly elevating levels within the plasma before being regulated by homeostatic mechanisms (e.g. Mg^{2+}, Oikari and Rankin, 1985; Ca^{2+}, Baldisserotto et al., 2004; reviewed by Wood and Bucking, 2010). Once in the blood, ions that are not utilized or stored are filtered out by the kidneys and excreted as urine (McDonald and Grossell, 2006;

reviewed by Grossell, 2010). The importance of dietary levels of various ions such as Na^+, K^+, Zn^{2+}, Ca^{2+}, PO_4^-, and Mg^{2+} have been investigated in both FW- and SW-acclimated fish.

3.1.1 : Dietary Intake of Ions is Essential for Growth and Survival

It was long assumed that the diet of fish played only a minor role in the acquisition of essential ions (Wood and Bucking, 2010). This assumption has since been challenged and largely disproven through studies investigating the effects of feeding fish isocaloric and isonitric diets containing varied ion concentrations and observing how these impact the overall health of fish, including growth rates, feeding rates, and survival, as well as the transcription of genes thought to be involved in the regulation and transport of those ions such as Na^{2+} (e.g. Gatlin et al., 1992; Smith et al., 1989, 1995; Salman and Eddy, 1988; Mzengereza and Kang'ombe, 2015), K^+ (e.g. Shearer, 1988; Wilson and El Naggar, 1992; Shiau and Hsieh, 2001a, 2001b; Liang et al., 2014; Zhu et al., 2014), Zn^{2+} (e.g. Spry et al., 1989; Prabhu et al., 2017, 2018; Akram et al., 2019; Watanabe et al., 1993; National Research Council, 2011; Tacon, 1992; Lall et al., 2002; Rider et al., 2010), Ca^{2+} (e.g. Hossain and Yoshimatsu, 2014; Song et al., 2017; Robinson et al., 1986; Zafar and Khan; 2019; Hossain and Furuichi, 1998, 1999a, b, 2000a, b; Ogino and Takeda, 1976; Watanabe et al., 1980), and PO_4^- (e.g. Zafar and Khan, 2018; Lall, 2002; Roy and Lall, 2003; Shen et al., 2016; Xie et al., 2016; Yao et al., 2014; Bureau and Cho, 1999; Mai et al., 2006; Avila et al., 2000). While all the above ions are essential for animal health, many go beyond the scope of my study. I have therefore only included specific examples of studies involving dietary Na^+, Mg^{2+}, both directly relevant to this study, and Ca^{2+}, as it is thought to serve similar physiological functions to Mg^{2+} and is also divalent.

The importance of dietary Na^+ intake in fish is dependent on the ionic composition of the environment (e,g, salinity, pH), and species-specific characteristics. In FW acclimated teleosts,

ions are passively lost through diffusion to the hypoionic environment across membranes such as the gills, excreted from the intestine, and small amounts are lost to the environment in the urine (reviewed by Evans et al., 2005). As a result, these fish must actively absorb ions from the environment across their gills, or from the food they eat (e.g. Evans et al., 2005; Wood and Bucking, 2011).

In the euryhaline red drum (*Sciaenops ocellatus*), for example, it was demonstrated that FW-acclimated fish experienced increased growth and feed efficiency when NaCl was added into the diet, whereas no significant improvements to growth or feed efficiency were seen in fish acclimated to 6ppt brackish water, and no significant improvement to growth but a significant decrease in feed efficiency was observed in fish acclimated to 35ppt SW, suggesting that dietary sodium may play an essential role in ionoregulation when the ionic composition of the environment is insufficient to compensate for diffusive losses across the gills and through the urine (Gatlin et al., 1992). Smith et al. (1989) demonstrated in FW salmonids that under conditions where food is readily available such as in the summertime or in captivity, dietary uptake of Na^+ occurs at a similar rate to branchial uptake, but in the winter, when less food is available, or under fasted conditions in the laboratory, branchial uptake of Na^+ is greater than dietary uptake (Smith et al., 1989). Ingested Na^+ in rainbow trout (*Oncorhynchus mykiss*) is rapidly absorbed across the intestine, with faecal concentrations of Na^+ being low, even when fish were fed high-Na^+ diets (Salman and Eddy, 1988), and increased dietary salt loads led to increased branchial Na^+ efflux with reduced branchial Na^+ influx (Smith et al., 1995). Absorption of Na^+ across the intestine is not only important for balancing Na^+ levels within the blood, but the increased expression and activity of Na^+/K^+-ATPase (Nka) within the gut also influences the expression and function of various other enzymes that rely on Na^+ gradients to

drive the movement of other ions and molecules such as carbohydrates and amino acids across the intestinal mucosa and into the blood, which may explain improvements in growth and feed efficiency in FW fish fed diets supplemented with NaCl (Mzengereza and Kang'ombe, 2015).

Calcium (Ca^{2+}) also serves a variety of key physiological roles in fish including growth, influencing cellular permeability, mineralization of bones and scales, nerve signalling, muscle contraction, blood clotting, and osmoregulation (Hossain and Yoshimatsu, 2014; Song et al., 2017). The primary sites of Ca^{2+} absorption in fish are the gills and intestines (Flik and Verbost, 1993). It was long assumed that the Ca^{2+} requirement of fish was met solely by absorption across the gills and skin, especially in marine environments (Robinson et al., 1986). The ability of fish to acquire sufficient environmental Ca^{2+} through branchial transport seems to be largely species-specific, making dietary Ca^{2+} supplementation essential for certain fish species, regardless of environmental salinity (Zafar and Khan; 2019).

For example, in certain species of marine fish such as the tiger puffer (*Takifugu rubripes*), giant croaker (*Nibea japonica*), scorpion fish (*Sebastiscus marmoratus*), and Japanese sea bass (*Lateolabrax japonicus*), dietary Ca^{2+} requirements have been reported (Hossain and Furuichi, 1998, 1999a, 2000a; Song et al., 2017, respectively). In FW fish, many species have a dietary requirement for Ca^{2+} due to low environmental concentrations, however, certain species such as chum salmon (*Oncorhynchus keta*) and common carp (*Cyprinus carpio*) have been reported as not having a dietary Ca^{2+} requirement (Ogino and Takeda, 1976; Watanabe et al., 1980, respectively), so long as the amount of ambient Ca^{2+} is sufficient such as in hard water (Hossain and Yoshimatsu, 2014). Consequently, in soft water environments such as those surrounding the Canadian Shield, Scandinavia, and the Amazon basin (e,g, Rodgers 1984;

Gonzalez et al., 2005; reviewed by Wood and Bucking, 2011), dietary Ca^{2+} uptake would be comparatively more important.

It has been shown that the diet may contribute over half of the required Mg^{2+} that FW fish use to survive, with only a small amount coming from the environment (Bijvelds et al., 1998; reviewed by Wood and Bucking, 2011), and when fish are fed diets that lack sufficient Mg^{2+}, health complications such as reduced growth and increased mortality have been documented. In fact, multiple studies have demonstrated that when insufficient dietary Mg^{2+} is provided, the gills were unable to absorb enough Mg^{2+} from the surrounding water to sufficiently compensate for the loss in dietary Mg^{2+} (e.g. Shim and Ng, 1988; Ogino and Chiou, 1976; Ogino et al., 1978; Gaitlin et al., 1982). In contrast, dietary Mg^{2+} in saltwater acclimated fish does not demonstrate any net absorption from the GIT (Bucking et al., 2009), likely reflecting the increased (excess) amount of environmental Mg^{2+} available.

The absorption of Mg^{2+} across the intestinal mucosa in fish is thought to occur via both active and passive processes in a region-specific manner (e.g. Bucking and Wood 2007; Kodzhahinchev et al., 2018) with the anterior regions of the gut having a higher amount of passive transport, and the posterior regions having more active transport (Bucking and Wood, 2007; Kodzhahinchev et al., 2018). It has also been demonstrated that when FW goldfish (*C. auratus*) are fed a diet rich in Mg^{2+}, the amount of transcellular absorption seems to decrease (Kodzhahinchev et al., 2018) and the presence of *slc41a1* mRNA increased in response to elevated dietary Mg^{2+} (Kodzhahinchev et al., 2017).

The specific mechanisms of Mg^{2+} transport from dietary sources in fish have yet to be fully elucidated. This is despite a growing body of evidence detailing the importance of acquiring sufficient Mg^{2+} (Chapter 1) as well as the importance of the diet in osmo- and

ionoregulatory processes (Reviewed by Wood and Bucking, 2011). Kodzhahinchev et al. (2017) suggested the involvement of Slc41a1 in the transport of dietary Mg^{2+} across intestinal cells by demonstrating significant decreases in intestinal *slc41a1* expression after FW goldfish (*C. auratus*) were fed diets containing decreased levels of Mg^{2+}. Though these findings have provided useful and novel insights into the transport of Mg^{2+} from ingested food, they only provide a part of the picture when it comes to Mg^{2+} homeostasis in fish. Other genes believed to be involved in Mg^{2+} transport in teleosts, such as *trpm6/7*, *cnnm3*, and *slc41a2/a3* have only received attention in the context of salinity acclimation experiments, or alterations in environmental concentrations of Mg^{2+}. These findings, while invaluable to our understanding of Mg^{2+} homeostasis in teleosts, do not properly account for the large role of the diet in the absorption of Mg^{2+} in these animals. The purpose, therefore, of this chapter was to address the largely understudied roles of Slc41a1/a2, Trpm7, and Cnnm3 on the transport of dietary Mg^{2+} in sailfin mollies by comparing gene expression in the gills, kidneys, and intestines of fish acclimated to 0ppt FW or 35ppt SW fed either a control diet of commercial pellets, or a Mg^{2+}-rich diet.

Based on previous findings on the influence of environmental salinity on the expression of these transporters, as well as the models that I developed and presented in Chapter 2, it was hypothesized that the expression of the transporters of interest would change in response to additional dietary Mg^{2+}. Based on my predictive models (Figures 2-4), I predicted that *slc41a1/a2* should be upregulated to support their role in excretion, whereas *cnnm3* and *trpm7* should be downregulated to decrease absorption. I further hypothesized that environmental salinity would have an impact on how the expression of my target genes would change in response to increased dietary Mg^{2+}. I predicted that dietary Mg^{2+} supplementation would have a

greater affect on gene expression in FW- acclimated fish than in SW-acclimated fish due to a decrease in intestinal divalent cation permeability in SW acclimated fish. Finally, I hypothesized that increasing the amount of dietary Mg^{2+} would lead to changes in the plasma Mg^{2+}, predicting that there would be a rapid increase in plasma Mg^{2+} followed by a decrease back to physiological concentrations driven by regulation of my target genes.

3.2 : Materials and Methods

3.2.1 : Animal Husbandry

Animals were housed in glass aquaria as detailed in Chapter 2.2.

3.2.2 : Dietary Manipulations

To determine the impact of dietary magnesium on transporter expression, adult sailfin mollies were separated randomly and equally into 4 testing groups following a 21-day acclimation to laboratory conditions. Control and Mg^{2+}-rich diets were prepared following the protocol of Kodzhahinchev et al. (2017). Mg^{2+} contents of control and test diets were measured using ISME (see Chapter 2.2.7 for detailed ISME protocol). Commercial pellets were ground in a mortar and pestle, mixed into a paste using reverse osmosis (RO) water, and passed through a syringe before being baked for 24h at 65°C. Baked food was then broken into pellets of similar size to commercial pellets and stored at -20°C before use. Animals were fed a quantity of pellets pertaining to the size of the fish (~5% body mass) in each respective tank at the same time each day and given 30 minutes to feed. Fish were divided into 4 groups: FW-acclimated fish fed commercial pellets ([Mg^{2+}] =781.06± 10.98 μmol/g dry weight), FW-acclimated fish fed a Mg^{2+}-rich diet (commercial pellets with 110mmol Mg^{2+} added), SW-acclimated fish fed commercial pellets, and SW-acclimated fish fed a Mg^{2+}-rich diet. Feeding trials were carried out over the span of 7 days. At 3 and 7 days of each treatment, fish were sampled from each tank at random (N=4), and gills, kidneys, and intestines (divided into anterior and posterior segments) were sampled.

3.2.3 : Primer Design and Optimization

Primers were designed and optimized according to the protocol detailed in Chapter 2.2 with no modifications. Refer to table 1 for primer sequences and PCR conditions.

3.2.4 : RNA Extraction, cDNA Synthesis, and qPCR Analysis

RNA extraction, cDNA synthesis and qPCR reactions were carried out according to the protocols detailed in Chapter 2.2.

3.2.5 : Determining Plasma Mg^{2+} Concentration

Quantification of plasma Mg^{2+} levels for each test group were carried out according to the protocol detailed in Chapter 2.2.

3.2.6 : Predicting Structure of Mg^{2+} Transporters

Structural predictions for Slc41a1, Slc41a2, and Cnnm3 were generated using the I-TASSER server (Yang et al., 2015) using the I-TASSER method (Wu et al, 2007; Zhang, 2007; reviewed by Zhang, 2008). Amino acid sequences of target proteins (retrieved from the Ensembl genome browser) in sailfin mollies and a commonly used mammalian model for comparison (*M. musculus*) were input into the I-TASSER server where they were threaded through a representative PDB structure library (pairwise sequence identity cut-off set to 70%) to determine the most likely folding of the structure using a combination of the hidden Markov model (Karplus et al., 1998), PSI-BLAST (Altschul et al., 1997), and aligned using the Needleman-Wunsch and Smith-Waterman alignment algorithms (Needleman and Wunsch, 1970; Smith and Waterman, 1981, respectively). Continuous fragments are then used to reassemble full-length models while discontinuous fragments are modelled using *ab initio* modeling (Zhang et al.,

2003). The conformational space of the structure was then predicted using replica-exchange Monte Carlo Simulations (Zhang et al., 2003) and trajectories were clustered by SPICKER (Zhang and Skolnick, 2004a). Generated PDB structures were then searched by the TM-align program to generate a more accurate simulation of the structure (Zhang and Skolnick, 2005). Reliability of predicted structures were determined using C-Score (Zhang and Skolnick, 2004b), TM-Score (Zhang and Skolnick, 2004c), and RMSD (Root Mean Square Deviation) (Kabsch, 1976).

3.2.7 : Statistics

Statistical analyses were carried out in Sigmaplot 14.5 (Systat). For all data, normality, homogeneity of variance, and Grubb's tests were carried out as specified in Chapter 2.2. If the data passed normality and homogeneity of variance tests, a two-way ANOVA analysis was carried out on the data to test for statistical significance using time and diet as the two independent variables. Tukey's posthoc test for multiple pairwise comparisons was used on statistically significant results ($p<0.05$ for all tests).

3.3 : Results

3.3.1 : Integrative Effects of Diet and Environment on Transporter Expression

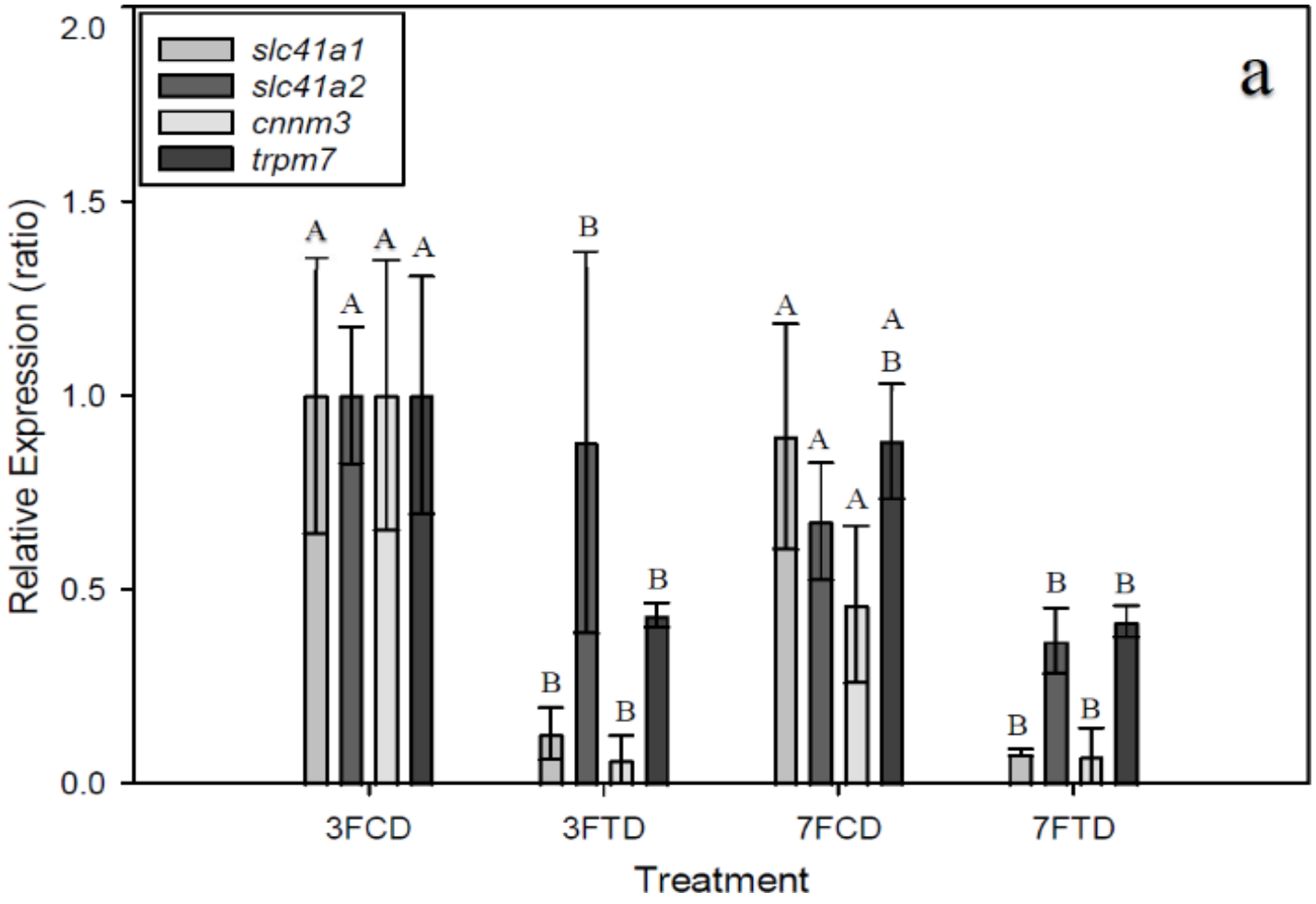

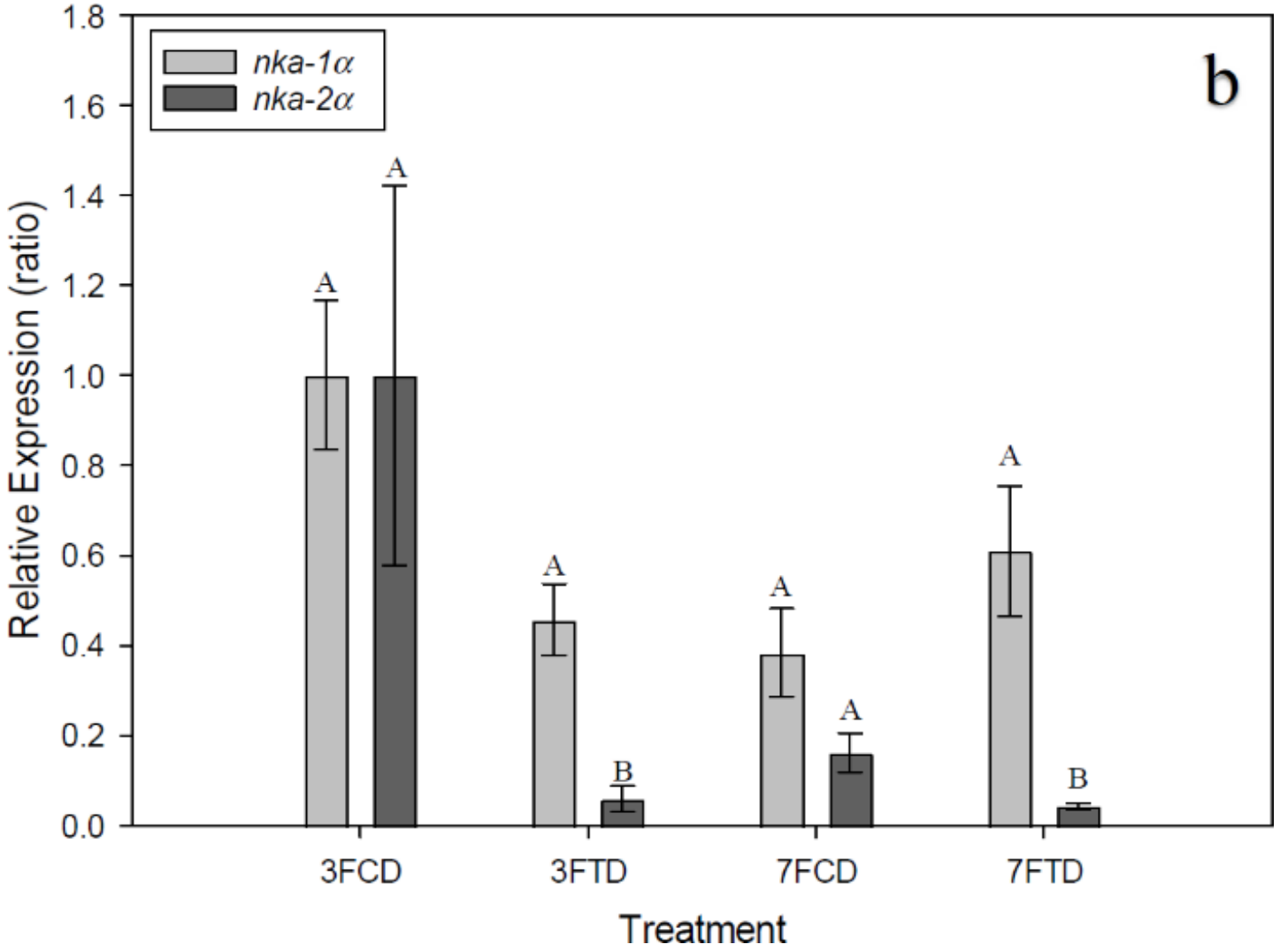

Figure 15: Relative mRNA expression of Mg^{2+} transporters (a) and *nka* isoforms (b) in the gills of *P. latipinna* in 0ppt FW at 3 and 7 days of consuming either a control diet (CD; $[Mg^{2+}]$ = 781.06± 10.98 µmol/g dry weight) or a Mg^{2+}-rich diet (TD; Control diet + 110mmol $MgCl_2$) (n=4). Bars represent the mean ± SEM of the ratio of gene expression when compared to the 3-day control group (set to 1.00). Statistical significance was determined using 2-way ANOVA (diet x time) followed by Tukey's post hoc test for multiple pairwise comparisons. Bars that do not share the same letter are significantly different from one another ($p<0.05$). Comparisons between genes were not made.

Significant decreases in the expression of *slc41a1*, *cnnm3*, and *trpm7* were observed in the gills of FW-acclimated fish after 3 days of consuming a Mg^{2+}-rich diet ($P<0.001$, $P=0.008$, $P<0.001$, $P=0.025$, respectively), a decrease that was maintained after 7 days of consuming the test diet (Figure 15a). Further, at 7 days, *slc41a2* had also significantly decreased (Figure 15a). No significant interactions between diet and time were observed for the magnesium transporters (Figure 15a). Levels of *nka-1α* did not change in response to consumption of a Mg^{2+}-rich diet ($P=0.331$), or to time of exposure ($p=0.164$), however there was a significant interaction between diet and time ($P=0.03$). Expression of *nka-2α* decreased significantly in response to the test diet ($P=0.002$) after 3 days, with no significant effects of time being observed ($P=0.253$) or any interaction between factors ($P=0.155$) (Figure 15b).

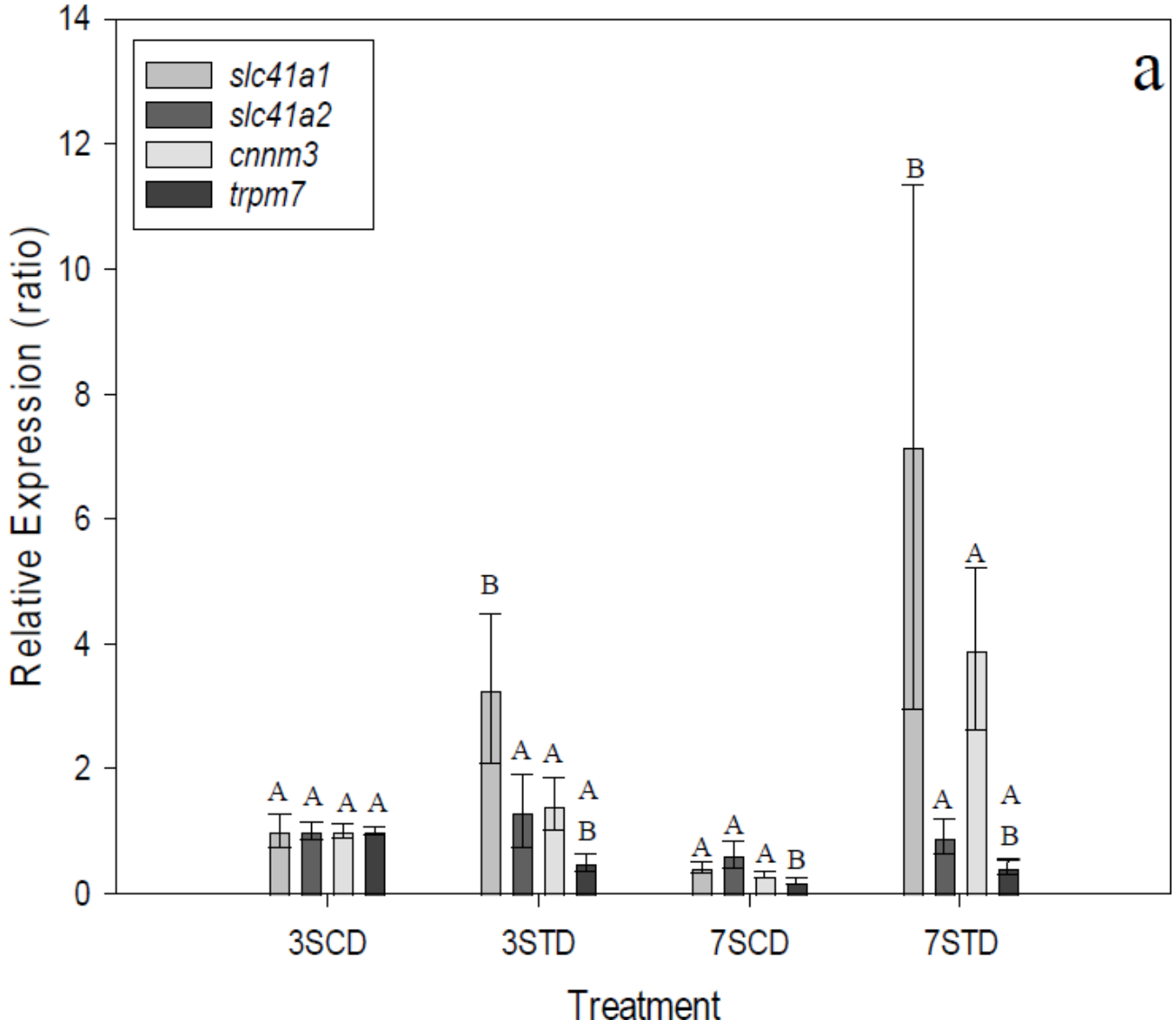
a
slc41a1
slc41a2
cnnm3
trpm7
Relative Expression (ratio)
0
2
4
6
8
10
12
14
A A A A
B A A A B
A A A B
B A A A B
3SCD
3STD
7SCD
7STD
Treatment

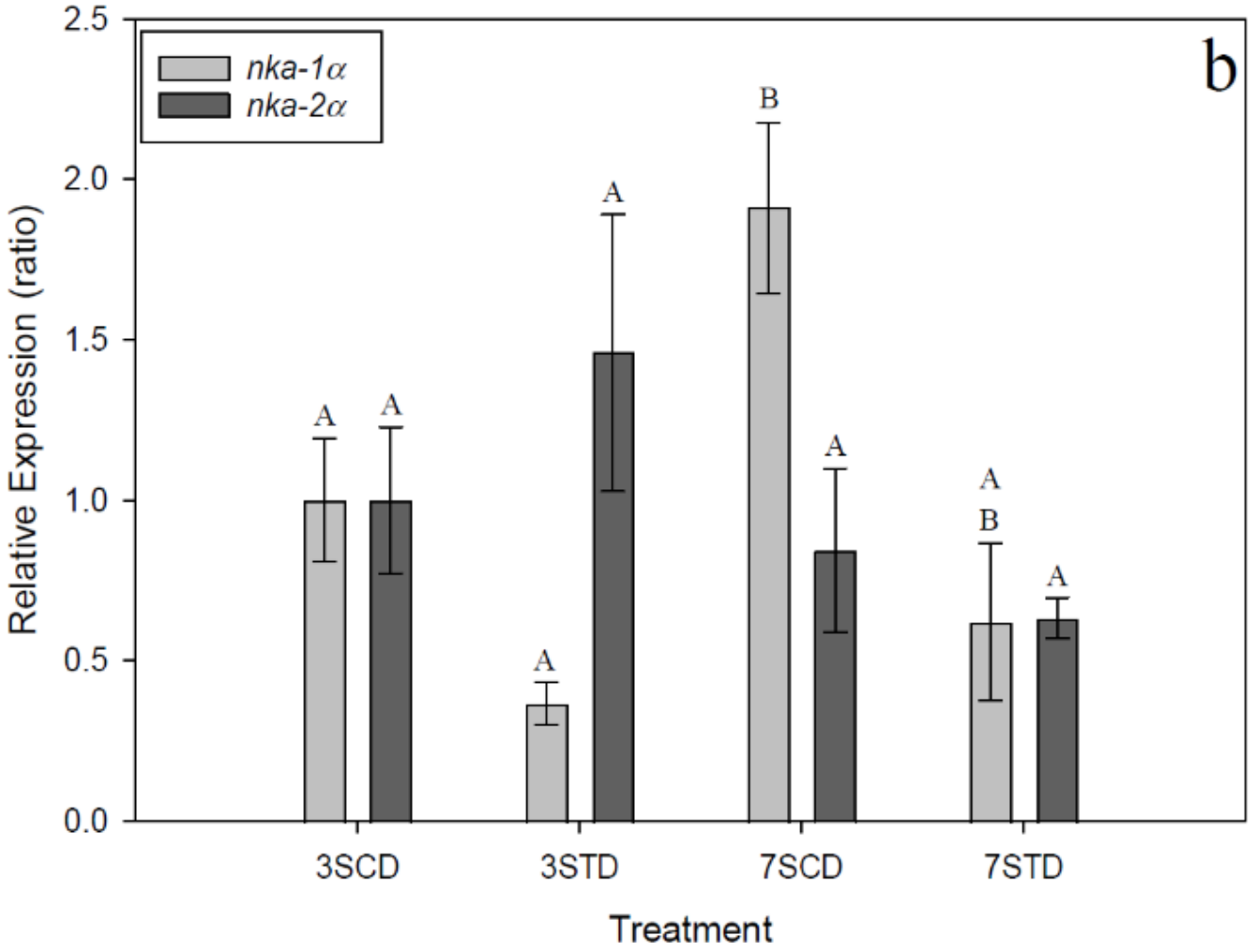

Figure 16: Relative mRNA expression of Mg^{2+} transporters (a) and *nka* isoforms (b) in the gills of *P. latipinna* in 35ppt SW at 3 and 7 days of consuming either a control diet (CD; $[Mg^{2+}]$ = 781.06± 10.98 µmol/g dry weight) or a Mg^{2+}-rich diet (TD; Control diet + 110mmol $MgCl_2$) (n=4). Bars represent the mean ± SEM of the ratio of gene expression when compared to the 3-day control group (set to 1.00). Statistical significance was determined using 2-way ANOVA (diet x time) followed by Tukey's post hoc test for multiple pairwise comparisons. Bars that do not share the same letter are significantly different from one another. Comparisons between genes were not made.

In SW- acclimated fish, *slc41a1* expression in the gills of fish fed the test diet was significantly higher than the levels seen in the control group (P=0.042), with no significant influence of time (P=0.668) or interaction of diet and time (P=0.978). No significant changes in the expression of *slc41a2* or *cnnm3* were observed in the gills of SW-acclimated fish fed either diet (P=0.498, P=0.524, respectively). No influence of time (P=0.385, P=0.245, respectively) or interaction between diet and time (P=0.976, P=0.613, respectively) was observed for either *slc41a2* or *cnnm3*. *trpm7* expression was not affected by dietary manipulations in the gills of SW-acclimated fish (P=0.312), however expression did significantly decrease in response to the time of exposure (P=0.007). A significant interaction between factors was observed for *trpm7* (P=0.019) (Figure 16a). *nka-1α* expression increased after 7 days in SW (P=0.039). The influence of diet was also determined to be significant (P=0.033), with no significant interaction between diet and time was observed (P=0.769). *nka-2α* expression did not change in the gills of SW-acclimated fish after 7 days of consuming either diet (diet: p=0.872; time: P=0.152; diet x time: P=0.493) (Figure 16b).

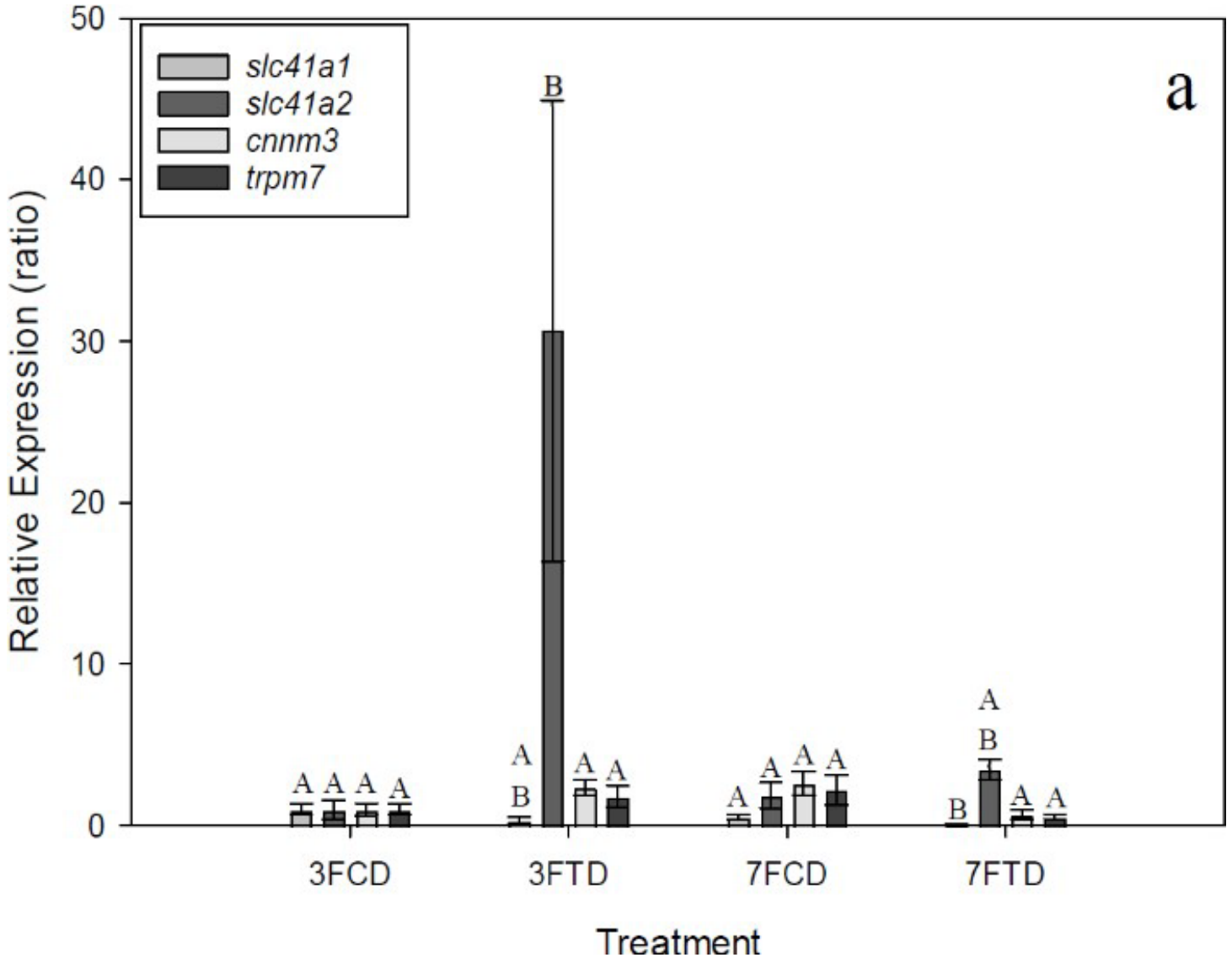
slc41a1
slc41a2
cnnm3
trpm7
a
Relative Expression (ratio)
50
40
30
20
10
0
A A A A
A B
B
A A
A A A A
B A B
A A
3FCD
3FTD
7FCD
7FTD
Treatment

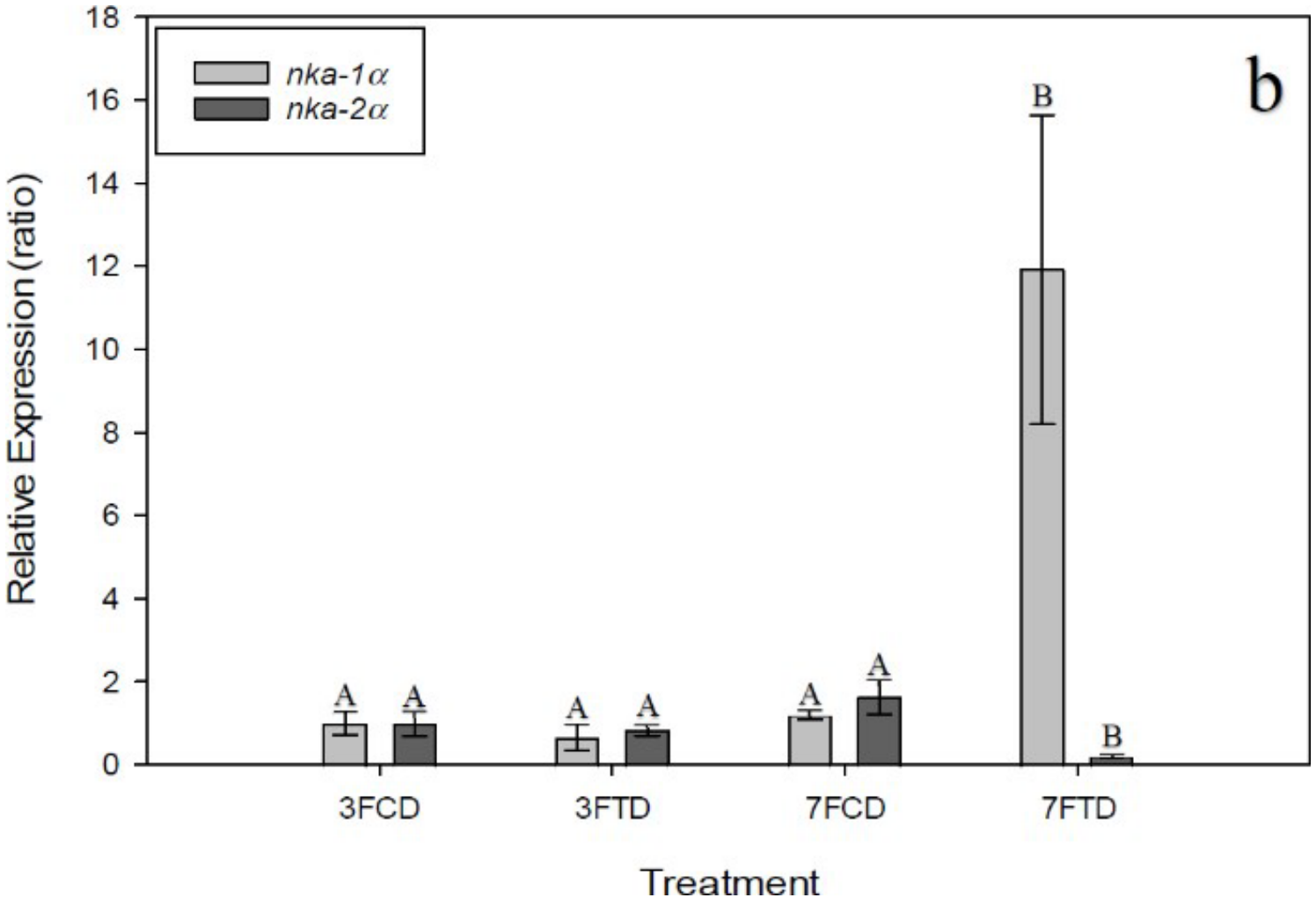

Figure 17: Relative mRNA expression of Mg^{2+} transporters (a) and *nka* isoforms (b) in the anterior intestines of *P. latipinna* in 0ppt FW at 3 and 7 days of consuming either a control diet (CD; [Mg^{2+}] = 781.06± 10.98 µmol/g dry weight) or a Mg^{2+}-rich diet (TD; Control diet + 110mmol $MgCl_2$) (n=4). Bars represent the mean ± SEM of the ratio of gene expression when compared to the 3-day control group (set to 1.00). Statistical significance was determined using 2-way ANOVA (diet x time) followed by Tukey's post hoc test for multiple pairwise comparisons. Bars that do not share the same letter are significantly different from one another ($p<0.05$). Comparisons between genes were not made.

In the anterior intestines of FW-acclimated fish, quantities of *slc41a1* mRNA decreased significantly after 7 days of consuming a Mg^{2+}-rich diet (P=0.043). *slc41a1* expression was not affected by time (P=0.205), and no interaction between diet and time was observed (P=0.652). Quantities of *slc41a2* mRNA significantly increased with dietary treatments (P=0.007), but the results were not affected by time (P=0.667). There was no significant interaction between factors for *slc41a2* (P=0.168). No significant changes were observed in *cnnm3* mRNA in this tissue (diet: P=0.634; time: P=0.955, respectively). *Trpm7* expression was also unchanged, with no statistically significant changes observed due to diet (P=0.869), or time (P=0.928), and no interaction between factors (P=0.498) (Figure 17a). Levels of *nka-1α* mRNA significantly increased after 7 days of consuming the test diet (P<0.001), whereas levels of *nka-2α* mRNA significantly decreased after 7 days of receiving the test diet (P=0.011) (Figure 17b). There were significant interactions between diet and time in the cases of both *nka* isoforms (P=0.031, P=0.015, respectively), so either time or dietary Mg^{2+} could have driven these changes.

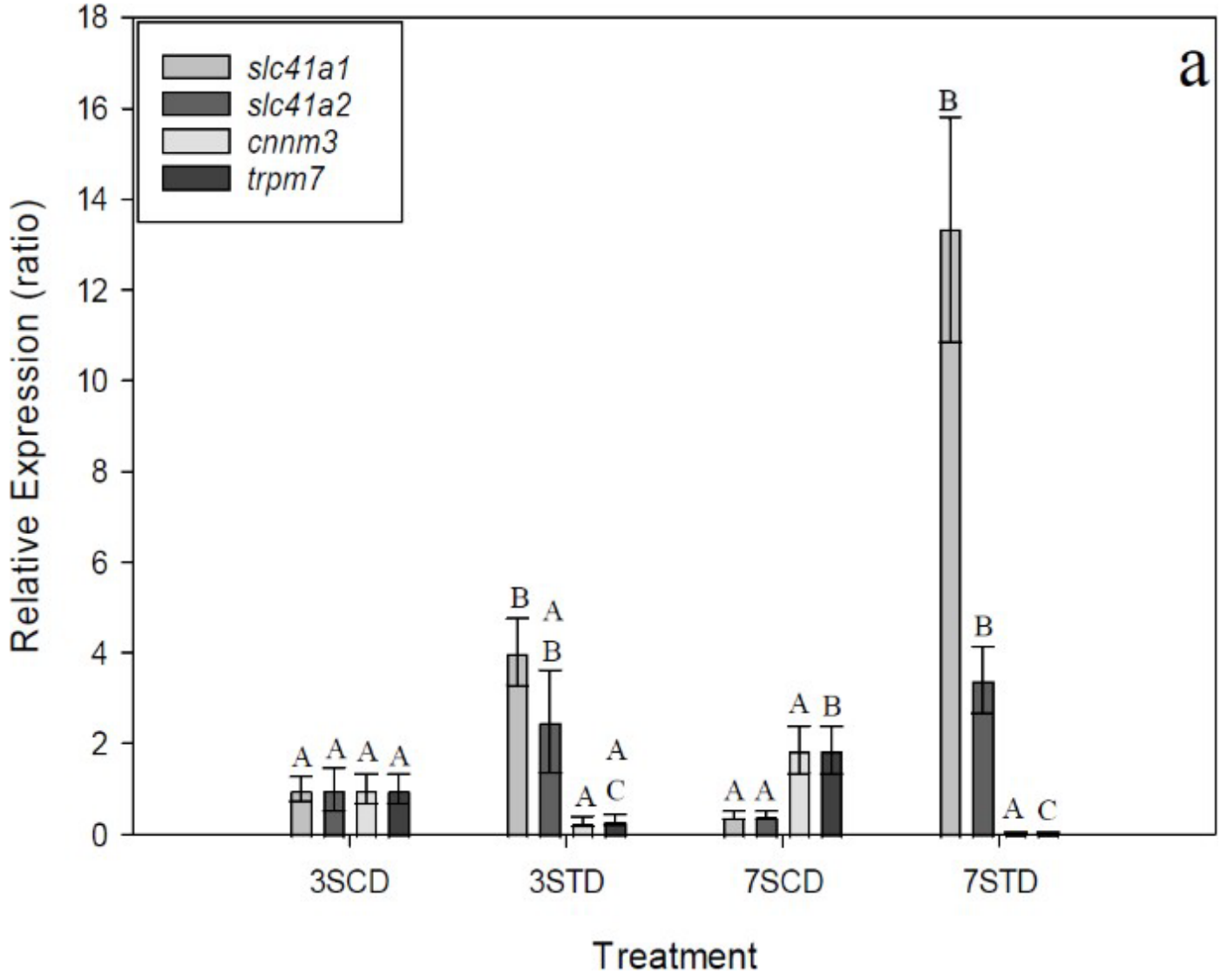
a
slc41a1
slc41a2
cnnm3
trpm7
Relative Expression (ratio)
0
2
4
6
8
10
12
14
16
18
A A A A
B A
B
A C
A A
A B
B
B
A C
3SCD
3STD
7SCD
7STD
Treatment

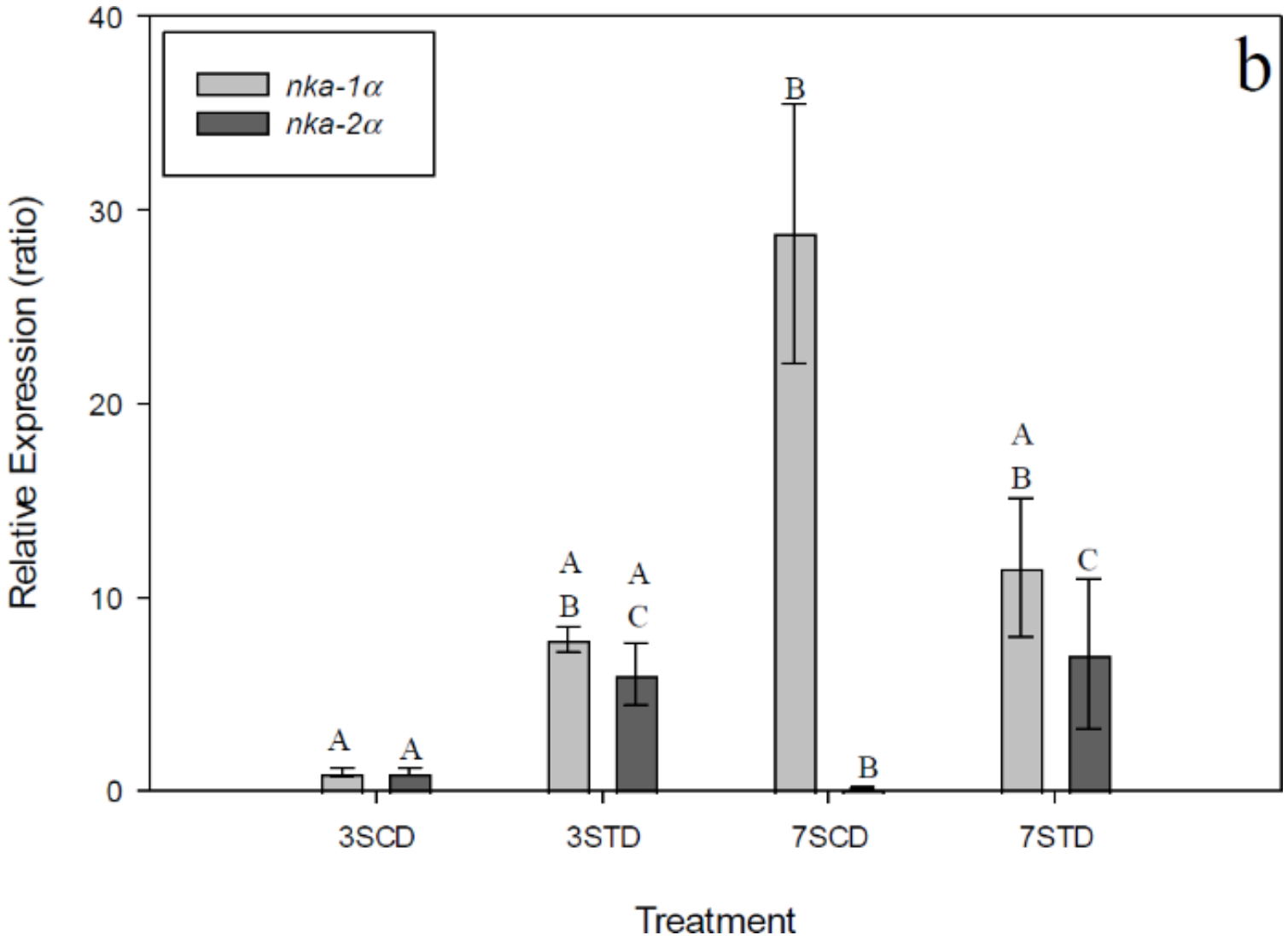

Figure 18: Relative mRNA expression of Mg^{2+} transporters (a) and *nka* isoforms (b) in the anterior intestines of *P. latipinna* in 35ppt SW at 3 and 7 days of consuming either a control diet (CD; $[Mg^{2+}]$ = 781.06± 10.98 µmol/g dry weight) or a Mg^{2+}-rich diet (TD; Control diet + 110mmol $MgCl_2$) (n=4). Bars represent the mean ± SEM of the ratio of gene expression when compared to the 3-day control group (set to 1.00). Statistical significance was determined using 2-way ANOVA (diet x time) followed by Tukey's post hoc test for multiple pairwise comparisons. Bars that do not share the same letter are significantly different from one another. Comparisons between genes were not made.

In the anterior intestines of SW-acclimated fish, the expression of *slc41a1* mRNA increased significantly in response to dietary Mg^{2+} (P=0.003: Figure 18a), but no significant influence of time on expression was observed (P=0.978). No significant interaction was observed between diet and time for *slc41a1* (P=0.096). Likewise, *slc41a2* expression in the anterior intestine increased significantly after 7 days of consuming the test diet. These changes were attributed to increased dietary Mg^{2+} (P=0.014) and not time (P=0.333). No significant interaction between diet and time was observed for *slc41a2* (P=0.146). A significant change in *cnnm3* mRNA was observed in response to time (P<0.001), and diet (P<0.001), however a significant interaction between factors (P=0.002) made it difficult to determine the main cause of these changes. *Trpm7* expression significantly increased after 7 days of exposure to the control diet (P=0.001), but a significant decrease from the 3-day control group was observed after 7 days of consuming the test diet (P=0.048). No significant interaction between diet and time was observed (P=0.054) (Figure 18a). Consuming a Mg^{2+}-rich diet did not result in a significant change in *nka-1α* expression after 7 days (P=0.946), however exposure to SW for 7 days when consuming the control diet resulted in a significant increase in its expression (P=0.016). A significant interaction between diet and time was observed for *nka-1α* (0.019) and therefore an accurate determination of cause for the change in expression could not be reliably determined. *nka-2α* expression increased significantly after 7 days of consuming either diet, with an observed decrease in expression between 3 and 7 days of the control treatment (P=0.018), and an increase in between the 3-day control group and 7-day test group (P<0.001). No significant interaction between diet and time was observed for *nka-2α* (P=0.148) (Figure 18b).

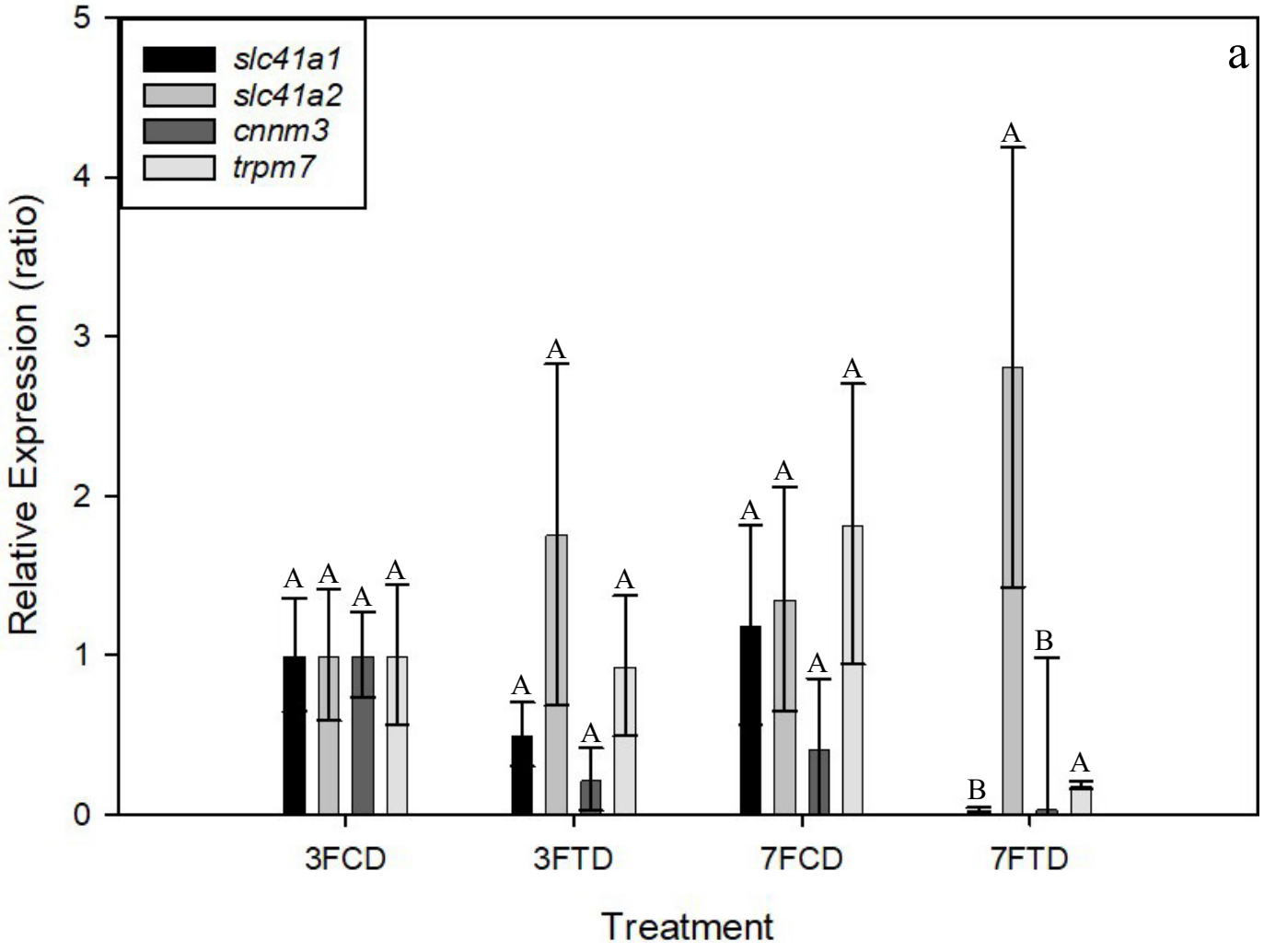
a
slc41a1
slc41a2
cnnm3
trpm7
Relative Expression (ratio)
0
1
2
3
4
5
A A A A
A A A
A A A
B B A
3FCD
3FTD
7FCD
7FTD
Treatment

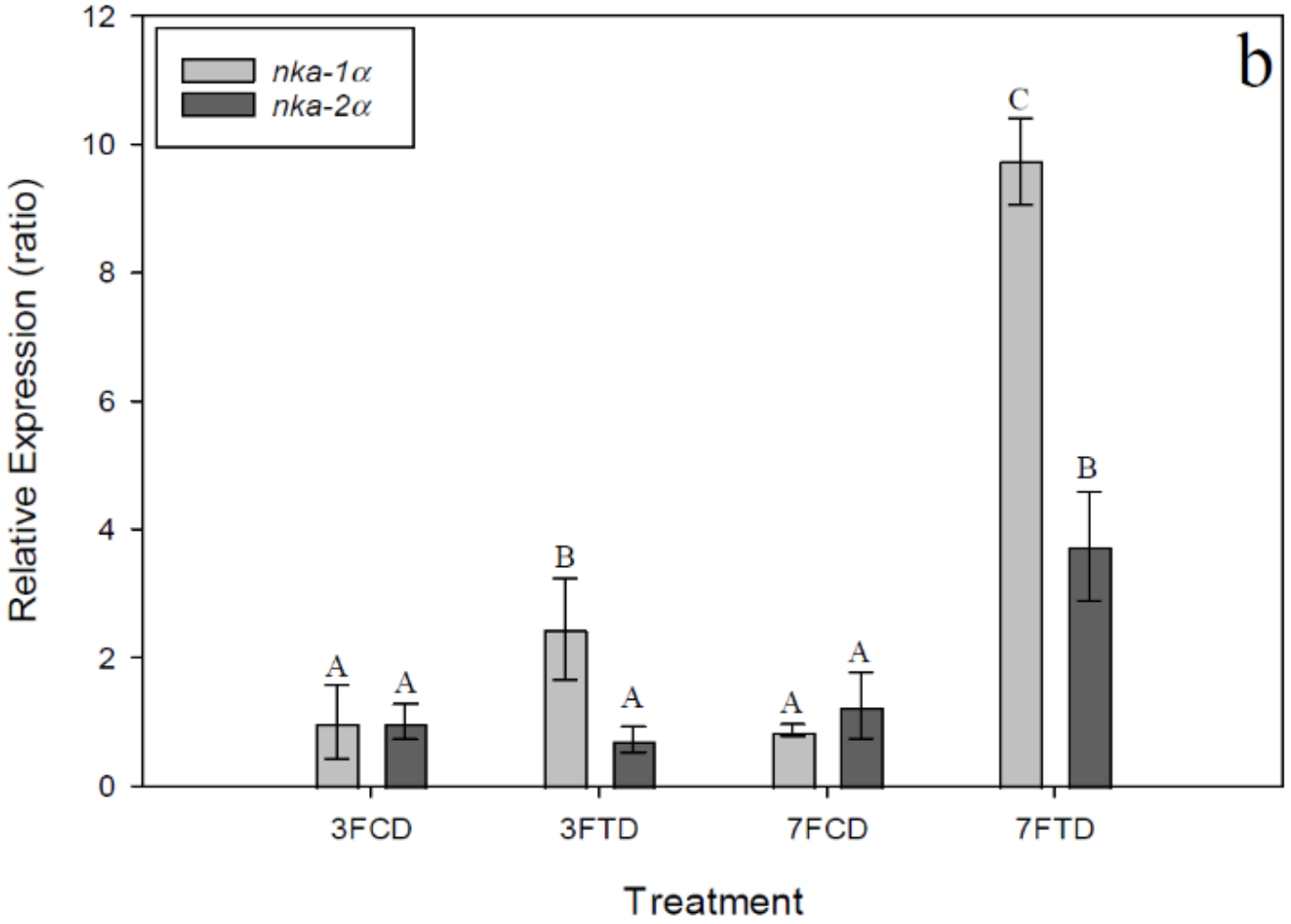

Figure 19: Relative mRNA expression of Mg^{2+} transporters (a) and *nka* isoforms (b) in the posterior intestines of *P. latipinna* in 0ppt FW at 3 and 7 days of consuming either a control diet (CD; [Mg^{2+}] = 781.06± 10.98 µmol/g dry weight) or a Mg^{2+}-rich diet (TD; Control diet + 110mmol $MgCl_2$) (n=4). Bars represent the mean ± SEM of the ratio of gene expression when compared to the 3-day control group (set to 1.00). Statistical significance was determined using 2-way ANOVA (diet x time) followed by Tukey's post hoc test for multiple pairwise comparisons. Bars that do not share the same letter are significantly different from one another. Comparisons between genes were not made.

In the posterior intestine of FW-acclimated *P. latipinna*, *slc41a1* levels significantly decreased by 7 days in response to dietary Mg^{2+} (P=0.006) and time (P=0.023) with no significant interaction between the two factors (P=0.304). *cnnm3* expression also decreased significantly after consuming the test diet for 7 days (P=0.034) with no significant impact of time (P=0.749) or interaction between diet and time (P=0.148). No significant changes in quantities of *trpm7* mRNA were observed in this tissue (Time: P=0.558; Diet: P=0.176; Diet x Time: P=0.100) (Figure 19a). *slc41a2* levels remained consistent within this tissue after consuming additional dietary Mg^{2+} (P=0.431), regardless of time (P=0.300), and no significant interaction between factors was observed (P=0.233) (Figure 19a). Expression of *nka-1α* increased significantly after 3 days of consuming the Mg^{2+}-rich diet (P=0.028) and increased again between 3 and 7 days of the test diet (P=0.013). These changes were attributed to either diet (P<0.001) and time (P=0.019), but no significant interaction between factors was observed (P=0.178). *nka-2α* levels also increased after 7 days of consuming the test diet. The observed changes could have been due dietary Mg^{2+} (P=0.008), or time (P=0.018), but a significant interaction between factors made determining the cause of these changes difficult (P=0.038) (Figure 19b).

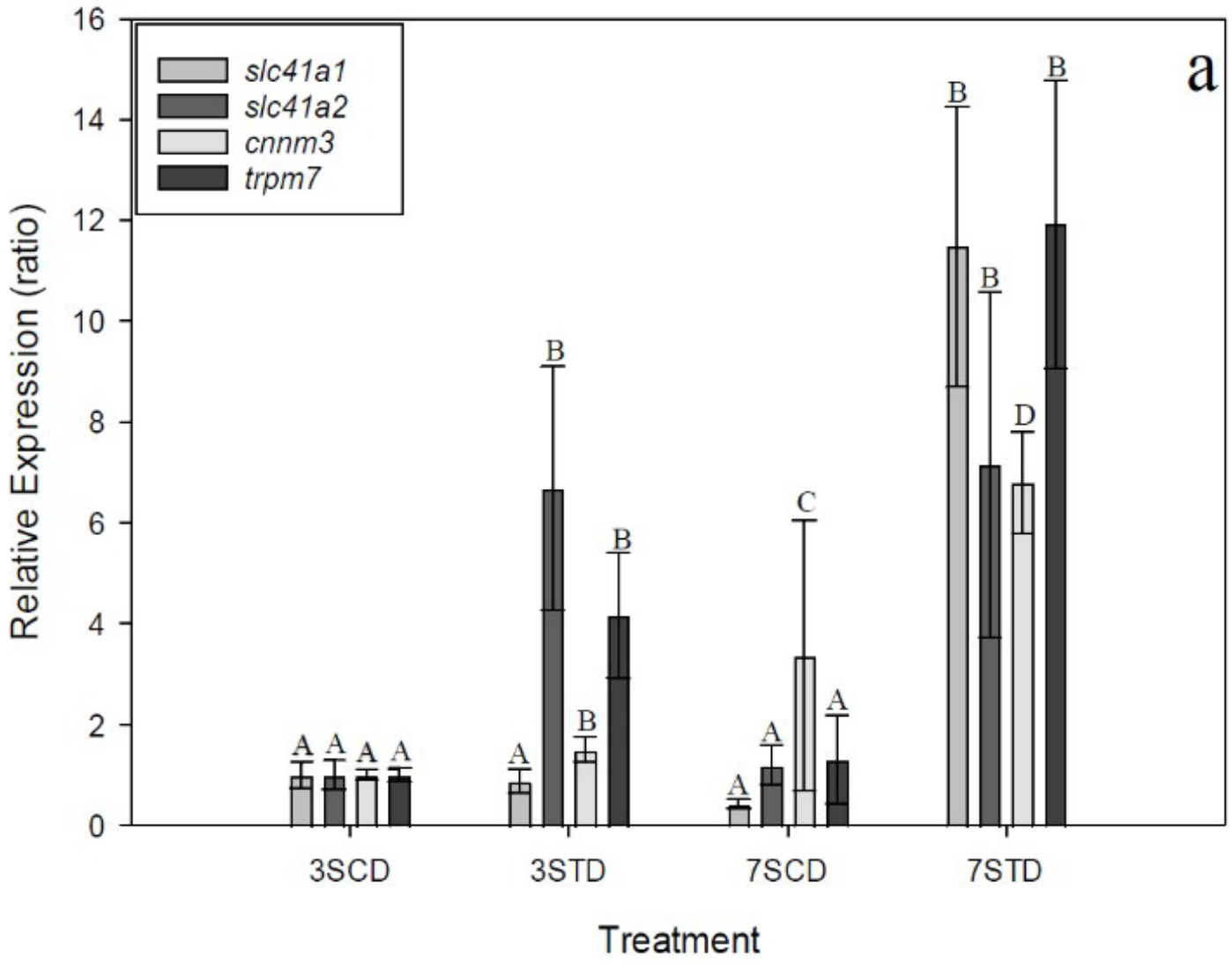
a
slc41a1
slc41a2
cnnm3
trpm7
Relative Expression (ratio)
0
2
4
6
8
10
12
14
16
A A A A
A B B B
A A C A
B B D B
3SCD
3STD
7SCD
7STD
Treatment

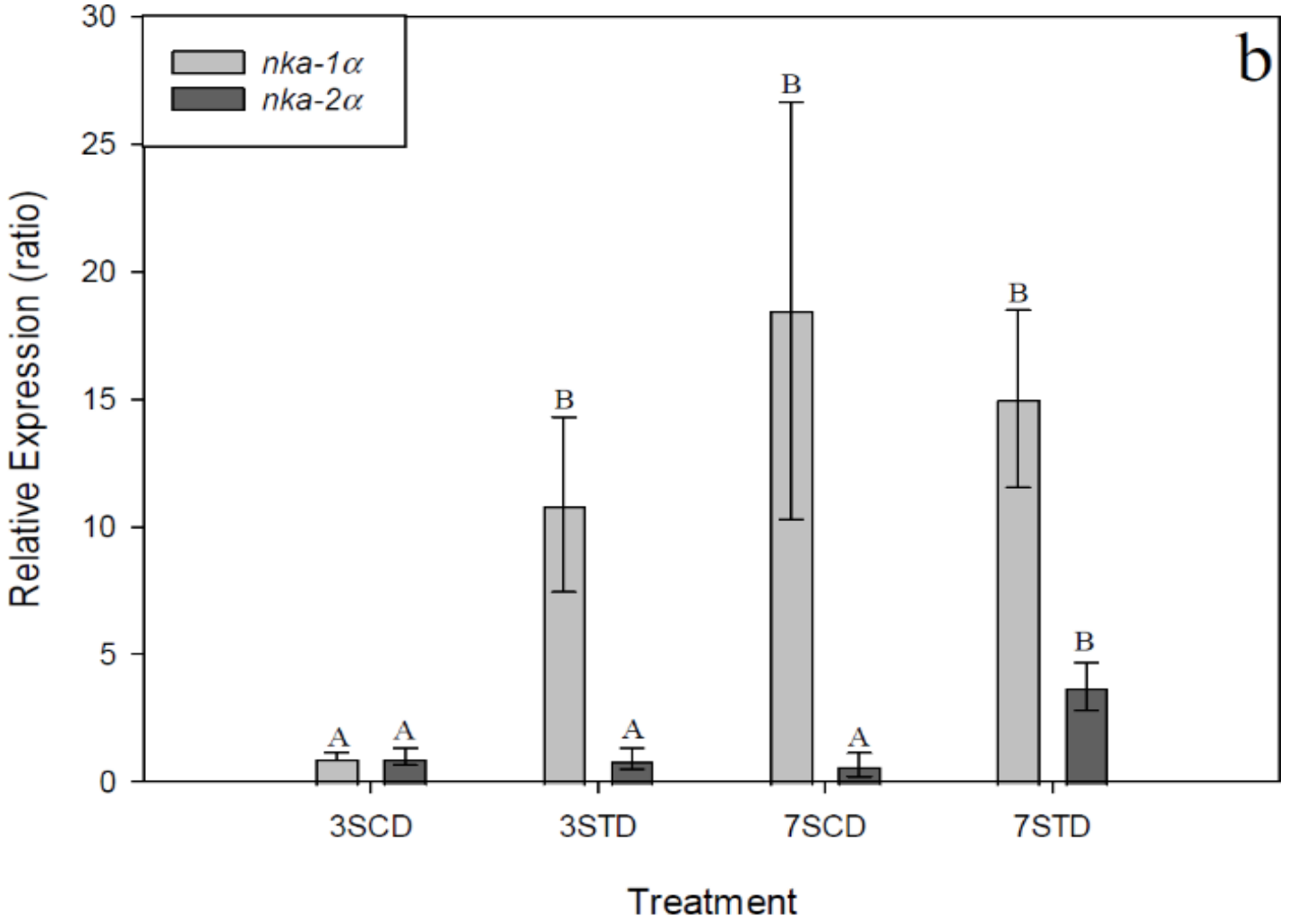

Figure 20: Relative mRNA expression of Mg^{2+} transporters (a) and *nka* isoforms (b) in the posterior intestines of *P. latipinna* in 35ppt SW at 3 and 7 days of consuming either a control diet (CD; $[Mg^{2+}]$ = 781.06± 10.98 µmol/g dry weight) or a Mg-rich diet (TD; Control diet + 110mmol $MgCl_2$) (n=4). Bars represent the mean ± SEM of the ratio of gene expression when compared to the 3-day control group (set to 1.00). Statistical significance was determined using 2-way ANOVA (diet x time) followed by Tukey's post hoc test for multiple pairwise comparisons. Bars that do not share the same letter are significantly different from one another. Comparisons between genes were not made.

In the posterior intestines of SW-acclimated fish, *slc41a1* expression increased significantly after 7 days. Diet ($P<0.001$) and time ($P=0.028$) were both determined to be significant, and a significant interaction between diet and time ($P<0.001$) was observed. A significant increase in *slc41a2* mRNA was observed within 3 days of consuming the test diet ($P=0.040$). No significant effect of time ($P=0.852$) or interaction between factors ($P=1.000$) were observed. Significant differences in *cnnm3* mRNA were observed between all 4 tested groups. There was a significant effect of time ($P<0.001$), diet ($P<0.001$) and a significant interaction between factors ($P<0.001$) making the cause of these changes difficult to determine. *trpm7* mRNA significantly increased in response to increased dietary Mg^{2+} ($P=0.007$) with no significant impact of time ($P=0.957$), or significant interaction between the two factors ($P=0.138$) (Figure 20a). *nka-1α* expression was significantly higher in the 3-day test group than it was in the 3-day control group ($P=0.019$) with no significant changes between the 3-day and 7-day test groups ($P=0.368$). Interestingly, a significant increase could also be seen when comparing 3-day and 7-day control groups ($P=0.007$). No significant interaction between diet and time of exposure was observed for *nka-1α* ($P=0.155$). *nka-2α* expression was significantly higher than all other groups after 7 days of receiving the test diet ($P=0.038$). Time was not considered to be a significant factor in this change in expression ($P=0.963$), however there was a significant interaction between diet and time ($P=0.015$) (Figure 20b)

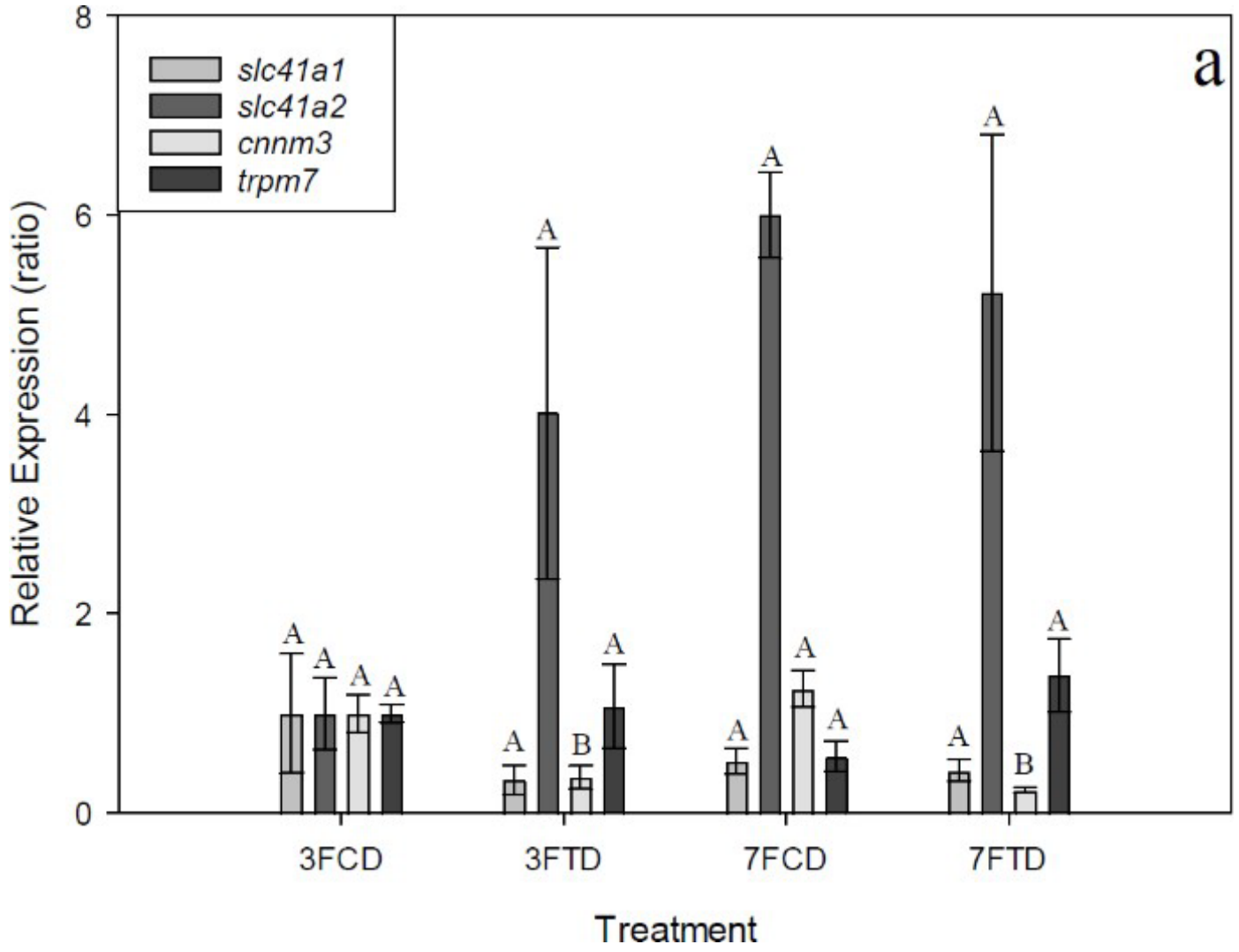
a
slc41a1
slc41a2
cnnm3
trpm7
Relative Expression (ratio)
0
2
4
6
8
A
A
A
A
A
B
A
A
A
A
A
A
A
B
A
3FCD
3FTD
7FCD
7FTD
Treatment

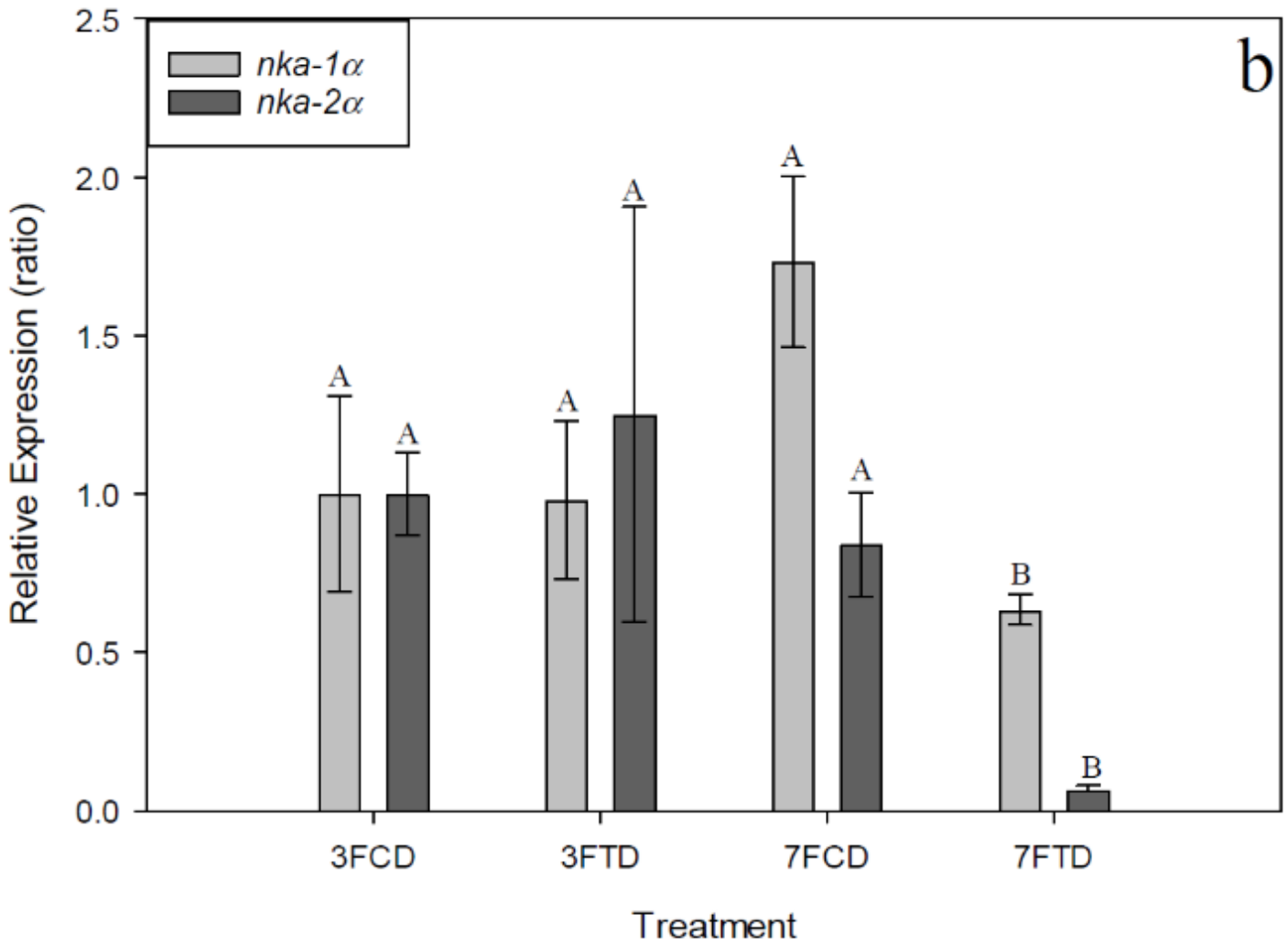

Figure 21: Relative mRNA expression of Mg^{2+} transporters (a) and *nka* isoforms (b) in the kidneys of *P. latipinna* in 0ppt FW at 3 and 7 days of consuming either a control diet (CD; $[Mg^{2+}]$ = 781.06± 10.98 µmol/g dry weight) or a Mg^{2+}-rich diet (TD; Control diet + 110mmol $MgCl_2$) (n=4). Bars represent the mean ± SEM of the ratio of gene expression when compared to the 3-day control group (set to 1.00). Statistical significance was determined using 2-way ANOVA (diet x time) followed by Tukey's post hoc test for multiple pairwise comparisons. Bars that do not share the same letter are significantly different from one another. Comparisons between genes were not made.

In the kidneys of FW-acclimated fish, consuming a Mg^{2+}-rich diet for 7 days did not lead to a significant change in *slc41a1* expression (Time: P=0.542; Diet: P=0.344; Diet x Time: P=0.545) (Figure 21a). *slc41a2* expression within this tissue was also unchanged (Diet: P=0.090; Time: P=0.514; Diet x Time: P=0.279) (Figure 21a). A significant decrease in *cnnm3* mRNA was observed in between the control and test groups. The change in expression was attributed to diet (P<0.001), with no significant differences in between time points for either diet group (P=0.745) and no significant interaction between diet and time was observed (P=0.300) (Figure 21a). Diet (P=0.299) and time (P=0.772) did not result in a significant change in the expression of *trpm7* mRNA throughout 7 days of dietary manipulations, however a statistically significant interaction between diet and time was observed (P=0.03) (Figure 21a). 7 days of consuming the test diet led to a significant decrease in the expression of *nka-1α* mRNA. Time was a significant contributor to these changes (P=0.007), but diet was not (P=0.345) however there was a significant relationship between diet and time (P=0.001) (Figure 21b). A significant decrease in the level of *nka-2α* mRNA was also observed in the 7-day test group, however it was not attributed to diet (P=0.068) or time (0.414). Again, a significant interaction between factors was observed (P=0.022) (Figure 21b).

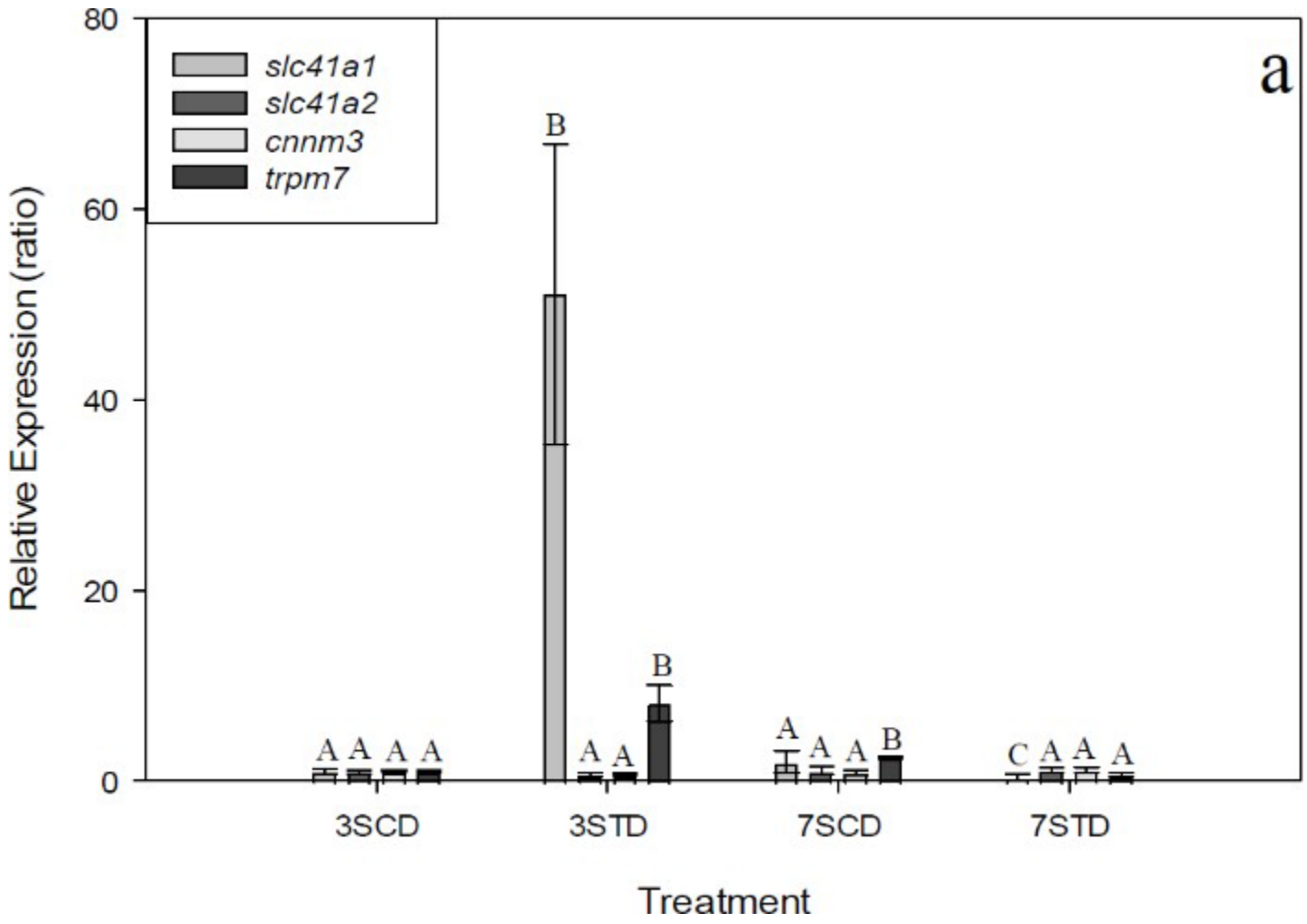
a
slc41a1
slc41a2
cnnm3
trpm7
Relative Expression (ratio)
80
60
40
20
0
A A A A
B
A A
B
A A A B
C A A A
3SCD
3STD
7SCD
7STD
Treatment

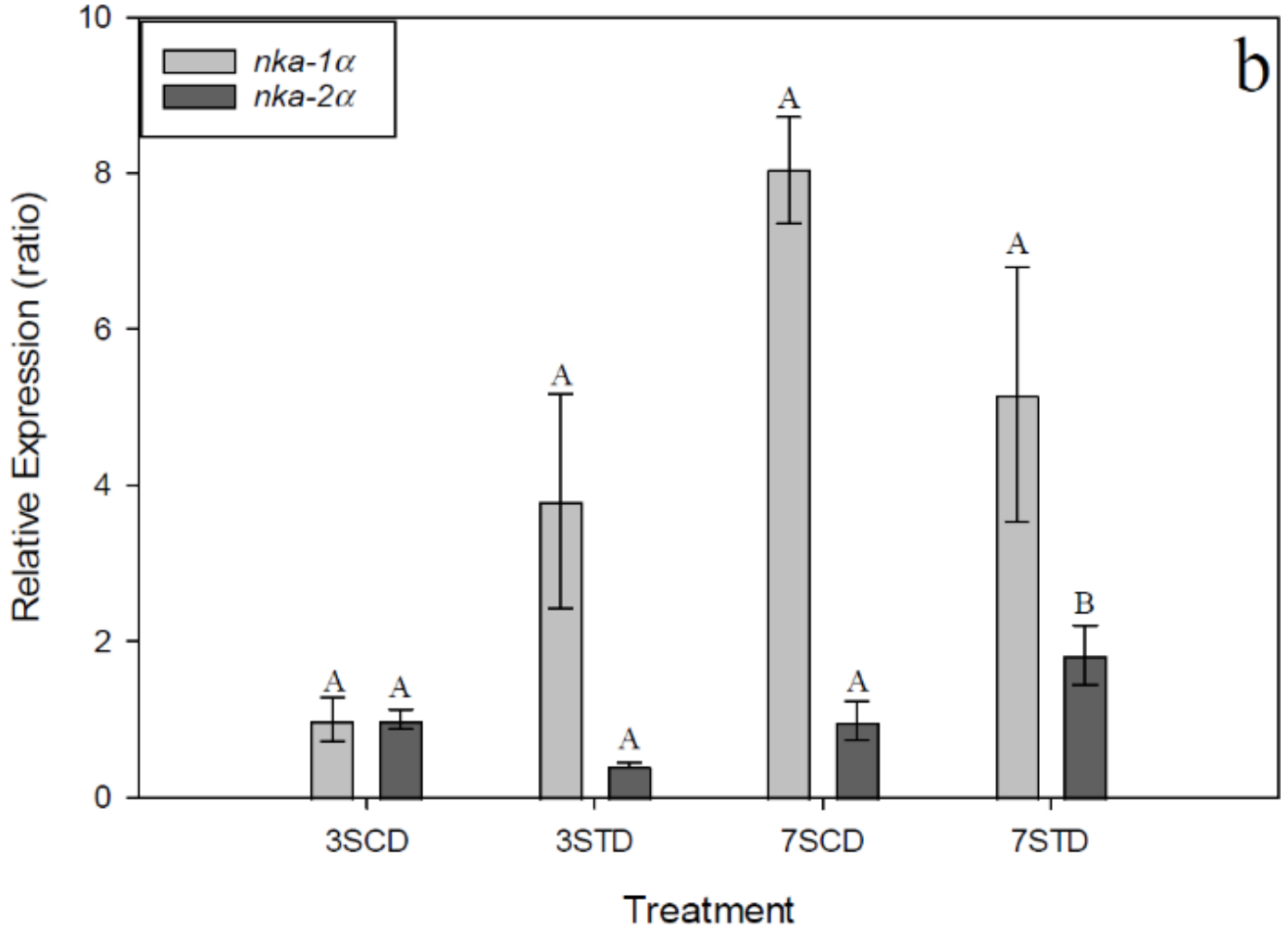

Figure 22: Relative mRNA expression of Mg^{2+} transporters (a) and *nka* isoforms (b) in the kidneys of *P. latipinna* in 35ppt SW at 3 and 7 days of consuming either a control diet (CD; $[Mg^{2+}]$ = 781.06± 10.98 µmol/g dry weight) or a Mg^{2+}-rich diet (TD; Control diet + 110mmol $MgCl_2$) (n=4). Bars represent the mean ± SEM of the ratio of gene expression when compared to the 3-day control group (set to 1.00). Statistical significance was determined using 2-way ANOVA (diet x time) followed by Tukey's post hoc test for multiple pairwise comparisons. Bars that do not share the same letter are significantly different from one another. Comparisons between genes were not made.

In the kidneys of SW-acclimated fish, *slc41a1* expression significantly increased after 3 days of consuming a Mg^{2+}-rich diet ($P<0.001$). Interestingly, after 7 days of consuming the test diet, the expression of *slc41a1* mRNA decreased significantly from the 3-day test group ($P<0.001$) to a level significantly lower than the 7-day control group ($P=0.045$). A significant interaction between diet and time was observed ($P<0.001$), therefore these changes may have been caused by either factor or both (Figure 22a). *slc41a2* quantities in the kidneys of SW-acclimated fish were not affected by dietary Mg^{2+} (Diet: $P=0.711$; Time: $P=0.472$; Diet x Time: $P=0.616$). *cnnm3* mRNA did not significantly change in the kidneys throughout this experiment (Diet: $P=0.461$; Time: $P=0.986$; Diet x Time: $P=0.202$) (Figure 22a). Consuming additional dietary Mg^{2+} led to a significant increase in *trpm7* quantities ($P<0.001$). Interestingly, *trpm7* expression was higher in the 7-day control group than in the 3-day control group ($P=0.036$). After consuming the test diet for 7 days, *trpm7* levels normalized back to control levels ($P<0.001$). Time of exposure had a significant effect on *trpm7* expression in the kidneys of SW-fish ($P=0.020$), and no significant effect of diet was detected ($P=0.269$) however a significant interaction between diet and time was detected ($P<0.001$) (Figure 22a). *nka-1α* expression did not change significantly in the kidneys of SW-acclimated fish after 7 days of receiving the test diet (Diet: $P=0.066$; Time: $P=0.677$; Diet x Time: $P=0.252$). The level of *nka-2α* mRNA was not significantly different in between the test and control groups after 3 days of feeding ($P=0.186$). Relative quantities of *nka-2α* in the 7-day test group was significantly higher than the levels observed in the 7-day control group ($P=0.048$). The influence of increased dietary Mg^{2+} was not determined to be significant ($P=0.661$), but there was a significant effect of time on the observed changes ($P=0.030$). A significant interaction between diet and time was also observed for *nka-2α* in the kidneys of SW-acclimated fish ($P=0.026$) (Figure 22b).

3.3.2 : Effects of Environment and Diet on Mg^{2+} Concentrations in Plasma

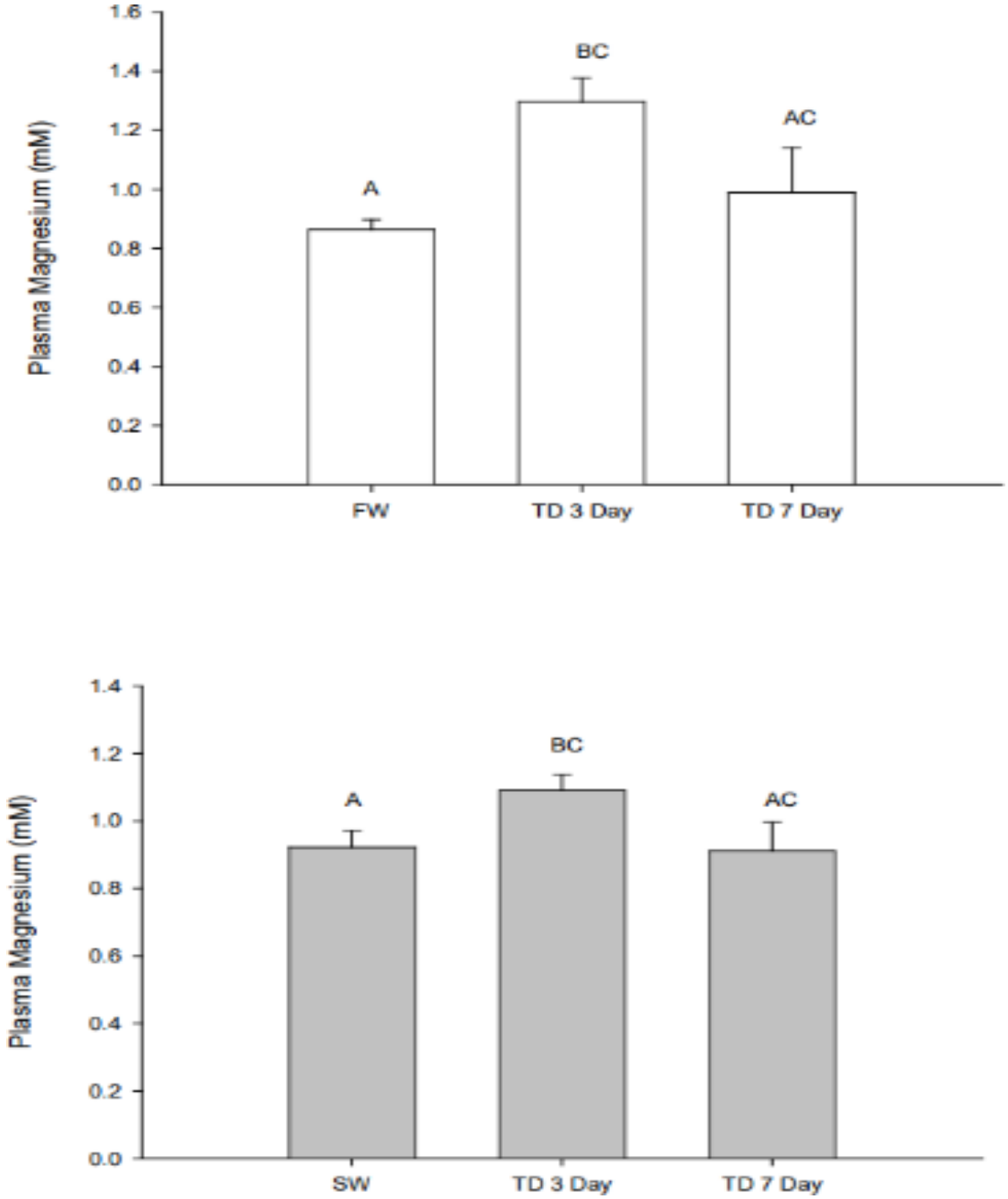

Figure 23: Concentration of Mg^{2+} (mM) in the plasma of *P. latipinna* acclimated to 0ppt FW (top) or 35ppt SW (bottom) at 3 and 7 days of consuming either a control diet (CD; $[Mg^{2+}]$ = 781.06± 10.98 µmol/g dry weight) or a Mg^{2+}-rich diet (TD; Control diet + 110mmol $MgCl_2$) using the Ion-Selective Microelectrode Technique (ISME) on pooled samples of plasma (n=2). Bars represent the mean plasma concentration + SEM. Statistical significance was determined using a 2-way ANOVA (diet x salinity; $p<0.05$), followed by Tukey's post hoc test for multiple pairwise comparisons. Bars that do not share a letter are significantly different from one another.

NOTE: plasma calcium was also measured to ensure that changes observed were not driven by changes in calcium that were being detected by the magnesium ionophore. There were no significant changes in calcium. Data examined but not shown.

It was determined that environmental salinity did not significantly impact the concentration of Mg^{2+} in the blood ($p=0.328$), however consuming a Mg^{2+}-rich diet did lead to a significant increase in the concentration of Mg^{2+} within the plasma of fish acclimated to either salinity treatment ($p=0.009$). No significant interaction between salinity and diet were found in this experiment ($p=0.297$). A post hoc analysis of the data determined that the concentration of Mg^{2+} in the plasma of fish fed a Mg^{2+}-rich diet for 3 days was significantly higher than that of the control group ($p=0.007$). After 7 days of consuming the test diet, the amount of Mg^{2+} in the plasma decreased from the levels measured at 3 days, albeit not significantly ($p=0.075$), to levels seen in the control group ($p=0.780$) (Figure 23).

3.3.3 : Structural Predictions of Mg^{2+} Transporters from Known Amino Acid Sequences

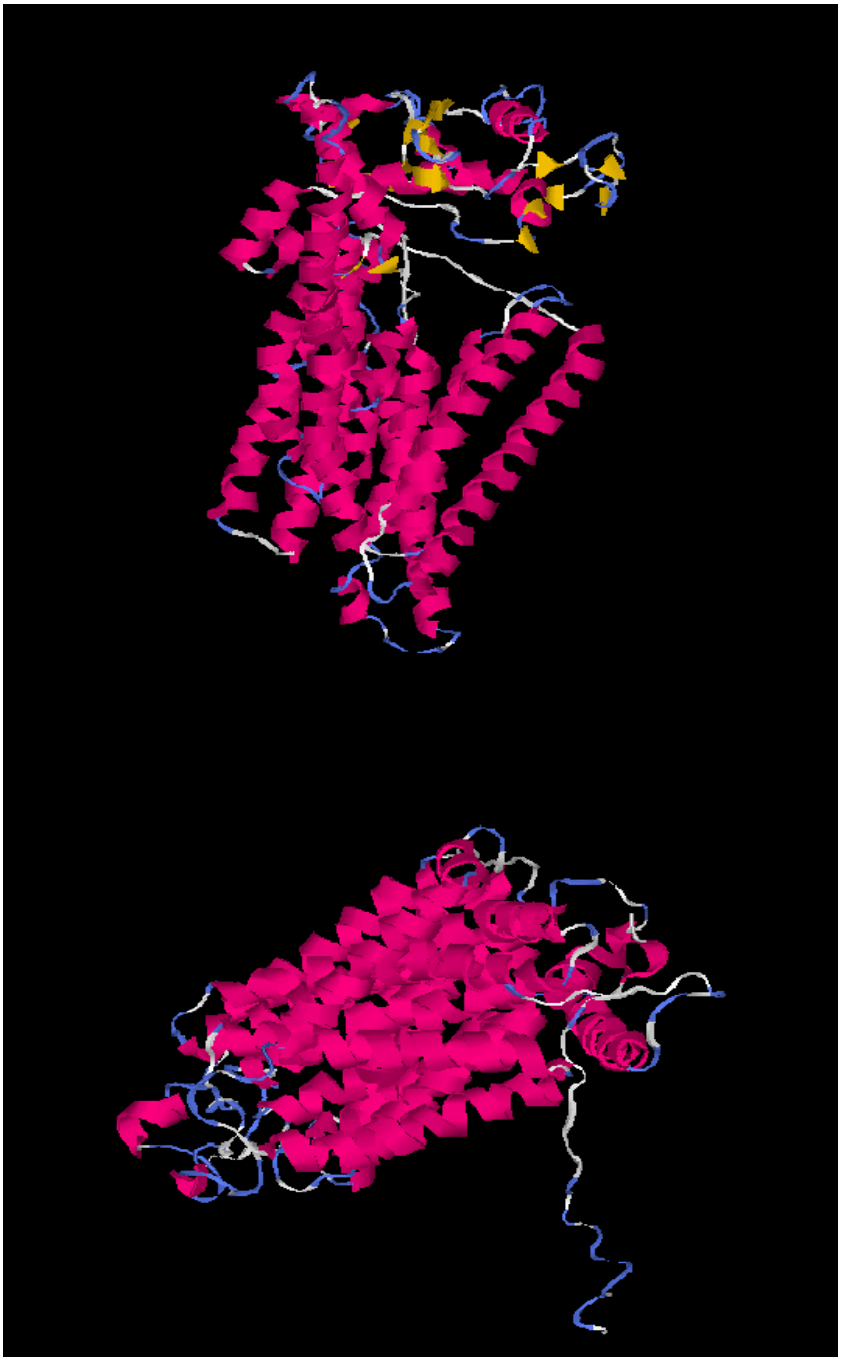

Figure 24: Predicted molecular structure of *slc41a1* in *P. latipinna* (top) and *M. musculus* (bottom) as predicted by I-TASSER (Yang and Zhang, 2015). In *P. latipinna*, the predicted model registered a C-score of -0.49, an estimated TM-score of 0.65±0.15 and an estimated RMSD of 8.6±4.3Å. In *M. musculus*, the predicted model registered a C-score of -1.88, an estimated TM-score of 0.49±0.15 and an estimated RMSD of 11.9±4.4Å. C-score is a quantitative measurement of confidence for a predicted structure and ranges from -5 to 2 where a higher score represents a more accurate prediction. C-score >-1.5 is a model of correct global topology. TM-score and RMSD are predicted based on C-score and overall protein length. TM-scores ≥0.5 can be assumed to have the same topology/fold in SCOP/CATH. RMSD is the root-mean-square deviation of a prediction and higher scores indicate a less reliable prediction.

I-TASSER predictions for *slc41a1* in both *P. latipinna* and *M. musculus* produced proteins with C-scores <-1.50 (-2.07 and -1.96, respectively) and therefore may not be entirely accurate. The TM-scores, however, for each predicted structure (0.47±0.15 and 0.48±0.15, respectively) fall approximately within the acceptable range (TM≥0.5) suggesting the topology of the predicted structures was correct. High RMSD scores (12.5±4.3Å and 12.1±4.4Å, respectively) were given for both predicted structures, suggesting that there may be a region within the predicted protein that did not fold correctly or was mismatched (Figure 24).

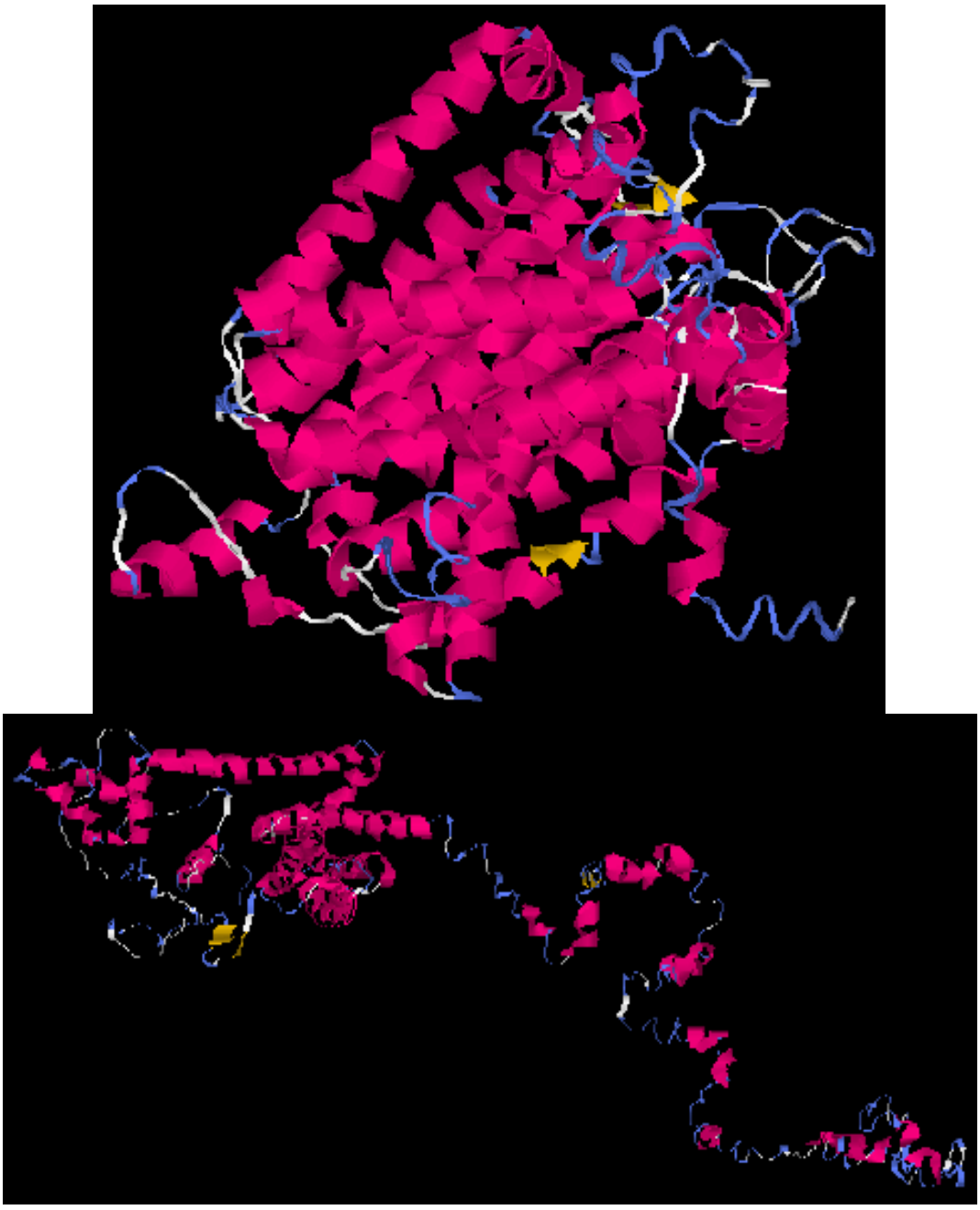

Figure 25: Predicted molecular structure of *slc41a2* in *P. latipinna* (top) and *M. musculus* (bottom) as predicted by I-TASSER (Yang and Zhang, 2015). In *P. latipinna*, the predicted model registered a C-score of -2.77, an estimated TM-score of 0.40±0.13 and an estimated RMSD of 14.5±3.7Å. In *M. musculus*, the predicted model registered a C-score of -1.96, an estimated TM-score of 0.48±0.15 and an estimated RMSD of 12.1±4.4Å. C-score is a quantitative measurement of confidence for a predicted structure and ranges from -5 to 2 where a higher score represents a more accurate prediction. C-score >-1.5 is a model of correct global topology. TM-score and RMSD are predicted based on C-score and overall protein length. TM-scores ≥0.5 can be assumed to have the same topology/fold in SCOP/CATH. RMSD is the root-mean-square deviation of a prediction and higher scores indicate a less reliable prediction.

The predicted molecular structure of *slc41a2* is shown in Figure 25. The predicted structure for this protein in *P. latipinna* produced a C-score of -2.77, a TM-score of 0.40±0.13, and an RMSD of 14.5±3.7Å. The given scores for this prediction suggest a low level of confidence, although the TM-score is high enough that it is unlikely to be an entirely random orientation (TM<0.17 would indicate a random similarity).

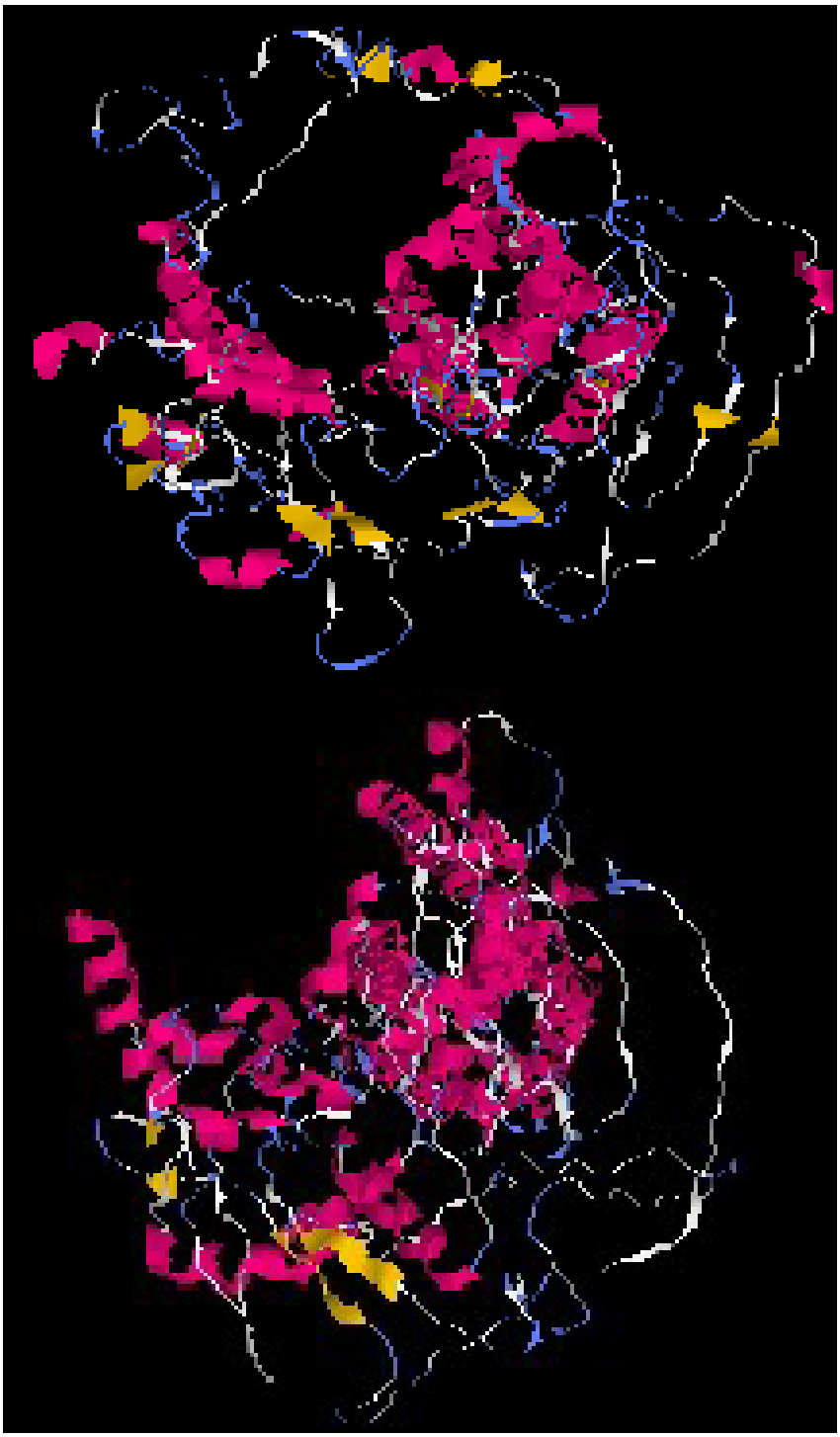

Figure 26: Predicted molecular structure of *cnnm3* in *P. latipinna* (top) and *M. musculus* (bottom) as predicted by I-TASSER (Yang and Zhang, 2015). In *P. latipinna*, the predicted model registered a C-score of -2.18, an estimated TM-score of 0.46±0.15, and an estimated RMSD of 13.6±4.0Å. In *M. musculus*, the predicted model registered a C-score of -1.54, an estimated TM-score of 0.53±0.15 and an estimated RMSD of 11.8±4.5Å. C-score is a quantitative measurement of confidence for a predicted structure and ranges from -5 to 2 where a higher score represents a more accurate prediction. C-score >-1.5 is a model of correct global topology. TM-score and RMSD are predicted based on C-score and overall protein length. TM-scores ≥0.5 can be assumed to have the same topology/fold in SCOP/CATH. RMSD is the root-mean-square deviation of a prediction and higher scores indicate a less reliable prediction.

The structure of *cnnm3* in *P. latipinna* as predicted by I-TASSER (Figure 26; Yang and Zhang, 2015) registered C-score of -2.18, an estimated TM-score of 0.46±0.15, and an RMSD of 13.6±4.0Å. With the given scores, it is likely that the structure is of the correct topology, although the overall prediction quality (as represented by C-score) is lower than desired (C-score≥ -1.50 is ideal). The high RMSD suggests that there may be an error within the prediction.

3.4 : Discussion

3.4.1 : Effects of Diet and Environment on Mg^{2+}in the Plasma

Acclimation of *P. latipinna* to 0ppt FW or 35ppt SW did not lead to significant differences in plasma [Mg^{2+}] when fish were fed a diet of commercial pellets. This was expected, as I had observed this result in a previous experiment (Figure 6, Chapter 2.3.2). I then wanted to determine what effect, if any, consuming a Mg^{2+}-rich diet would have on fish acclimated to either 0ppt FW or 35ppt SW. I hypothesized that consuming additional dietary Mg^{2+} would lead to changes in plasma Mg^{2+} concentrations and predicted that levels would increase as the additional Mg^{2+} was absorbed across the intestines and into the blood. I further predicted that these levels would normalize to maintain homeostasis.

Indeed, under both environmental conditions, increasing dietary Mg^{2+} led to an initial increase in plasma Mg^{2+} levels followed by normalization (Figure 23). Increasing dietary Mg^{2+} has been shown experimentally to be correlated with elevated plasma [Mg^{2+}] in the euryhaline Nile tilapia (*Oreochromis niloticus*) fed a low protein diet (Dabrowska et al., 1989). Further, insufficient dietary Mg^{2+} has been linked to decreased levels of Mg^{2+} in the plasma of carp (*Cyprinus carpio*, Ogino and Chou, 1976), and rainbow trout (*Oncorhynchus mykiss*, Cowey et al., 1977). None of the above studies observed, however, a return to normal values as the time of exposure to the diet increased, perhaps speaking to the ability of sailfin mollies to rapidly regulate internal ion levels. Interestingly, consumption of a Mg^{2+}-rich diet for 28 days did not lead to significant changes in plasma [Mg^{2+}] in goldfish, although changes in renal SLC41a1 expression during their experiment may suggest that increased urinary output of Mg^{2+} effectively normalized any changes in plasma Mg^{2+} (Kodzhahinchev et al., 2017).

3.4.2 : Effects of Diet and Environment on Transporter Expression

3.4.2.1 : Effects of Diet and Environment on Branchial Transporter Expression

Due to the significant role the diet plays in Mg^{2+} homeostasis (Chapter 3.1), it was hypothesized that increasing dietary Mg^{2+} would lead to quantifiable changes in my genes of interest. Since Slc41a1 is thought to serve an excretory role, and Slc41a2 shares a high degree of genetic similarity to Slc41a1, I predicted that the relative quantities of *slc41a1* and *slc41a2* mRNA would increase in response to elevated dietary Mg^{2+}. Based on my previous experiments (Chapter 2), I believed that Cnnm3 and Trpm7 were likely serving an absorptive role, predicting that increasing dietary Mg^{2+} would lead to decreased expression of both genes.

Furthermore, dietary ions are thought to play a larger role in the physiological needs of fish acclimated to FW than in those acclimated to SW. It was therefore hypothesized that environmental salinity would impact the influence of dietary Mg^{2+} on my genes of interest. More specifically, I predicted that consuming a Mg^{2+}-rich diet would have a larger impact on the expression of my genes of interest in FW-acclimated fish than in SW-acclimated fish.

In FW-acclimated fish, consuming a Mg^{2+}-rich diet led to decreased expression of *slc41a1*, *slc41a2*, *cnnm3*, *trpm7*, and *nka-2α* mRNA (Figures 15a and 15b) but did not affect relative quantities of *nka-1α* mRNA (Figure 15b). Dietary sources are thought to supply the majority of Mg^{2+} required for survival in FW fish (reviewed by Wood and Bucking, 2011). This may explain the downregulation of my target genes within this tissue in FW acclimated fish. Indeed, in Chapter 2, I proposed that Slc41a1, Slc41a2, Cnnm3, and Trpm7 formed an avenue for absorption of environmental magnesium, a proposal that was mostly upheld (or at least not refuted) by the responses to elevated environmental magnesium. Here, elevated dietary

magnesium could be providing sufficient magnesium for homeostasis, thus allowing for a downregulation in branchial absorptive pathways (Figure 2) (Arjona et al., 2019).

In the gills of SW-acclimated fish, however, genetic expression of *slc41a1* and *nka-1α* increased, with no changes being observed for other genes of interest (Figures 16a and 16b, respectively). This suggested an excretory role for Slc41a1, in opposition to what was observed in the gills of FW-acclimated fish (Figure 15a). However, although environmental Mg^{2+} restriction led to upregulation of branchial *slc41a1* in zebrafish (Arjona et al., 2019; suggesting a role in magnesium absorption), dietary Mg^{2+} restriction led to downregulation of branchial *slc41a1* in goldfish (Kodzhahinchev et al., 2017), supporting a role in magnesium secretion and mirroring the results I observed in SW-acclimated fish fed a Mg^{2+}-rich diet (Figure 16a). Furthermore, SW acclimation has led to upregulation of *slc41a1* in the kidneys of mefugu (Islam et al., 2013) and gulf toadfish (Hansen et al., 2021), further supporting an excretory role.

It is therefore possible that my results (Figures 15 and 16) may be explained by multiple scenarios: First, the diet (and therefore the intestines) of FW acclimated fish are thought to contribute more to Mg^{2+} uptake than the environment (and by extension, the gills) (reviewed by Wood and Bucking, 2011). Therefore, increasing dietary Mg^{2+} would decrease the need for branchial absorption, leading to downregulation (Figure 15).

In SW acclimated fish, intestinal Mg^{2+} absorption decreases as the overall permeability of the intestines to divalent cations decreases. If Slc41a1 is indeed serving an absorptive role in the gills of sailfin mollies, and intestinal absorption is decreased, it is possible that an increase in branchial Mg^{2+} absorption could be occurring to compensate (Figure 16a). Since Slc41a1 is thought to be an NME, more intracellular Na^{+} would be required to support this change, explaining the increase in *nka-1α* mRNA I observed (Figure 16b).

In the second scenario, Slc41a1 is involved in excretion, not absorption. In FW acclimated fish, the gills actively transport ions across the apical membrane and into the cell to maintain homeostasis. It is therefore possible that the decrease in branchial *slc41a1* I observed in FW acclimated fish fed the test diet (Figure 15a) was not to decrease Slc41a1-mediated absorption, but rather due to the decrease in Trpm7 at the basolateral membrane reducing intracellular Mg^{2+} and ultimately the need for Slc41a1-mediated excretion. In SW-acclimated fish fed the test diet, I saw a clear increase in *slc41a1* and *nka-1α* (Figures 16a and 16b, respectively) to remove excess Mg^{2+} that had accumulated in the cell, while the expression of other studied genes remained stable.

Unfortunately, the influence of dietary Mg^{2+} on branchial expression of *slc41a1* mRNA in the gills of SW-acclimated fish, or the influence of dietary Mg^{2+} on the expression of any of my other genes of interest in the gills of fish regardless of environmental salinity have not been previously investigated, making my study the first to look at branchial Mg^{2+} homeostasis on a wholistic level under these conditions. Consequently, comparisons to other studies were difficult to make.

From my observations (Figure 15a), Slc41a2 may serve an absorptive role in the gills of sailfin mollies acclimated to FW, supported by previous literature using *trpm7*-deficient DT40 cells where Slc41a2 was able to rescue Mg^{2+} absorption (Sahni et al., 2007). It is also possible that Slc41a2 is serving a role in excretion like that of Slc41a1, however compensation at the levels of other ionoregulatory epithelia such as the intestines (Figures 17a-20a) may have sufficiently compensated for the initial change in plasma Mg^{2+} (Figure 23), making branchial excretion via Slc41a2 unnecessary. The lack of change observed in the gills of SW-acclimated fish (Figure 16a) is likely reflective of a change in intestinal permeability, and potentially

changes at the renal level (discussed in Chapter 2.4). In support of a role in Mg^{2+} excretion, a previous study observed significantly elevated *slc41a2* quantities in the gills of Atlantic salmon after SW acclimation (Esbaugh et al., 2014). It has also been proposed that Slc41a2 may function in a dose-dependent manner (Sahni et al., 2007), further supporting the notion that changes at the level of other tissues or potentially other genes may have contributed to the regulation of *slc41a2* I observed in this tissue.

The relationship between branchial *cnnm3* expression and dietary Mg^{2+} has also not been previously quantitatively investigated in a euryhaline fish. The observed decrease in FW (Figure 15a) suggests an absorptive role, and if Cnnm3 was serving an excretory role in this tissue it should have been upregulated in SW acclimated fish fed the test diet. In contrast to this prediction, no significant changes were observed in the SW group (Figure 16a). Previous studies that have investigated *cnnm3* expression in fish have all focused on environmental manipulations and have focused primarily on genetic changes within the kidneys (Islam et al., 2014; Hansen et al., 2021). Both studies observed upregulation of *cnnm3* in response to SW-acclimation, and both concluded similarly that Cnnm3 likely played a role in Mg^{2+} excretion. Indeed, the downregulation of branchial *cnnm3* in FW-acclimated fish in response to elevated dietary Mg^{2+} may suggest an excretory role, however, the lack of change I observed in SW-acclimated fish fed the test diet, along with the likely basolateral localization of Cnnm3 (as demonstrated in the kidneys of euryhaline mefugu; Islam et al., 2014) could tell a different story. While Cnnm3 may be removing Mg^{2+} from the cell, the resultant increase in Mg^{2+} in the lateral intercellular space would move passively down a concentration gradient. In a FW-acclimated fish, this would mean the loss of Mg^{2+} to the environment which would be physiologically undesirable. I therefore still believe that Cnnm3 is playing an overall absorptive role in the gills of sailfin mollies.

The downregulation of *trpm7* in FW-acclimated fish (Figure 15a) may have been to decrease absorption, and the lack of change in response to dietary Mg^{2+} in SW-acclimated fish (Figure 16a) further supports this idea, as passive basolateral entry through Trpm7 would be necessary for apical Mg^{2+} excretion to occur. A role for Trpm7 in passive Mg^{2+} absorption has been proposed based on evidence from mammalian models (e.g. Schlingmann et al., 2002; Voets et al., 2004; Giménez-Mascarell et al., 2018), as well as in fish (Hansen et al., 2021) and my results agree with previous studies.

Finally, *nka* isoforms are thought to drive NME-mediated Mg^{2+} transport by establishing Na^{+} gradients (e.g. Hansen et al., 2021). Since all studied Mg^{2+} transporters were also downregulated (Figure 15a), the requirement for exchange via Nka in FW would be decreased, potentially explaining the downregulation of *nka-2α* in FW (Figure 15b). In SW, the increase of *nka-1α* mRNA (Figure 16b) that occurred in tandem with an increase in branchial *slc41a1* levels (Figure 16a) supports the need for branchial excretion under these environmental conditions, as more NME-mediated excretion would require higher concentrations of intracellular Na^{+}. Indeed, significant increases in renal quantities of *nka* in gulf toadfish were observed during a hypersaline challenge in tandem with increases in various Mg^{2+} transporters (Hansen et al., 2021) and while they did not investigate dietary manipulations as I have done here, the same logic can be applied to my own observations.

Based on my findings, my proposed model of branchial Mg^{2+} transport (Figure 2) is still plausible. At the basolateral membrane, Trpm7 facilitates passive movement of Mg^{2+} down its concentration gradient (in FW this allows passive absorption into branchial cells). Nka isoforms along the basolateral membrane actively exchange extracellular K^{+} for intracellular Na^{+}. Cnnm3 uses extracellular Na^{+} gradients established by Nka isoforms at the basolateral membrane to

transport intracellular Mg^{2+} into the lateral membrane space, where it would follow its concentration gradient and either re-enter the plasma or be excreted across tight junctions (suggested by Hansen et al., 2021). I placed Slc41a1/a2 in an unknown position within branchial cells. I suspect that they may be removing Mg^{2+} from the cell in exchange for Na^{+}. If located on the basolateral membrane, then the function would be for absorption, however if they were found on the apical membrane, the role would likely be for secretion. It is possible that this occurs directly across the apical membrane, or through vacuole-mediated transport as was demonstrated in the kidneys of other euryhaline species (mefugu: Islam et al., 2013; mummichog: Chandra et al., 1997).

3.4.2.2 : Effects of Diet and Environment on Intestinal Transporter Expression

In the intestines of FW-acclimated fish, increasing dietary Mg^{2+} led to decreased expression of *slc41a1*, increased expression of *slc41a2* in the anterior intestine, with no change in *slc41a2* in the posterior intestine, and no changes in the expression of *cnnm3* or *trpm7* in either intestinal segment (Figure 17a (anterior), Figure 19a (posterior)). Expression of *nka-1α* increased when dietary Mg^{2+} was elevated, regardless of intestinal region (Figure 17b (anterior), Figure 19b (posterior)), but an apparent region-specific response in *nka-2α* was observed, with a decrease in the anterior intestines (Figure 17b) and an increase in the posterior intestine (Figure 19b). In contrast, in SW-acclimated fish fed the test diet, I observed increased expression of *slc41a1* and *slc41a2* regardless of intestinal section (Figure 18a (anterior), Figure 20a (posterior)). Genetic expression of *cnnm3* was unchanged in the anterior intestine (Figure 18a) but increased in the posterior intestine (Figure 20a). *trpm7* expression decreased in the anterior intestine (Figure 18a) but increased in the posterior intestine (Figure 20a). The expression of *nka-1α* increased (similarly to freshwater) while *nka-2α* also increased in SW-acclimated fish fed

the test diet along the entire intestine (Figure 18b (anterior), Figure 20b (posterior)), while there was a decrease in the anterior in freshwater (Figure 18b).

In a previous study involving goldfish fed a Mg^{2+}-restricted diet, researchers observed a decrease in intestinal *slc41a1* mRNA which, when taken alongside their observations in other regulatory tissues, led researchers to propose that Slc41a1 is serving a role in Mg^{2+} excretion, and that the downregulation they observed in the intestines was to improve dietary assimilation (Kodzhahinchev et al., 2017). Interestingly, increasing dietary Mg^{2+} did not lead to changes in intestinal *slc41a1*, with changes instead being observed in the kidneys of goldfish (Kodzhahinchev et al., 2017). It is therefore possible that my observed decrease in intestinal *slc41a1* (Figure 17a (anterior), Figure 18a (posterior)) was not indicative of a role in absorption, but rather indicative of a decrease in excretion, allowing any excess Mg^{2+} to be filtered out via the kidneys. This excretory role becomes clearer when fish were acclimated to SW, as the levels of *slc41a1* were elevated (Figure 18a (anterior), Figure 20a (posterior)), likely to prevent excess intracellular Mg^{2+} accumulation that would disturb the osmotic gradient required for intestinal water gain. The observed changes in intestinal *slc41a2* also supported an excretory role. In FW, the brief increase I observed in the anterior intestine (Figure 17a) was likely to compensate for the sudden increase in intracellular Mg^{2+}, but eventually these levels returned to normal, remaining stable throughout the posterior intestine (Figure 19a). In SW, however, *slc41a2* was upregulated throughout the entire intestine (Figure 18a (anterior), Figure 20a (posterior)). Although this study is the first to quantitatively investigate the relationship between dietary Mg^{2+} and intestinal *slc41a2* expression, a comparable study found increased *slc41a2* expression in Atlantic salmon during SW-acclimation, indicating that it may serve an excretory role in other euryhaline species (Esbaugh et al., 2014).

A decrease in intestinal *cnnm3* in response to elevated dietary Mg^{2+} in FW and SW (Figures 17a-20a) is suggestive of an absorptive role supporting previous observations, as well as my predictions. The lack of change in intestinal *trpm7* expression in FW fish (Figure 17a (anterior), Figure 19a (posterior)) may suggest that the intestines may not be tightly regulating the passive movement of Mg^{2+}, but instead are relying on the regulation of active transporters such as NMEs. In support of an absorptive role (e.g. Schlingmann et al., 2002; Voets et al., 2004; Giménez-Mascarell et al., 2018; Hansen et al., 2021), as well as my own predictions, I observed a decrease in *trpm7* expression in the anterior intestines of SW-acclimated fish fed the test diet (Figure 18a).

Finally, increasing dietary Mg^{2+} led to increased *nka-1α* and decreased *nka-2α* within the anterior intestines of FW-acclimated fish (Figure 17b). In SW-acclimated fish, *nka-1α* expression increased due to environmental salinity, but did not change significantly in response to consuming the test diet (Figure 19b). *nka-2α* levels increased in response to elevated dietary Mg^{2+} in this tissue (Figure 19b). The major contributing factor to these changes could not be reliably determined, however, as a significant interaction between diet and time was determined. In the posterior intestines of FW-acclimated fish, consuming a Mg^{2+}-rich diet led to increases in both *nka-1α* and *nka-2α* (Figure 18b). In SW-acclimated fish, both time of exposure and dietary Mg^{2+} led to increases in *nka-1α* levels, whereas only dietary Mg^{2+} was attributed to an increase in *nka-2α* within this tissue (Figure 20b). My findings are interesting, as they demonstrate not only the response of Nka transporters to changes in Na^{+} but also to changes in Mg^{2+}, highlighting their role in driving the function of other transporters. Indeed, decreasing dietary Mg^{2+} has been shown to decrease intestinal Nka activity in grass carp (*Ctenopharyngodon Idella*), supporting my own observations (Wei et al., 2018).

The observed changes in the intestines in response to dietary manipulations support the cellular model I proposed in Chapter 2 (Figure 3) whereby apical Trpm7 facilitates the passive absorption of luminal Mg^{2+} across the apical membrane of enterocytes while Cnnm3 at the basolateral membrane exchanges serosal Na^{+} for intracellular Mg^{2+} using gradients established by basolateral Nka, facilitating Mg^{2+} absorption into the blood. Slc41a1 and Slc41a2 associated with the apical membrane exchange extracellular Na^{+} for intracellular Mg^{2+}, facilitating apical excretion.

3.4.2.3 : Effects of Diet and Environment on Renal Transporter Expression

Consuming additional dietary Mg^{2+} did not significantly alter quantities of *slc41a1*, *slc41a2*, or *trpm7* in the kidneys of FW fish, but a decrease in *cnnm3* expression was observed (Figure 21a), as well as decreases in both *nka* isoforms (Figure 21b). In contrast, when SW-acclimated fish were fed the test diet an initial increase in *slc41a1* and *trpm7* was observed before returning to normal values (Figure 22a), *nka-2α* was also found to increase in fish acclimated to SW (Figure 22b). Levels of all other studied transporters remained stable in SW.

In goldfish, elevating dietary Mg^{2+} led to a significant increase in renal *slc41a1* transcripts (Kodzhahinchev et al., 2017), supporting an excretory role, as has been proposed in other fish species when environmental salinity was manipulated (e.g. Islam et al., 2013; Hansen et al., 2021). An excretory role may explain the observed increase in SW-acclimated fish, and the lack of a contradicting change in the FW test group does not disagree with this role. It is possible that Slc41a1 is being regulated on multiple levels- in fact, it has been previously suggested that Slc41a1 may be recycled by endosomes when Mg^{2+} levels within the cell are in the desired range (Mandt et al., 2008), and indeed, a vacuolar localization has been experimentally demonstrated in other euryhaline fish (e.g. mefugu, Islam et al., 2013; mummichog, Chandra et al., 1997). A

similar “recycling” process may also explain the lack of significant changes in *slc41a2* in either salinity, as I suspect that, based on genetic similarity to *slc41a1*, it should serve a similar role and thus be regulated similarly.

A relationship between renal *cnnm3* quantities and dietary Mg^{2+} intake has not previously been established in euryhaline fish but based on the results of my salinity experiments (Chapter 2), I believed Cnnm3 to be serving an absorptive role. More specifically, I believed that Cnnm3 is pumping Mg^{2+} into the lateral space in exchange for intercellular Na^{+} that accumulates through Nka activity at the basolateral membrane, after which Mg^{2+} moves passively back into the plasma. My results here (Figures 21a and 22a) suggest that Cnnm3 is indeed serving an absorptive role in this tissue. Finally, Trpm7 has been proposed to form a transmembrane channel that allows the passive movement of Mg^{2+} to occur down its gradient. In the kidneys of mammalian models, Trpm7 is apically localized, facilitating reabsorption from the glomerular filtrate (e.g. Voets et al., 2004; Giménez-Mascarell et al., 2018), although this has not been previously demonstrated in fish, the results from both environmental (Chapter 2) and dietary manipulations are in support of this role and positioning within the kidneys of sailfin mollies. My prediction here is somewhat at odds with previous predictions made, whereby a basolateral position was suggested for Trpm7 in the kidneys of gulf toadfish (Hansen et al., 2021). One possible cause for the differences in findings between my study and others is that gulf toadfish are aglomerular, and as such a full switch from net ionic absorption in hypoionic environments to net secretion in hyperionic environments may never occur as it would in glomerular teleosts such as sailfin mollies (Hansen et al., 2021).

The results of my experiment support my proposed cellular model (Figure 4), whereby basolateral Nka establishes extracellular Na^{+} gradients that drive Cnnm3-mediated Mg^{2+}

transport into the lateral membrane space. Mg^{2+} in the lateral membrane space then diffuses into the preurine through tight junctions or returns to the plasma depending on the concentration gradient in between the plasma and preurine. Intracellular Mg^{2+} that is not transported by Cnnm3 is exchanged for Na^{+} by Slc41a1/a2 across vacuolar membranes before being trafficked to the apical membrane and being released into the preurine. Apically localized Trpm7 then facilitates passive Mg^{2+} reabsorption across the apical membrane.

3.4.3 : Predictions of Molecular Structures of Mg^{2+} Transporters

To learn more about the molecular structure of Slc41a1, Slc41a2, Cnnm3, and Trpm7, I retrieved the amino acid sequence of each protein from Ensembl and entered them into the I-TASSER server (Yang and Zhang, 2015). Predicted molecular structures for each were then generated, along with scores to describe the confidence of the predictions. Unfortunately, the computing capacity of the I-TASSER server only allows for the input of amino acid sequences up to 1500 residues, and therefore structural predictions for Trpm7 could not be made using this software. The low C-scores generated for Slc41a1 (Figure 24), Slc41a2 (Figure 25), and Cnnm3 (Figure 26) in *P. latipinna* suggested poor prediction quality, despite the TM-scores being in a range consistent with predictions of correct topology. I was unsure if these low C-scores were due to the sequences themselves, or due to the use of a less studied model organism. To test this, I repeated the experiment using amino acid sequences from mice (*M. musculus*) and found that the confidence scores were consistent with those observed for *P. latipinna*. This is unfortunate, as accurately predicting the molecular structure of a protein can reveal vital information about its biological function and could potentially help to determine the causes of some inconsistent findings in between my observations and those from earlier investigations.

3.4.4 : Conclusions and Future Perspectives

To establish a relationship between dietary Mg^{2+} and transporter expression I fed a Mg^{2+}-rich diet to sailfin mollies acclimated to both FW and SW. I predicted, based on what is currently known of my genes of interest, that genes suspected to serve roles in Mg^{2+} excretion (*slc41a1*, *slc41a2*) would be upregulated, and genes thought to serve absorptive roles (*cnnm3*, *trpm7*) would be downregulated. I further hypothesized that environmental salinity would affect the regulation of my genes of interest, predicting to see more pronounced differences in FW-acclimated fish than in SW-acclimated fish due to perceived differences in dietary ion requirements. Finally, I hypothesized that increasing dietary Mg^{2+} would affect plasma Mg^{2+} levels, predicting an increase that would potentially be compensated for on a genetic level. Indeed, the results revealed that increasing dietary Mg^{2+} led to an initial increase in plasma Mg^{2+} concentrations regardless of salinity, and levels were quickly normalized (Figure 25). Furthermore, I was able to see tissue-dependent differences in the regulation of my genes of interest that differed depending on environmental conditions. In FW-acclimated fish, increasing dietary Mg^{2+} led to decreased expression of my genes of interest in the gills (Figure 17), whereas only those involved in Mg^{2+} excretion seemed to be downregulated in the intestines (Figures 19 and 21). In the kidneys, *cnnm3* and *nka* were the only target genes that were regulated at the genetic level (Figure 23).

Based on my findings, I believe that my genes of interest are being regulated in response to both dietary and environmental Mg^{2+}, and that gills, intestines, and kidneys play different roles in handling dietary Mg^{2+} that may differ depending on the salinity of the environment. In all cases, the data supports the previous cellular models I suggested (Figures 4-6); Trpm7 is facilitating passive Mg^{2+} entry into the cell, where NMEs utilize the gradients established by

basolaterally localized Nka isoforms to drive Mg^{2+} excretion. Cnnm3 is likely on the lateral membrane, as has been previously demonstrated in mefugu (Islam et al., 2014), and Slc41a1/a2 are likely localized to the membranes of apically associated vacuoles, as has been demonstrated in mummichog (Chandra et al., 1997) and mefugu (Islam et al., 2013), although its localization in branchial cells is less obvious.

Chapter 4: Conclusions, Limitations, Significance, and Future Perspectives

4.1 : Conclusions

The purpose of this thesis was to learn more about how environmental and dietary Mg^{2+} are handled by the gills, intestines, and kidneys of fish at the genetic level to gain a more wholistic understanding of Mg^{2+} homeostasis in animals. First, I wanted to confirm that genes involved directly in Mg^{2+} transport were expressed ubiquitously in tissues of sailfin mollies regardless of environmental salinity. I expected to observe ubiquitous expression of my genes of interest due to their known physiological roles in fish and mammals (Chapter 2.1), and that levels would differ in a tissue-specific manner. Indeed, this was the case in sailfin mollies, and I also found that the tissue-specific distribution of my target genes was altered in response to environmental salinity.

My next objective was to determine how increased environmental salinity would influence the expression of my genes of interest in the gills, intestines, and kidneys of sailfin mollies. Based on previous studies, I expected that Slc41a1 and Cnnm3 would be involved in Mg^{2+} excretion by using Na^{+} gradients established by Nka at the basolateral membrane, and that Mg^{2+} entry would occur passively via Trpm7. Due to its genetic similarity to Slc41a1, I expected Slc41a2 to serve a similar physiological function. I therefore hypothesized that my genes of interest would be regulated at the genetic level, more specifically predicting to see downregulation of *trpm7*, and upregulation of all other genes, ultimately decreasing absorption and increasing excretion. I also hypothesized that SW acclimation would lead to changes in Mg^{2+} levels within the plasma, predicting that increasing environmental Mg^{2+} would temporarily increase levels within the plasma. I was surprised to find that not all genes of interest changed

across all target tissues, and that the expression of *slc41a1* and *cnnm3* decreased during salinity acclimation. Some of my observations may have been due to the lack of change in plasma Mg^{2+} levels, potentially due to the ability of sailfin mollies to rapidly acclimate to environmental changes, a characteristic that allows them to survive in their estuarine environments.

With plasma levels being maintained, I suspect that the consistent downregulation of my target genes was reflective of a decreased demand for excretion, and not a role for these genes in absorption. When no changes were observed for a specific gene in any given tissue, I attributed this to sufficient compensation by other genes of interest within that tissue, sufficient compensation by other tissues, or regulation at the protein level which I was not able to observe with my methods. I then sought to compare sailfin mollies to other model organisms that have been used to achieve similar results, predicting that species specific variations in the genetic codes for these transporters may shed some light on some inconsistencies within the literature. Indeed, phylogenetic analyses revealed distributions that were largely familial, with no clear influence of habitat on the distribution of species within the resultant trees. It is therefore possible that the coding sequences for my genes of interest have evolved many times throughout history, and that some inconsistencies in currently available literature may be in part due to species-specific regulation of these genes.

Finally, I sought to learn about the integrated effects of environmental salinity and dietary Mg^{2+} on the expression of my genes of interest, and on plasma Mg^{2+} contents. Based on what was observed during my SW acclimation experiments (Chapter 2), I expected to find rapid regulation of plasma Mg^{2+} that would be driven by transcriptional regulation of my genes of interest. I also suspected that excess dietary Mg^{2+} would be handled differently depending on environmental salinity due to the different roles the diet is thought to play in species acclimated

to FW as opposed to SW species. I found that plasma Mg^{2+} levels were initially elevated in fish fed the test diet, but those levels were rapidly normalized. At the genetic level, I saw transcriptional regulation in all tissues that may have accounted for the changes I observed in the plasma (Figure 23). Furthermore, these genetic changes were often different depending on environmental salinity, as I predicted based upon the different physiological challenges fish face when living in FW versus SW.

When taken together, my results suggest that all target genes were playing significant roles in ionic homeostasis within the gills, kidneys, and intestines of sailfin mollies. It was also evident that these genes were likely serving roles in other tissues regardless of environmental conditions as they were expressed in all studied tissues. Furthermore, it was found that manipulating environmental and dietary Mg^{2+} initiated regulation at the genetic level, allowing the animals to survive in all treatments. Based on my findings, I constructed predictive cellular models for all genes of interest in the gills, kidneys, and intestines to gain a more wholistic understanding of the tissue-specific cellular function each gene was serving (Figures 2-4). I hope that future researchers will be able to compare their findings with my models, and that they may serve as a catalyst for critical discussion about the integrated roles these genes are playing in all animals.

4.2 : Limitations

Many of the findings I have reported throughout this thesis are novel. For example, *slc41a2* has not been previously investigated in a euryhaline fish under similar experimental conditions. The impact of dietary Mg^{2+} on the expression of many of my genes of interest was also largely unexplored, and my study was the first to achieve this in a euryhaline fish acclimated to different salinities. One limitation to my study was, therefore, the relative lack of previous

data with which to draw meaningful comparisons. Further, although the coding sequences for my genes of interest within sailfin mollies were available online, designing specific primers for certain relevant genes such as TRPM6, NKA-1β and SLC41a3 (as studied by Hansen et al., 2021) was extremely difficult, perhaps speaking to the novelty of my model organism and this area of research.

To better understand the handling of Mg^{2+} in sailfin mollies at a holistic level, I initially sought to collect urine and study how urinary Mg^{2+} concentrations would change throughout each treatment. Unfortunately, the relatively small size of sailfin mollies made extracting consistent volumes of urine for reliable data extremely difficult. Samples were often contaminated with blood which would have interfered with the reliability of the data, and the volume collected from individuals within a test group was often too small to properly analyze.

Finally, when using software to predict the molecular structure of Slc41a1, Slc41a2, and Cnnm3, the confidence scores of the resultant structures were consistently low. I assumed that these scores were due to the novelty of the model organism I used but repeating the experiment using the same genes in mice produced similarly low confidence scores. Furthermore, functional predictions of my genes based on the structures predicted by I-TASSER were also statistically unlikely. I-TASSER was also unable to process the full coding sequence for Trpm7 due to its size being larger than the maximum allowable threshold on their server. This made it impossible to complete structural predictions of Trpm7 in a way that would yield meaningful results, as breaking the coding sequence into smaller portions would undoubtedly negatively impact structural integrity.

4.3 : Significance and Future Perspectives

Despite the vital roles Mg^{2+} is known to play in animals, the study of its regulation is still in its infancy, especially in non-mammalian models. My study was the first to quantitatively investigate the integrated influence of dietary and environmental Mg^{2+} on the genetic regulation of known Mg^{2+} transporters in a euryhaline fish. Working to establish a more holistic understanding of the mechanisms at the genetic level is significant as understanding the function and regulation of these genes at both an individual level and as they work in tandem within cells may allow future scientists to better understand and respond to diseases and conditions associated with hypomagnesemia, or mutations within my genes of interest. Further, understanding dietary assimilation of Mg^{2+} in fish may provide economic benefits as fish farms continue to optimize the composition of fish feed to be more cost effective.

Although my results largely agree with the findings of previous studies, further insight on how these genes are regulated under similar experimental conditions in a wide variety of models would greatly benefit our understanding of what these genes are doing within the cell. Cellular localization of my genes of interest would also help validate my proposed cellular models (Figures 2-4). Studying my targets at the protein level would also be valuable to defining a clearer picture of how each protein functions and how they are regulated. Finally, the use of electrophysiological techniques such as the Scanning Ion-selective Electrode Technique (SIET) or Ussing Chambers in tandem with molecular and genetic evidence would help to strengthen my findings and conclusions

Chapter 5: References

Akram, Z., Fatima, M., Shah, S. Z. H., Afzal, M., Hussain, S. M., Hussain, M., ... & Akram, K. (2019). Dietary zinc requirement of *Labeo rohita* juveniles fed practical diets. *Journal of Applied Animal Research*, 47(1), 223-229.

Ando, M., Mukuda, T., & Kozaka, T. (2003). Water metabolism in the eel acclimated to sea water: from mouth to intestine. *Comparative Biochemistry and Physiology Part B: Biochemistry and Molecular Biology*, 136(4), 621-633.

Arjona, F. J., Chen, Y. X., Flik, G., Bindels, R. J., & Hoenderop, J. G. (2013). Tissue-specific expression and in vivo regulation of zebrafish orthologues of mammalian genes related to symptomatic hypomagnesemia. *Pflügers Archiv-European Journal of Physiology*, 465(10), 1409-1421.

Arjona F. J., Latta F., Mohammed S. G., Thomassen M., Van Wijk E., Bindels R. J. M., Hoenderop J. G. J., de Baaij J. H. F. (2019) SLC41A1 is essential for magnesium homeostasis in vivo. *Pflügers Archiv-European Journal of Physiology*, 471(6), 845-860.

Avila, E. M., Tu, H., Basantes, S., & Ferraris, R. P. (2000). Dietary phosphorus regulates intestinal transport and plasma concentrations of phosphate in rainbow trout. *Journal of Comparative Physiology B*, 170(3), 201-209.

Baldisserotto, B., Kamunde, C., Matsuo, A., & Wood, C. M. (2004). Acute waterborne cadmium uptake in rainbow trout is reduced by dietary calcium carbonate. *Comparative Biochemistry and Physiology Part C: Toxicology & Pharmacology*, 137(4), 363-372.

Baldisserotto, B., Chowdhury, M. J. & Wood, C. M. (2006), In vitro analysis of intestinal absorption of cadmium and calcium in rainbow trout fed with calcium- and cadmium-supplemented diets. *Journal of Fish Biology*, 69(3), 658-667.

Beyenbach, K. W. (1995). Secretory electrolyte transport in renal proximal tubules of fish, in *Cellular and Molecular Approaches to Fish Ionic Regulation*, (C. M. Wood & T. J. Shuttleworth eds), 85-105, Academic Press.

Beyenbach, K. W. (2000). Renal handling of magnesium in fish: from whole animal to brush border membrane vesicles. *Frontiers in Bioscience-Landmark*, 5(3), 712-719.

Beyenbach, K. W. (2004). Kidneys sans glomeruli. *American Journal of Physiology. Renal Physiology*, 286(5), F811-F827.

Bijvelds, M. J., Flik, G., Kolar, Z. I., & Wendelaar Bonga, S. E. (1996). Uptake, distribution and excretion of magnesium in *Oreochromis mossambicus*: dependence on magnesium in diet and water. *Fish Physiology and Biochemistry*, 15(4), 287-298.

Bijvelds, M. J., Velden, J. A., Kolar, Z. I., & Flik, G. (1998). Magnesium transport in freshwater teleosts. *The Journal of Experimental Biology*, 201(13), 1981-1990.

Boisen, A. M., Amstrup, J., Novak, I. & Grosell, M. (2003). Sodium and chloride transport in soft water and hard water acclimated zebrafish (*Danio rerio*). *Biochimica et Biophysica Acta*. 1618(2), 207-218.

Bucking, C., & Wood, C. M. (2006a). Water dynamics in the digestive tract of the freshwater rainbow trout during the processing of a single meal. *Journal of Experimental Biology*, 209(10), 1883-1893.

Bucking, C., & Wood, C. M. (2006b). Gastrointestinal processing of Na^+, Cl^-, and K^+ during digestion: implications for homeostatic balance in freshwater rainbow trout. *American Journal of Physiology-Regulatory, Integrative and Comparative Physiology*, 291(6), R1764-R1772.

Bucking, C., & Wood, C. M. (2007). Gastrointestinal transport of Ca^{2+} and Mg^{2+} during the digestion of a single meal in the freshwater rainbow trout. *Journal of Comparative Physiology B*, 177(3), 349-360.

Bucking, C., & Wood, C. M. (2009). The effect of postprandial changes in pH along the gastrointestinal tract on the distribution of ions between the solid and fluid phases of chyme in rainbow trout. *Aquaculture Nutrition*, 15(3), 282-296.

Bucking, C., Landman, M. J., & Wood, C. M. (2010). The role of the kidney in compensating the alkaline tide, electrolyte load, and fluid balance disturbance associated with feeding in the freshwater rainbow trout, *Oncorhynchus mykiss*. *Comparative Biochemistry and Physiology Part A: Molecular & Integrative Physiology*, 156(1), 74-83.

Bureau, D. P., & Cho, C. Y. (1999). Phosphorus utilization by rainbow trout (*Oncorhynchus mykiss*): Estimation of dissolved phosphorus waste output. *Aquaculture,* 179(1-4), 127-140.

CABI Invasive Species Compendium (2019, November 20th). *Poecilia latipinna* (sailfin molly) datasheet. Cabi.org. https://www.cabi.org/isc/datasheet/68203.

Chandra, S., Morrison, G. H., & Beyenbach, K. W. (1997). Identification of Mg-transporting renal tubules and cells by ion microscopy imaging of stable isotopes. *American Journal of Physiology-Renal Physiology*, 273(6), F939-F948.

Chasiotis H., Kolosov D., Bui P., & Kelly S. P. (2012). Tight junctions, tight junction proteins and paracellular permeability across the gill epithelium of fishes: a review. *Respiratory Physiology and Neurobiology*, 184(3), 269-81.

Choe, K. P., Morrison-Shetlar, A. I., Wall, B. P., & Claiborne, J. B. (2002). Immunological detection of Na^+/H^+ exchangers in the gills of a hagfish, *Myxine glutinosa*, an elasmobranch, *Raja erinacea*, and a teleost*, Fundulus heteroclitus*. *Comparative Biochemistry and Physiology Part A: Molecular & Integrative Physiology*, 131(2), 375-385.

Claiborne, J. B., Blackston, C. R., Choe, K. P., Dawson, D. C., Harris, S. P., Mackenzie, L. A., & Morrison-Shetlar, A. I. (1999). A mechanism for branchial acid excretion in marine fish: identification of multiple Na^+/H^+ antiporter (NHE) isoforms in gills of two seawater teleosts. *Journal of Experimental Biology*, 202(3), 315-324.

Dabrowska, H., Meyer-Burgdorff, K. H., & Gunther, K. D. (1991). Magnesium status in freshwater fish, common carp (*Cyprinus carpio, L.*) and the dietary protein-magnesium interaction. *Fish Physiology and Biochemistry*, 9(2), 165-172.

Dantzler, W. H. (2003). Regulation of renal proximal and distal tubule transport: sodium, chloride and organic anions. *Comparative Biochemistry and Physiology Part A: Molecular & Integrative Physiology*, 136(3), 453-478.

D'Cruz, L. M., & Wood, C. M. (1998). The influence of dietary salt and energy on the response to low pH in juvenile rainbow trout. *Physiological Zoology*, 71(6), 642-657.

De Baaij, J. H., Hoenderop, J. G., & Bindels, R. J. (2015). Magnesium in man: implications for health and disease. *Physiological Reviews*, 95(1), 1-46.

Ding, T., Shi, Y., Duan, W., Hu, S., & Zhao, Z. (2020). Immunohistochemical characterization and change in location of branchial ionocytes after transfer from freshwater to seawater in the euryhaline obscure puffer, *Takifugu obscurus*. *Journal of Comparative Physiology B*, 190(5), 585-596.

Doyle, D., Carney Almroth, B., Sundell, K., Simopoulou, N., & Sundh, H. (2022). Transport and barrier functions in rainbow trout trunk skin are regulated by environmental salinity. *Frontiers in Physiology*, 13, 882973.

Elizondo, M. R., Budi, E. H., & Parichy, D. M. (2010). Trpm7 regulation of in vivo cation homeostasis and kidney function involves stanniocalcin 1 and fgf23. *Endocrinology*, 151(12), 5700-5709.

Esbaugh, A. J., Kristensen, T., Takle, H., & Grosell, M. (2014). The effects of sustained aerobic swimming on osmoregulatory pathways in atlantic salmon *Salmo salar* smolts. *Journal of fish biology*, 85(5), 1355–1368.

Evans, D. H. (1984). 8- The Roles of Gill Permeability and Transport Mechanisms in Euryhalinity. In *Fish physiology*, (Hoar, W. S. & Randall, D. J. eds), 10(B), 239-283. Academic Press.

Evans, D. H., Piermarini, P. M., & Choe, K. P. (2005). The multifunctional fish gill: dominant site of gas exchange, osmoregulation, acid-base regulation, and excretion of nitrogenous waste. *Physiological Reviews*, 85, 97-111.

Evans, D. H. (2008). Teleost fish osmoregulation: what have we learned since August Krogh, Homer Smith, and Ancel Keys. *American Journal of Physiology-Regulatory, Integrative and Comparative Physiology*, 295(2), R704-R713.

FAO. 2020. The State of World Fisheries and Aquaculture 2020. In brief. Sustainability in action. Rome.

Fleig, A., Schweigel-Röntgen, M., & Kolisek, M. (2013). Solute carrier family SLC41: what do we really know about it?. *Wiley Interdisciplinary Reviews: Membrane Transport and Signaling*, 2(6), 227-239.

Flik, G., & Verbost, P. M. (1993). Calcium transport in fish gills and intestine. *Journal of Experimental Biology*, 184(1), 17-29.

Foskett, J. K., Bern, H. A., Machen, T. E., & Conner, M. (1983). Chloride cells and the hormonal control of teleost fish osmoregulation. *Journal of Experimental Biology*, 106(1), 255-281.

Fredericq, L. (1901). Sur la concentration moléculaire du sang et des tissus chez les animaux aquatiques. *Bulletin de la Classe des Sciences.* Académie Royale de Belgique.

Froese, R. and D. Pauly. Editors. 2022. FishBase. World Wide Web electronic publication.www.fishbase.org, version (02/2022).

Galvez, F., Reid, S. D., Hawkings, G., & Goss, G. G. (2002). Isolation and characterization of mitochondria-rich cell types from the gill of freshwater rainbow trout. *American Journal of Physiology-Regulatory, Integrative and Comparative Physiology*, 282(3), R658-R668.

Gatlin III, D. M., MacKenzie, D. S., Craig, S. R., & Neill, W. H. (1992). Effects of dietary sodium chloride on red drum juveniles in waters of various salinities. *The Progressive Fish-Culturist*, 54(4), 220-227.

Gatlin III, D. M., Robinson, E. H., Poe, W. E., & Wilson, R. P. (1982). Magnesium requirement of fingerling channel catfish and signs of magnesium deficiency. *The Journal of nutrition*, 112(6), 1182-1187.

Giménez-Mascarell, P., Schirrmacher, C. E., Martínez-Cruz, L. A., & Müller, D. (2018). Novel aspects of renal magnesium homeostasis. *Frontiers in Pediatrics*, 6, 77.

Gonzalez R. J., Cooper J., & Head D. (2005). Physiological responses to hyper-saline waters in sailfin mollies (*Poecilia latipinna*). *Comparative Biochemistry and Physiology A: Molecular & Integrative Physiology*. 142(4), 397-403.

Gonzalez, R. J. (2012). The physiology of hyper-salinity tolerance in teleost fish: a review. *Journal of Comparative Physiology B*, *Biochemical, Systems, and Environmental Physiology*, 182(3), 321-329.

Goss, G. G., Adamia, S., & Galvez, F. (2001). Peanut lectin binds to a subpopulation of mitochondria-rich cells in the rainbow trout gill epithelium. *American Journal of Physiology-Regulatory, Integrative and Comparative Physiology*, 281(5), R1718-R1725.

Goytain, A., & Quamme, G. A. (2005). Functional characterization of human SLC41A1, a Mg^{2+} transporter with similarity to prokaryotic MgtE Mg^{2+} transporters. *Physiological genomics*, 21(3), 337-342.

Griffith, R. W. (1974). Environment and salinity tolerance in the genus *Fundulus*. *Copeia*, 1974(2), 319-331.

Griffith, M. B. (2017). Toxicological perspective on the osmoregulation and ionoregulation physiology of major ions by freshwater animals: teleost fish, Crustacea, aquatic insects, and Mollusca. *Environmental Toxicology and Chemistry*, 36(3), 576-600.

Griffiths, A. B. (1892). On the blood of the Invertebrata. *Proceedings of the Royal Society of Edinburgh*, 18, 288-294.

Groenestege, W. M. T., Hoenderop, J. G., Van Den Heuvel, L., Knoers, N., & Bindels, R. J. (2006). The epithelial Mg^{2+} channel transient receptor potential melastatin 6 is regulated by dietary Mg^{2+} content and estrogens. *Journal of the American Society of Nephrology*, 17(4), 1035-1043.

Grosell, M. (2006). Intestinal anion exchange in marine fish osmoregulation. *Journal of Experimental Biology*, 209(15), 2813-2827.

Grosell, M. (2010). The multifunctional gut of fish 4- The role of the gastrointestinal tract in salt and water balance. In *Fish Physiology* (Grosell, M. Farrell, A. P. Brauner C. J. eds), 30, 135-164. Academic Press.

Grosell, M., Hogstrand, C., Wood, C. M., & Hansen, H. J. M. (2000). A nose-to-nose comparison of the physiological effects of exposure to ionic silver versus silver chloride in the European eel (*Anguilla anguilla*) and the rainbow trout (*Oncorhynchus mykiss*). *Aquatic Toxicology*, 48(2-3), 327-342.

Hansen, N. G. W., Madsen, S. S., Brauckhoff, M., Heuer, R. M., Schlenker, L. S., Engelund, M. B., & Grosell, M. (2021). Magnesium transport in the aglomerular kidney of the Gulf toadfish (*Opsanus beta*). *Journal of Comparative Physiology B*, 191(5), 865-880.

Hawkings, G. S., Galvez, F., & Goss, G. G. (2004). Seawater acclimation causes independent alterations in Na^+/K^+-and H^+-ATPase activity in isolated mitochondria-rich cell subtypes of the rainbow trout gill. *Journal of experimental biology*, 207(6), 905-912.

Henry RP, Lucu C, Onken H, Weihrauch D (2012) Multiple functions of the crustacean gill: osmotic/ionic regulation, acid-base balance, ammonia excretion, and bioaccumulation of toxic metals. *Frontiers in Physiology*, 3(431), 431.

Heron, V. (2018). Calcium, phosphate and magnesium disorders. In *Fluid and Electrolyte Disorders*. IntechOpen.

Hossain, M. A., & Yoshimatsu, T. (2014). Dietary calcium requirement in fishes. *Aquaculture nutrition*, 20(1), 1-11.

Houillier, P. (2014). Mechanisms and regulation of renal magnesium transport. *Annual review of physiology*, 76, 411-430.

Hickman Jr, C. P. (1968). Urine composition and kidney tubular function in southern flounder, *Paralichthys lethostigma*, in sea water. *Canadian Journal of Zoology*, 46(3), 439-455.

Hickman, C. P., & Trump, B. F. (1969). The kidney, in *Fish Physiology,* (W. S. Hoar and D. J. Randall eds), 91–239. Academic Press.

Hirano, T., & Mayer-Gostan, N. (1976). Eel esophagus as an osmoregulatory organ. *Proceedings of the National Academy of Sciences*, 73(4), 1348-1350.

Hiroi, J., McCormick, S. D., Ohtani-Kaneko, R., & Kaneko, T. (2005). Functional classification of mitochondrion-rich cells in euryhaline Mozambique tilapia (*Oreochromis mossambicus*) embryos, by means of triple immunofluorescence staining for Na^+/K^+-ATPase, $Na^+/K^+/2Cl^-$cotransporter and CFTR anion channel. *Journal of Experimental Biology*, 208(11), 2023-2036.

Hossain, M. A., & Furuichi, M. (1998). Availability of environmental and dietary calcium in tiger puffer. *Aquaculture International*, 6, 121-132.

Hossain, M. A., & Furuichi, M. (1999a). Effect of deletion of calcium supplement from purified diet on growth and bone mineralization in red sea bream. *Journal of the Faculty of Agriculture Kyushu University*, 44(1), 91-97.

Hossain, M. A., & Furuichi, M. (1999b). Necessity of dietary calcium supplement in black sea bream. *Fisheries Science*, 65(6), 893-897.

Hossain, M. A., & Furuichi, M. (2000). Essentiality of dietary calcium supplement in fingerling scorpion fish (*Sebastiscus marmoratus*). *Aquaculture*, 189(1-2), 155-163.

Hossain, M. A. (2000). Essentiality of dietary calcium supplement in redlip mullet (*Liza haematocheila*). *Aquaculture Nutrition*, 6(1), 33-38.

Hossain, M. A., & Yoshimatsu, T. (2014). Dietary calcium requirement in fishes. *Aquaculture Nutrition*, 20(1), 1-11.

Hurd, T. W., Otto, E. A., Mishima, E., Gee, H. Y., Inoue, H., Inazu, M., ... & Hildebrandt, F. (2013). Mutation of the Mg^{2+} transporter SLC41A1 results in a nephronophthisis-like phenotype. *Journal of the American Society of Nephrology*, 24(6), 967-977.

Hwang, P.P., Lee, T. H. (2007) New insights into fish ion regulation and mitochondrion-rich cells. *Comparative Biochemistry & Physiology A*: *Molecular & Integrative* Physiology, 148(3), 479–497

Hwang, P. P., Lee, T. H., & Lin, L. Y. (2011). Ion regulation in fish gills: recent progress in the cellular and molecular mechanisms. *American Journal of Physiology-Regulatory, Integrative and Comparative Physiology*, 301(1), R28-R47.

Islam, Z., Hayashi. N,, Yamamoto, Y., Doi, H., Romero, M. F., Hirose, S., & Kato, A. (2013). Identification and proximal tubular localization of the Mg^{2+} transporter, Slc41a1, in a

seawater fish. *American Journal of Physiology-Regulatory, Integrative, and Comparative Physiology*, 305(4), R385–R396.

Islam, Z., Hayashi, N., Inoue, H., Umezawa, T., Kimura, Y., Doi, H., Romero, M. F., Hirose, S., & Kato, A. (2014). Identification and lateral membrane localization of cyclin M3, likely to be involved in renal Mg^{2+} handling in seawater fish. *American Journal of Physiology-Regulatory, Integrative, and Comparative Physiology*, 307(5), R525–R537.

Kang, C. K., Tsai, S. C., Lee, T. H., & Hwang, P.P. (2008). Differential expression of branchial Na^+/K^+-ATPase of two medaka species, *Oryzias latipes* and *Oryzias dancena*, with different salinity tolerances acclimated to fresh water, brackish water and seawater. *Comparative Biochemistry & Physiology* 151(4), 566–575

Kjoss, V. A., Kamunde, C. N., Niyogi, S., Grosell, M., & Wood, C. M. (2005). Dietary Na does not reduce dietary Cu uptake by juvenile rainbow trout. *Journal of fish biology*, 66(2), 468-484.

Klinck, J. S., Green, W. W., Mirza, R. S., Nadella, S. R., Chowdhury, M. J., Wood, C. M., & Pyle, G. G. (2007). Branchial cadmium and copper binding and intestinal cadmium uptake in wild yellow perch (*Perca flavescens*) from clean and metal-contaminated lakes. *Aquatic toxicology*, 84(2), 198-207.

Kodzhahinchev, V., Kovacevic, D., & Bucking, C. (2017). Identification of the putative goldfish (*Carassius auratus*) magnesium transporter SLC41a1 and functional regulation in the gill, kidney, and intestine in response to dietary and environmental manipulations. *Comparative Biochemistry & Physiology*, 206, 69–81.

Kolisek, M., Nestler, A., Vormann, J., & Schweigel-Röntgen, M. (2012). Human gene SLC41A1 encodes for the Na^+/Mg^{2+} exchanger. *American Journal of Physiology-Cell Physiology*, 302(1), C318-C326.

Komiya, Y., & Runnels, L. W. (2015). TRPM channels and magnesium in early embryonic development. *The International Journal of Developmental Biology*, 59(7-9), 281.

Krogh, A. (1937). Osmotic regulation in fresh water fishes by active absorption of chloride ions. *Zeitschrift für vergleichende Physiologie*, 24(5), 656-666.

Krogh, A. (1938). The active absorption of ions in some freshwater animals. *Zeitschrift für vergleichende Physiologie*, 25, 335-350.

Kültz, D. (2012). The combinatorial nature of osmosensing in fishes. *Physiology*, 27(4), 259-275.

Kültz, D. (2015). Physiological mechanisms used by fish to cope with salinity stress. *The Journal of Experimental Biology*, 218(12), 1907-1914.

Kuz'mina, V. V. (2021). Specific features of nutrient transport in the digestive tract of fish. *Journal of Evolutionary Biochemistry and Physiology*, 57(2), 175-184.

Kwong, R.W.M., Kumai, Y., & Perry, S.F. (2013). The role of aquaporin and tight junction proteins in the regulation of water movement in larval zebrafish (*Danio rerio*). *PLoS ONE* 8(8), e70764.

Lai, K. P., Li, J. W., Gu, J., Chan, T. F., Tse, W. K. F., & Wong, C. K. C. (2015). Transcriptomic analysis reveals specific osmoregulatory adaptive responses in gill mitochondria-rich cells and pavement cells of the Japanese eel. *BMC genomics*, 16(1), 1-17.

Lall, S. P. (2002). The minerals. In: *Fish Nutrition* (J. E. Halver and R. W. Hardy, eds), pp. 261-307

Larsen, E. H., Willumsen, N. J., Møbjerg, N., & Sørensen, J. N. (2009). The lateral intercellular space as osmotic coupling compartment in isotonic transport. *Acta Physiologica*, 195(1), 171-186.

Larsen, E.H., Deaton, L.E., Onken, H., O'Donnell, M., Grosell, M., Dantzler, W.H., & Weihrauch, D. (2014). Osmoregulation and excretion. In: *Comparative Physiology, American Physiological Society* (Hicks, J., & Wang, T. eds), Blackwell, 4(2), 405-573. Wiley.

Laurent, P., Chevalier, C., & Wood, C. M. (2006). Appearance of cuboidal cells in relation to salinity in gills of *Fundulus heteroclitus*, a species exhibiting branchial Na^+ but not Cl^- uptake in freshwater. *Cell and Tissue Research*, 325(3), 481-492.

Laverty, G., & Skadhauge, E. (2012). Adaptation of teleosts to very high salinity. *Comparative Biochemistry and Physiology Part A: Molecular & Integrative Physiology*, 163(1), 1-6.

Loewen, T. N., Carriere, B., Reist, J. D., Halden, N. M., & Anderson, W. G. (2016). Linking physiology and biomineralization processes to ecological inferences on the life history of fishes. *Comparative Biochemistry and Physiology Part A: Molecular & Integrative Physiology*, *202*, 123-140.

Li, M., Jiang, J., & Yue, L. (2006). Functional characterization of homo-and heteromeric channel kinases TRPM6 and TRPM7. *The Journal of General Physiology*, *127*(5), 525-537.

Liang, J. J., Yang, H. J., Liu, Y. J., & Tian, L. X. (2014). Dietary potassium requirement of juvenile grass carp (*Ctenopharyngodon idella Val.*) based on growth and tissue potassium content. *Aquaculture Research*, 45(4), 701-708.

Lin, H., Pfeiffer, D. C., Vogl, A. W., Pan, J., & Randall, D. J. (1994). Immunolocalization of H^+-ATPase in the gill epithelia of rainbow trout. *Journal of Experimental Biology*, 195(1), 169-183.

Loretz, C. A. (1995). Cellular and molecular approaches to fish ionic regulation 2-electrophysiology of ion transport in teleost intestinal cells. In *Fish physiology* (Wood, C. M., & Shuttleworth, T. J. eds), 14, 25-56. Academic Press.

Loretz, C. A., Pollina, C., Hyodo, S., Takei, Y., Chang, W., & Shoback, D. (2004). cDNA cloning and functional expression of a Ca^{2+}-sensing receptor with truncated C-terminal

tail from the Mozambique tilapia (*Oreochromis mossambicus*). *Journal of Biological Chemistry*, 279(51), 53288-53297.

Madsen, S. S., Bollinger, R. J., Brauckhoff, M., & Engelund, M. B. (2020). Gene expression profiling of proximal and distal renal tubules in Atlantic salmon (*Salmo salar*) acclimated to fresh water and seawater. *American Journal of Physiology-Renal Physiology*, 319(3), F380-F393.

Mai, K. S., Zhang, C. X., Ai, Q. H., Duan, Q. Y., Xu, W., Zhang, L., & Tan, B. P. (2006). Dietary phosphorus requirement of large yellow croaker, *Pseudosciaena crocea*. *Aquaculture,* 251, 346–353.

Marshall, W. S. (2002). Na^+, Cl^-, Ca^{2+} and Zn^{2+} transport by fish gills: retrospective review and prospective synthesis. *Journal of Experimental Zoology*, 293(3), 264-283.

Marshall, W. S. (2012). Euryhaline fishes 8- osmoregulation in estuarine and intertidal fishes. In *Fish physiology* (McCormick, S. D., Farrell, A. P., Brauner, C. J. eds), 32, 395-434. Academic Press.

Marshall, W. S. and Grosell, M. (2006). Ion transport, osmoregulation and acid-base balance. In *Physiology of Fishes*. (Evans, D., & Claiborne, J. B. eds) 3, 177-230. Boca Raton: CRC Press.

McDonald, M. D., & Grosell, M. (2006). Maintaining osmotic balance with an aglomerular kidney. *Comparative Biochemistry and Physiology Part A: Molecular & Integrative Physiology*, *143*(4), 447-458.

McGuigan, J. A. S., Buri, A., Chen, S., Illner, H., & Lüthi, D. (1993). Some theoretical and practical aspects of the measurement of the intracellular free magnesium concentration in heart muscle: consideration of its regulation and modulation. *Magnesium and the Cell*, 91-120.

Musch, M. W., Orellana, S. A., Kimberg, L. S., Field, M., Halm, D. R., Krasny Jr, E. J., & Frizzell, R. A. (1982). $Na^+ - K^+ - Cl^-$ co-transport in the intestine of a marine teleost. *Nature*, 300(5890), 351-353.

Mzengereza, K., & Kang'Ombe, J. (2015). Effect of dietary salt (sodium chloride) supplementation on growth, survival and feed utilization of *Oreochromis shiranus* (Trewavas, 1941). *Journal of Aquatic Research & Development*, 7(1), 1-5.

National Research Council. (2011). *Nutrient requirements of fish and shrimp*. National Academies Press.

Natochin, Y. V., & Gusev, G. P. (1970). The coupling of magnesium secretion and sodium reabsorption in the kidney of teleost. *Comparative Biochemistry and Physiology*, 37(1), 107-111.

Nordlie, F.G., Haney, D. C., & Walsh, S.J. (1992). Comparisons of salinity tolerances and osmotic regulatory capabilities in populations of sailfin molly (*Poecilia latipinna*) from brackish and fresh waters. *Copeia*. 1992(3), 741-746.

Ogino, C. & Chiou, J. Y. (1976). Mineral requirements in fish. II. magnesium requirement of carp. *Bulletin of the Japanese Society of Scientific Fisheries*, 42, 71–75.

Ogino, C., Takashima, F. & Chiou, J. Y. (1978). Requirement of rainbow trout for dietary magnesium. *Bulletin of the Japanese Society of Scientific Fisheries,* 44(10), 1105–1108.

Ogino, C. & Takeda, H. (1976). Mineral requirements in fish. III. Calcium and phosphorus requirements in carp. *Nippon Suisan Gakkaishi*, 42, 793-799.

Oikari, A. O., & Rankin, J. C. (1985). Renal excretion of magnesium in a freshwater teleost, *Salmo gairdneri*. *Journal of Experimental Biology*, 117(1), 319-333.

Parmelee, J. T., & Renfro, J. L. (1983). Esophageal desalination of seawater in flounder: role of active sodium transport. *American Journal of Physiology-Regulatory, Integrative and Comparative Physiology*, 245(6), R888-R893.

Perry, S. F., Shahsavarani, A., Georgalis, T., Bayaa, M., Furimsky, M., & Thomas, S. L. Y. (2003). Channels, pumps, and exchangers in the gill and kidney of freshwater fishes: their role in ionic and acid-base regulation. *Journal of Experimental Zoology Part A: Comparative Experimental Biology*, 300(1), 53-62.

Pfaffl MW (2001). A new mathematical model for relative quantification in real-time RT-PCR. *Nucleic Acids Research*, 29, E45.

Pisam, M., & Rambourg, A. (1991). Mitochondria-rich cells in the gill epithelium of teleost fishes: an ultrastructural approach. In *International Review of Cytology* (Vol. 130, pp. 191-232). Academic Press.

Potts, W. T. W. (1954). The energetics of osmotic regulation in brackish-and fresh-water animals. *Journal of Experimental Biology*, 31(4), 618-630.

Potts, W. T. W., & Evans, D. H. (1967). Sodium and chloride balance in the killifish *Fundulus heteroclitus*. *The Biological Bulletin*, 133(2), 411-425.

Prabhu, P., Schrama, J. W., Fontagné-Dicharry, S., Mariojouls, C., Surget, A., Bueno, M., ... & Kaushik, S. J. (2017). Evaluating dietary supply of microminerals as a premix in a complete plant ingredient-based diet to juvenile rainbow trout (*Oncorhynchus mykiss*). *Aquaculture Nutrition*, 24(1), 539-547.

Prabhu, P. A. J., Stewart, T., Silva, M., Amlund, H., Ørnsrud, R., Lock, E. J., ... & Hogstrand, C. (2018). Zinc uptake in fish intestinal epithelial model RTgutGC: Impact of media ion composition and methionine chelation. *Journal of Trace Elements in Medicine and Biology*, *50*, 377-383.

Quamme, G. A. (2008). Recent developments in intestinal magnesium absorption. *Current Opinion in Gastroenterology,* 24(2)*,* 230–235.

Rider, S. A., Davies, S. J., Jha, A. N., Clough, R., & Sweetman, J. W. (2010). Bioavailability of co-supplemented organic and inorganic zinc and selenium sources in a white fishmeal-based rainbow trout (*Oncorhynchus mykiss*) diet. *Journal of Animal Physiology and Animal Nutrition*, 94(1), 99-110.

Robinson, E. H., Rawles, S. D., Brown, P. B., Yette, H. E., & Greene, L. W. (1986). Dietary calcium requirement of channel catfish *Ictalurus punctatus*, reared in calcium-free water. *Aquaculture*, 53(3-4), 263-270.

Rodgers, D. W. (1984). Ambient pH and calcium concentration as modifiers of growth and calcium dynamics of brook trout *Salvelinus fontinalis*. *Canadian Journal of Fisheries and Aquatic Sciences*, 41(12), 1774-1780.

Romani, A., & Scarpa, A. (1992). Regulation of cell magnesium. Archives of biochemistry and biophysics, 298(1), 1-12.

Roy, P. K., & Lall, S. P. (2003). Dietary phosphorus requirement of juvenile haddock (*Melanogrammus aeglefinus L.*). *Aquaculture*, *221*(1-4), 451-468.

Runnels, L. W., Yue, L., & Clapham, D. E. (2001). TRP-PLIK, a bifunctional protein with kinase and ion channel activities. *Science*, 291(5506), 1043-1047.

Ryazanova, L. V., Rondon, L. J., Zierler, S., Hu, Z., Galli, J., Yamaguchi, T. P., Mazur, A., Fleig, A., & Ryazanov, A. G. (2010). TRPM7 is essential for Mg^{2+} homeostasis in mammals. *Nature Communications* 1(1), 109.

Sahni, J., Nelson, B., & Scharenberg, A. M. (2007). SLC41A2 encodes a plasma-membrane Mg^{2+} transporter. *The Biochemical Journal*, 401(2), 505–513.

Sahni, J., & Scharenberg, A. M. (2013). The SLC41 family of MgtE-like magnesium transporters. *Molecular Aspects of Medicine*, 34(2-3), 620-628.

Salman, N. A., & Eddy, F. B. (1988). Effect of dietary sodium chloride on growth, food intake and conversion efficiency in rainbow trout (*Salmo gairdneri* (*Richardson*)). *Aquaculture*, 70(1-2), 131-144.

Schlingmann, K. P., Weber, S., Peters, M., Niemann Nejsum, L., Vitzthum, H., Klingel, K., ... & Konrad, M. (2002). Hypomagnesemia with secondary hypocalcemia is caused by mutations in TRPM6, a new member of the TRPM gene family. *Nature Genetics*, 31(2), 166-170.

Schlingmann, K. P., Waldegger, S., Konrad, M., Chubanov, V., & Gudermann, T. (2007). TRPM6 and TRPM7—gatekeepers of human magnesium metabolism. *Biochimica et Biophysica Acta -Molecular Basis of Disease*, 1772(8), 813-821.

Seo, M. Y., Mekuchi, M., Teranishi, K., Kaneko, T. (2013). Expression of ion transporters in gill mitochondrion-rich cells in Japanese eel acclimated to a wide range of environmental salinity. *Comparative Biochemistry & Physiology A: Molecular and Integrative Physiology*, 166, 323-332.

Shearer, K. D. (1988). Dietary potassium requirement of juvenile chinook salmon. *Aquaculture*, 73(1-4), 119-129.

Shearer, K. D. (1989). Whole body magnesium concentration as an indicator of magnesium status in rainbow trout (*Salmo gairdneri*). *Aquaculture*, 77(2-3), 201-210.

Shen, H. M., Chen, X. R., Chen, W. Y., Lin, S. M., Chen, Y. J., Zhang, L., & Luo, L. (2016). Influence of dietary phosphorus levels on growth, body composition, metabolic response and antioxidant capacity of juvenile snakehead (*Channa argus* × *Channa maculata*). *Aquaculture Nutrition*, 23(4), 662–670.

Shiau, S. Y., & Hsieh, J. F. (2001a). Quantifying the dietary potassium requirement of juvenile hybrid tilapia (*Oreochromis niloticus*× *O. aureus*). *British Journal of Nutrition*, 85(2), 213-218.

Shiau, S. Y., & Hsieh, J. F. (2001b). Dietary potassium requirement of juvenile grass shrimp *Penaeus monodon*. *Fisheries science*, 67(4), 592-595.

Shim, K. F., & Ng, S. H. (1988). Magnesium requirement of the guppy (*Poecilia reticulata* (*Peters*)). *Aquaculture*, 73(1-4), 131-141.

Shiraishi, K., Kaneko, T., Hasegawa, S., & Hirano, T. (1997). Development of multicellular complexes of chloride cells in the yolk-sac membrane of tilapia (*Oreochromis mossambicus*) embryos and larvae in seawater. *Cell and Tissue Research*, 288(3), 583-590.

Smith, N. F., Talbot, C., & Eddy, F. B. (1989). Dietary salt intake and its relevance to ionic regulation in freshwater salmonids. *Journal of Fish Biology*, 35(6), 749-753.

Smith, R. L., Thompson, L. J., & Maguire, M. E. (1995). Cloning and characterization of MgtE, a putative new class of Mg^{2+} transporter from Bacillus firmus OF4. *Journal of bacteriology*, 177(5), 1233-1238.

Song, J. Y., Zhang, C. X., Wang, L., Song, K., Hu, S. C., & Zhang, L. (2017). Effects of dietary calcium levels on growth and tissue mineralization in Japanese seabass, *Lateolabrax japonicus*. *Aquaculture Nutrition*, 23(3), 637-648.

Spry, D. J., & Wood, C. M. (1989). A kinetic method for the measurement of zinc influx in vivo in the rainbow trout, and the effects of waterborne calcium on flux rates. *Journal of Experimental Biology*, 142(1), 425-446.

Stuiver, M., Lainez, S., Will, F. C., Terryn, S., Günzel, D., Debaix, H., Sommer, K., Kopplin, K., Thumfart. J., Kampik, N. B., Querfeld, U., Willnow, T. E., Nemec, V., Wagner, C. A., Hoenderop, J. G., Devuyst, O., Knoers, N. V. A. M., Bindels, R. J., Meij, I. C., & Müller,

D. (2011). CNNM2, encoding a basolateral protein required for renal Mg^{2+} handling, is mutated in dominant hypomagnesemia. *American Journal of Human Genetics*, 88(3), 333– 343.

Swaminathan, R. (2003). Magnesium metabolism and its disorders. *The Clinical Biochemist Reviews*, 24(2), 47.

Tacon, A. G. (1992). Nutritional fish pathology: morphological signs of nutrient deficiency and toxicity in farmed fish. *Food & Agriculture Organization of the United Nations.* 85(2), 75.

Takvam, M., Wood, C. M., Kryvi, H., & Nilsen, T. O. (2021). Ion transporters and osmoregulation in the kidney of teleost fishes as a function of salinity. *Frontiers in Physiology*, 12, 664588.

Tang, C. H., Wu, W. Y., Tsai, S. C., Yoshinaga, T., & Lee, T. H. (2010). Elevated Na^+/K^+-ATPase responses and its potential role in triggering ion reabsorption in kidneys for homeostasis of marine euryhaline milkfish (*Chanos chanos*) when acclimated to hypotonic fresh water. *Journal of Comparative Physiology B*, 180, 813-824.

Taylor, J. R., & Grosell, M. (2006a). Feeding and osmoregulation: dual function of the marine teleost intestine. *Journal of Experimental Biology*, 209(15), 2939-2951.

Taylor, J. R., & Grosell, M. (2006b). Evolutionary aspects of intestinal bicarbonate secretion in fish. *Comparative Biochemistry and Physiology Part A: Molecular & Integrative Physiology*, 143(4), 523-529.

Teramoto, T., Lambie, E. J., & Iwasaki, K. (2005). Differential regulation of TRPM channels governs electrolyte homeostasis in the *C. elegans* intestine. *Cell Metabolism*, 1(5), 343-354.

Teramoto, T., Sternick, L. A., Kage-Nakadai, E., Sajjadi, S., Siembida, J., Mitani, S., ... & Lambie, E. J. (2010). Magnesium excretion in *C. elegans* requires the activity of the GTL-2 TRPM channel. *PloS One*, 5(3), e9589.

Teranishi, K., & Kaneko, T. (2010). Spatial, cellular, and intracellular localization of Na^+/K^+-ATPase in the sterically disposed renal tubules of Japanese eel. *Journal of Histochemistry & Cytochemistry*, 58(8), 707-719.

Verkman, A. S., & Thiagarajah, J. R. (2006). Physiology of water transport in the gastrointestinal tract. *Physiology of the Gastrointestinal Tract*, 4, 1827-1845.

Voets, T., Nilius, B., Hoefs, S., Van Der Kemp, A. W. C. M., Droogmans, G., Bindels, R. J. M., & Hoenderop, J. G. J. (2004). TRPM6 forms the Mg^{2+} infux channel involved in intestinal and renal Mg^{2+} absorption. *Journal of Biological Chemistry*, 279(1), 19-25.

Wabakken, T., Rian, E., Kveine, M., & Aasheim, H. C. (2003). The human solute carrier SLC41A1 belongs to a novel eukaryotic subfamily with homology to prokaryotic MgtE

Mg^{2+} transporters. *Biochemical and Biophysical Research Communications*, 306(3), 718-724.

Walsh, P. J., Blackwelder, P., Gill, K. A., Danulat, E., & Mommsen, T. P. (1991). Carbonate deposits in marine fish intestines: a new source of biomineralization. *Limnology and Oceanography*, 36(6), 1227-1232.

Watanabe, T., Murakami, A., Takeuchi, L., Nose, T. & Ogino, C. (1980) Requirement of chum salmon held in freshwater for dietary phosphorus. *Bulletin of the Japanese Society for the Science of Fish*, 46, 361–367.

Watanabe, T., Kiron, V., & Satoh, S. (1997). Trace minerals in fish nutrition. *Aquaculture*, 151(1-4), 185-207.

Wei, S. P., Jiang, W. D., Wu, P., Liu, Y., Zeng, Y. Y., Jiang, J., ... & Feng, L. (2018). Dietary magnesium deficiency impaired intestinal structural integrity in grass carp (*Ctenopharyngodon idella*). *Scientific Reports*, 8(1), 12705.

Whittamore, J. M. (2012). Osmoregulation and epithelial water transport: lessons from the intestine of marine teleost fish. *Journal of Comparative Physiology B*, 182(1), 1-39.

Wingert, R. A., Selleck, R., Yu, J., Song, H. D., Chen, Z., Song, A., ... & Davidson, A. J. (2007). The cdx genes and retinoic acid control the positioning and segmentation of the zebrafish pronephros. *PLoS Genetics*, 3(10), e189.

Wilson, R. P., & El Naggar, G. (1992). Potassium requirement of fingerling channel catfish, *Ictalurus puntatus*. *Aquaculture*, 108(1-2), 169-175.

Wilson, J. M., Laurent, P., Tufts, B. L., Benos, D. J.,Donowitz, M., Vogl, A. W. & Randall, D. J. (2000). NaCl uptake by the branchial epithelium in freshwater teleost fish: an immunological approach to ion-transport protein localization. *Journal of Experimental Biology*, 203, 2279-2296.

Wilson, R. W., Wilson, J. M., & Grosell, M. (2002). Intestinal bicarbonate secretion by marine teleost fish—why and how?. *Biochimica et Biophysica Acta -Biomembranes*, 1566(1-2), 182-193.

Wood, C. M., & Marshall, W. S. (1994). Ion balance, acid-base regulation, and chloride cell function in the common killifish, *Fundulus heteroclitus*: a euryhaline estuarine teleost. *Estuaries*, 17(1), 34.

Wood, C. M., Kajimura, M., Bucking, C., & Walsh, P. J. (2007). Osmoregulation, ionoregulation and acid–base regulation by the gastrointestinal tract after feeding in the elasmobranch (*Squalus acanthias*). *Journal of Experimental Biology*, 210(8), 1335-1349.

Wood, C. M., & Bucking, C. (2011). The multifunctional gut of fish 5- the role of feeding in salt and water balance. In *Fish physiology* (Grosell, M. Farrell, A. P. Brauner C. J. eds), 30, 165-212. Academic Press.

Wood, C. M., Bucking, C., & Grosell, M. (2010). Acid–base responses to feeding and intestinal Cl^- uptake in freshwater- and seawater- acclimated killifish, *Fundulus heteroclitus*, an agastric euryhaline teleost. *Journal of Experimental Biology*, 213(15), 2681-2692.

Xie, D., Han, D., Zhu, X., Yang, Y., Jin, J., Liu, H., & Xie, S. (2016). Dietary available phosphorus requirement for on-growing gibel carp (*Carassius auratus gibelio var. CAS III*). *Aquaculture Nutrition,* 48(6), 28411-2851.

Yamazaki, D., Funato, Y., Miura, J., Sato, S., Toyosawa, S., Furutani, K., Kurachi, Y., Omori, Y., Furukawa, T., Tsuda, T., Kuwabata, S., Mizukami, S., Kikuchi, K., & Miki, H. (2013). Basolateral Mg^{2+} extrusion via CNNM4 mediates transcellular Mg^{2+} transport across epithelia: a mouse model. *PLoS Genetics*, 9(12), e1003983-e1003983.

Yao, Y. F., Jiang, M., Wen, H., Wu, F., Liu, W., Tian, J., & Yang, C. G. (2014). Dietary phosphorus requirement of GIFT strain of Nile tilapia *Oreochromis niloticus* reared in fresh water. *Aquaculture Nutrition,* 20, 273–280.

Yu, Y., Chen, S., Xiao, C., Jia, Y., Guo, J., Jiang, J., & Liu, P. (2014). TRPM7 is involved in angiotensin II induced cardiac fibrosis development by mediating calcium and magnesium influx. *Cell Calcium*, 55(5), 252-260.

Zafar, N., & Khan, M. A. (2018). Determination of dietary phosphorus requirement of stinging catfish *Heteropneustes fossilis* based on feed conversion, growth, vertebrae phosphorus, whole body phosphorus, haematology and antioxidant status. *Aquaculture Nutrition*, 24(5), 1577-1586.

Zafar, N., & Khan, M. A. (2019). Quantification of dietary calcium requirement of fingerling *Heteropneustes fossilis* based on growth, feed conversion efficiency, mineralization and serum alkaline phosphatase activity. *Journal of Animal Physiology and Animal Nutrition*, 103(6), 1959-1968.

Zhu, W., Liu, M., Chen, C., Wu, F., Yang, J., Tan, Q., ... & Liang, X. (2014). Quantifying the dietary potassium requirement of juvenile grass carp (*Ctenopharyngodon idellus*). *Aquaculture*, 430, 218-223.